A molecular study on phospho-regulation of microtubule depolymerase MCAK via GTSE1

Inaugural - Dissertation
zur Erlangung des Doktorgrades
(Dr. rer.nat.)

Der Fakultät für Biologie
an der
Universität Duisberg - Essen

Vorgelegt von
Devika C Namboodiri
aus Kerala, Indien

durchgeführt am
Max Planck Institut für molekulare Physiologie
Abteilung für mechanistische Zellbiologie
AG Musacchio

April 2024

DOI: 10.17185/duepublico/82452
URN: urn:nbn:de:hbz:465-20241002-083706-2

Die der vorliegenden Arbeit zugrunde liegenden Experimente wurden am Max Planck Institut für molekulare Physiologie in der Abteilung für mechanistische Zellbiologie durchgeführt.

1. Gutachter: Prof. Dr. Andrea Musacchio
2. Gutachter: Dr. Stefan Westermann

Vorsitzender des Prüfungsausschusses: Dr. Perihan Nalbant

Tag der mündlichen Prüfung: 29.08.2024

Publications

Rondelet A*, Pozniakovsky A*, **Namboodiri D**, Cardoso da Silva R, Singh D, et al. ESI mutagenesis: a one-step method for introducing mutations into bacterial artificial chromosomes. Life Science Alliance (2020).

Abstract

Microtubules (MT) are essential components of the cellular cytoskeleton. During cell division, they form a highly dynamic structure called the mitotic spindle that is necessary for proper alignment and segregation of chromosomes. Hence it becomes crucial for the cell to ensure that the microtubule dynamics are strictly regulated in a spatio-temporal manner. This regulation is often orchestrated by the interplay of various Microtubule Associated Proteins (MAPs) and mitotic kinases in a complex and poorly understood coordination. The kinesin 13 family proteins (Kif2A, Kif2B and Kif2C/MCAK) are MAPs that execute a regulatory function on MT dynamics via their potent MT depolymerase activity. MCAK is required to establish the length and stability of astral microtubules during spindle assembly as well as to facilitate any microtubule-kinetochore attachment error correction process. We previously discovered a novel MCAK-inhibiting protein, GTSE1, whose loss in cells causes microtubule destabilization, resulting in spindle positioning defects and chromosome mis-alignment. We do not, however, understand how GTSE1 inhibits MCAK activity mechanistically, nor how it is regulated in cells. Here, we aim to elucidate this inhibitory mechanism at the molecular level, which we suspect will define a novel mechanism for the poorly understood, yet essential, cellular control of the potent Kinesin 13 MT depolymerase activities. We found that the interaction of GTSE1 with MCAK requires phosphorylation of GTSE1 on its T165 site by either of the mitotic kinases Aurora A or Aurora B in vitro. Further examination revealed a differential regulation of MCAK activity by GTSE1 that is dependent on the phosphorylation status of GTSE1. Phosphorylated GTSE1 was found to modulate MCAK activity in a more nuanced manner, suggesting a finely tuned regulatory mechanism, which could be vital for maintaining the fidelity of mitotic processes. This work will further our understanding of the spatio-temporal regulation of microtubule dynamics in mitosis.

List of Tables

List of Figures

List of Abbreviations

APC	Adenomatous Polyposis Coli
APC/C	Anaphase Promoting Complex/ Cdc25
ATP	Adenosine triphosphate
BACs	Bacterial Artificial Chromosomes
bp	basepair
CBB	Coomassie Brilliant Blue
Cdc	Cell division cycle
CDK	Cyclin Dependent Kinase
CENP	Centromeric Protein
CEP-135	Centrosomal Protein of 135 kDa
CHC	Clathrin Heavy Chain
CLASP	Cytoplasmic Linker Associated Protein
CLIP	Cytoplasmic Linker Protein
DAPI	4,6-diamidin-2-phenylindoldihydrochlorid
DMSO	Dimethyl sulfoxide
DNA	Deoxyribonucleic acid
DTT	Dithiothreitol
EB	End Binding
ECM	Extracellular Matrix
FBS	Fetal Bovine Serum
FL	Full length
G1	Growth 1
G2	Growth 2

GAK	Cyclin G-associated Kinase
GST	Glutathione S-transferase
GTP	Guanosine-5'-triphosphate
GTSE1	G2 and S phase expressed 1
HeLa	Henrietta Lacks
IP	Immunoprecipitation
kb	kilobase
kDa	kilo Dalton
KO	Knockout
LB	Luria-Bertani
LID	Leucine-Isoleucine-Aspartic Acid
M-phase	Mitotic phase
mA	milli Ampere
MAPs	Microtubule Associated Proteins
MARK2	MAP-microtubule Affinity Regulating Kinase
MCAK	Mitotic Centromere Associated Kinesin
min	minute
MPF	Maturation Promoting Factor
MS	Mass Spectrometry
MTOC	Microtubule Organizing Centre
NEBD	Nuclear Envelope Breakdown
PCR	Polymerase Chain Reaction
Plk1	Polo like Kinase 1
PTM	Post-translational Modification
RPE-1	Retinal Pigmented Epithelial
S-phase	Synthesis phase
SAC	Spindle Assembly Checkpoint

SDS-PAGE	Sodium Dodecyl Sulfate Polyacrylamide Gel Electrophoresis
siRNA	silencer RNA
SxIP	Serine-x-Isoleucine-Proline
RAN	RAs-related Nuclear
TACC3	Transforming Acid Coiled-coil Containing Protein 3
TCEP	Tris-(2-carboxyethyl)-phosphine
TPX2	Targeting Protein for Xklp2
V	Volts
wt	Wildtype
+TIP	Plus tip interacting proteins

Contents

1. Introduction

Faithful segregation of chromosomes during cell division is crucial for the maintenance of genomic stability. Therefore, chromosome segregation is a tightly regulated process that comprises multiple cellular signalling pathways and coordinated function of proteins and kinases. The cellular cytoskeleton, namely the microtubules, also takes part in the process by forming a structural apparatus called spindle that helps in the physical separation of chromosomes. It is within this spindle that many mitotic kinases phosphorylate its various substrates in order to ensure proper regulation of chromosomal movements and segregation. Any errors in these regulatory processes can lead to chromosome mis-segregation and instability (CIN). Persistent mis-segregation of chromosomes can eventually cause aneuploidy, a major hallmark of cancer. While there have been many comprehensive studies on cellular signalling and checkpoints during cell division, the differential regulation of microtubules via proteins and kinases are yet to be elucidated.

1.1. The Cell Cycle

A cell reproduces by duplicating and diving through an organised and controlled sequence of events known as the *cell cycle*. The major two stages of the cell cycle constitute the *S phase* (S for DNA synthesis) where the chromosomal DNA duplicates and the *M phase* (M for mitosis) where the duplicated chromosomes are segregated equally into two daughter cells followed by cell division (reviewed in Norbury and Nurse 1992). The cell prepares for each of these major stages during gap phases, namely G1 and G2. In G1, cells are metabolically active for preparation of DNA duplication during S phase and in G2, cells synthesise proteins before the start of M phase. Hence, traditionally the cell cycle comprises the four (G1, S, G2, M) phases (Figure 1) and among these, G1, S and G2 phases are collectively known as the *interphase* (Alberts B, Johnson A, 2002).

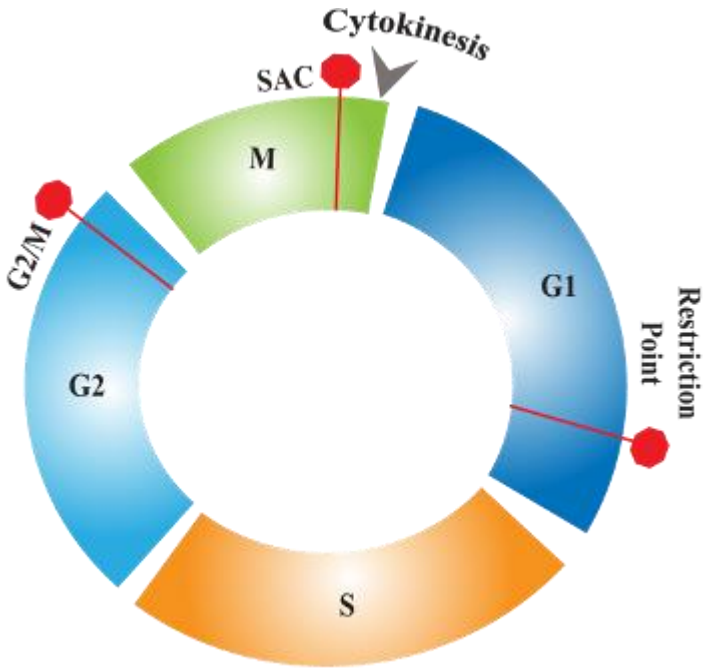

Figure 1. The Eukaryotic Cell Cycle

The cell duplicates its DNA during the S phase. The two gap phases (G1 and G2) provide more time for the cell to prepare for the next steps and safeguard cell cycle progression at quality control checkpoints. The duplicated chromosomes and cytoplasm are segregated equally into two daughter cells during mitosis (M phase) and cytokinesis, respectively. The three cell cycle checkpoints; restriction point, G2/M checkpoint and SAC are depicted in red.

The transition between different cell cycle phases is coordinated in a tightly regulated manner in order to ensure proper division of cells. In most eukaryotic cells, there are three major regulatory transitions, or checkpoints that control cell cycle progression. The first checkpoint is the restriction *point* (in mammalian cells) in late G1 that ensures if the external conditions for entry into S phase are constructive and that the signals for the growth and DNA replication are intact (Hartwell, 1971; Pardee, 1974). The second checkpoint G2/M is at the end of the G2 phase that ensures proper replication of DNA during S phase before the cell enters mitosis (reviewed in (Lukas et al., 2004)). The third checkpoint is called the spindle assembly checkpoint (SAC) that monitors proper chromosome attachments during metaphase and ensures accurate chromosome segregation (Musacchio & Salmon, 2007). The control system blocks progression through each of these checkpoints if it detects any unfavourable conditions within or outside the cell. If the control system senses problems in the completion of DNA replication, for example, it will hold the cell at the G2/M checkpoint until those problems are solved.

The cell cycle is catalysed primarily by complexes containing Cyclin Dependent Kinases (CDKs) and cyclins. Cdks are serine/threonine protein kinases that are activated at specific points in the cell cycle. The Cdks are critical for cell cycle progression as inactivation of these proteins prevents mitosis (Norbury & Nurse, 1992; Schafer, 1998). Much of the cell cycle regulation is determined by phosphorylation state. Cyclins perform multiple regulatory functions. Along with appropriate phosphorylation state of Cdks, binding to cyclins is another requirement for Cdk activation. Other major kinase families that are crucial in cell cycle control include Polo Like Kinase 1 (Plk1) and Aurora kinases (Aurora A and B). These kinases regulate protein phosphorylation in a spatiotemporal manner and play key roles during events like spindle assembly, chromosome segregation and cytokinesis. They are critical for avoiding errors during cell cycle progression (Barr et al., 2004; Carmena et al., 2009).

1.2. Mitosis

Once DNA duplication occurs in S phase, the cells progress through the G2 and enter the shortest and most dynamic stage at M phase. It begins with *mitosis* where cells condense and segregate the duplicated DNA pairs or sister chromatids equally into the two daughter nuclei. Mitosis traditionally constitutes five major stages, namely *prophase*, *prometaphase*, *metaphase*, *anaphase* and *telophase*. These phases together, also collectively called karyokinesis, is followed by the complete division of the mother cell to daughter cells known as *cytokinesis* (Alberts B, Johnson A, 2002). During prophase, the duplicated DNA condenses into discrete chromosomes by recruiting DNA binding proteins like the condensing complex. The sister chromatid pair that forms the chromosome is bound together by *cohesin*. Cohesin is largely removed from arms during prophase making the sister chromatids more resolved, but the remaining cohesin gets retained at the most constricted part of the chromosome, *centromere*. Outside the nucleus, the mitotic spindle begins to form as a result of microtubule nucleation at centrosomes positioned to the opposite side of the nucleus. This is followed by the breakdown of the nuclear envelope that marks the beginning of *prometaphase*. The microtubules that emanate from the centrosomes now start to form spindle-like structures and have access to the chromosomes. The microtubules dynamically assemble and disassemble while growing from centrosomes, thus undergoing a search and capture of chromosomes. The

most important part of the chromosomes for them to bind to the spindle microtubules is the *kinetochore*. They are multi protein complexes that are assembled at the centromere of each sister chromatid. Towards the end of prometaphase, the kinetochores of the sister chromatids bind to the microtubules from opposite poles starting off the *metaphase*.

At metaphase, the spindle attached chromosomes start aligning towards the middle of the cell on an imaginary line also known as the *metaphase plate*, to form a *bi-oriented* state. At this point, the SAC make sure that all the requirements including proper kinetochore-microtubule

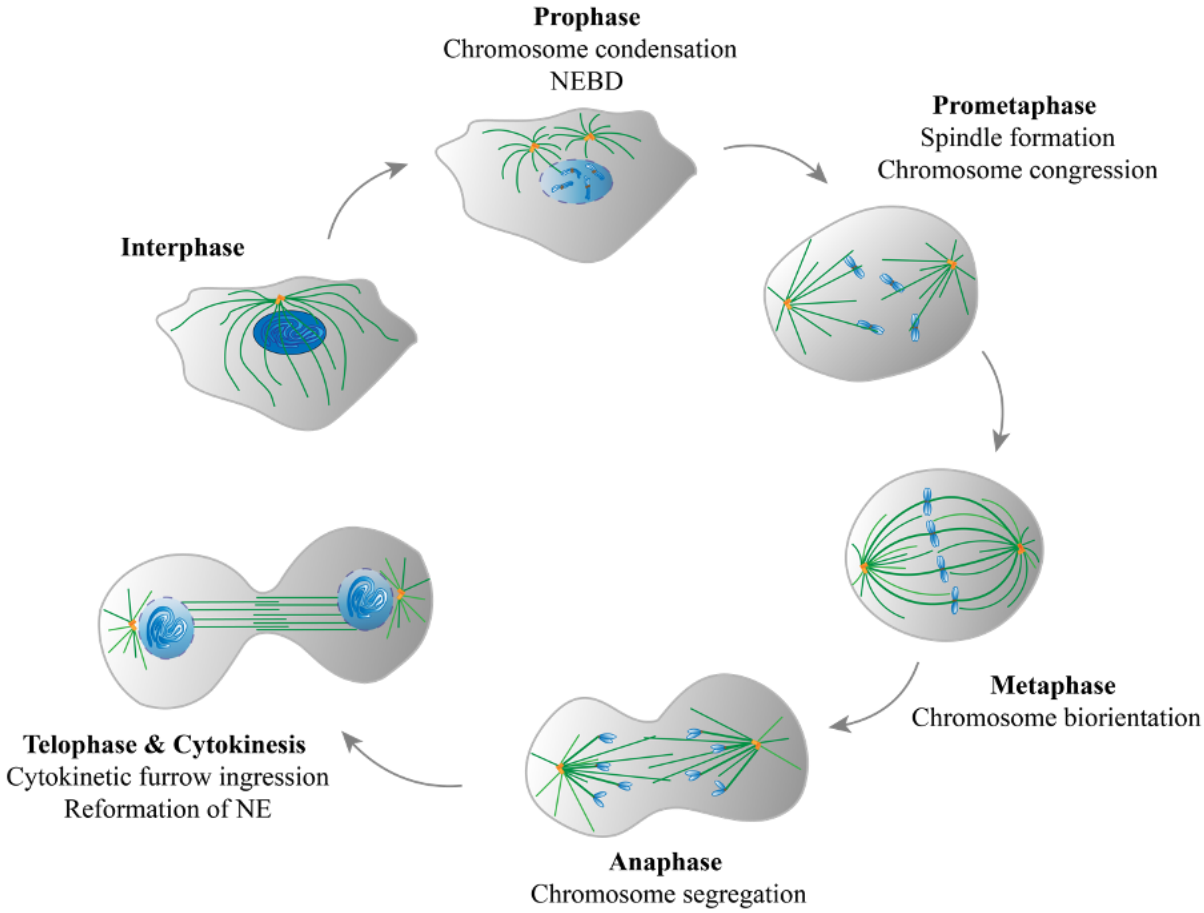

Figure 2. Schematic overview of phases in mitosis

During prophase, chromosomes replicated in S phase undergo condensation and the nuclear envelope (NE) disassembles. Chromosomes released into the cytoplasm are captured by spindle microtubules in prometaphase. The spindle also positions itself inside the cell. After biorientation of chromosomes in metaphase, sister chromatids are pulled to opposite poles in anaphase. Chromosomes decondense and NE reforms in telophase and cytokinesis complete mitosis.

attachments are satisfied in order to proceed to *anaphase* that begins with the cleavage of cohesin by a protein called *separase*. The sister chromatids are hence separated and are synchronously pulled towards the opposite poles of the cells by kinetochore attached microtubules and the spindle poles also move apart, both contributing to the segregation of chromosomes. The segregated chromosomes undergo de-condensation during *telophase* which is also followed by the reformation of individual nuclear envelopes forming two daughter nuclei. *Cytokinesis* is the last phase of cell division where the cytoplasm is divided into two by a contractile ring made of actin and myosin filaments that pinches the cell to form two daughter cells, each with a daughter nucleus.

1.3. Mitotic Kinases

Nearly every aspect of mitotic control involves protein phosphorylation. A significantly large portion of 518 kinases in the human kinome are dedicated to mitotic control. These kinases involved in mitosis, namely the *mitotic kinases* regulate both temporally and spatially in order to ensure the timely and proper execution of mitosis. The most prominent mitotic kinase is the Cdk1 as described before, which is also the founding member of the Cdk family of cell-cycle regulators. Recent studies have also discovered other kinase families that play crucial roles in mitotic regulation, some major ones being *Polo* family, *Aurora* family and *NIMA* (never in mitosis A) family. The activation of CDK-cyclinB during mitosis occurs through its phosphorylation by *CDK Activating Kinase complex* along with simultaneous phosphorylation of a phosphatase *Cdc25* by Plk1that can remove the inhibitory phosphorylations on Cdk1. Apart from role in Cdk1-cyclinB activation, Plk1 is also known to interplay along with Cdk1 by interacting with Cdk1 - primed substrates at different stages of mitosis (Takizawa & Morgan, 2000; Van Vugt & Medema, 2005). Similar crosstalk happens between Aurora Kinases and Plk1 as well. For instance, Plk1 primed substrate reverses the inhibitory effect on Aurora B during mitosis while Aurora A is known to activate Plk1 during G2/M phase with the help of cofactor *Bora*. While scientists have established much of Cdk1 based roles on cell cycle progression, the role of other kinases including Aurora Kinases in ensuring precise regulation of mitosis is yet to be elucidated in detail. Here I will describe further about the current understanding of the role of Aurora kinase family in mitosis which is relevant for the comprehension of this project.

1.3.1. Aurora Kinases

The Aurora genes that are relatively conserved throughout evolution, are characterised by 78-84% of identity between human and rodent orthologs (Katayama et al., 2003; Willems et al., 2018). The ancestral *AURK* gene known as *Ipl1* that gave rise to *AURKA* and *AURKB/AURKC* ancestral genes in invertebrates and some vertebrates were first identified in *Saccharomyces cerevisiae*. The mammalian version of *AURK* genes further evolved from duplication of genes from common ancestors of invertebrates and non-mammal vertebrates. In humans, there are three classes of Aurora kinases, namely *Aurora A*, *Aurora B* and *Aurora C*. While Aurora A and B are expressed in most normal cell types playing part in mitotic regulation, Aurora C is a *Chromosomal Passenger Complex (CPC)* protein functioning in meiotically-active germ cells.

1.3.1.1. Aurora A

The *Aurora* denotation, reminiscent of the North Pole, comes from the monopolar spindle formed upon mutations on the AURKA gene (Glover et al., 1995). Aurora A is localised at the centrosome during interphase, translocated to mitotic spindle during early mitosis and is a crucial player during the assembly of mitotic spindle. It gets locally activated by binding to its substrate, TPX2. This interaction blocks the access of *Protein Phosphatase 1* (PP1) to Aurora A, thus promoting the accumulation of active Aurora A by autophosphorylation. Depletion of TPX2 or addition of non-phosphorylatable form of Aurora A hence inhibits bipolar spindle assembly (Eyers et al., 2003; Kufer et al., 2002; Tsai & Zheng, 2005). Phosphorylation of CDC25B by Aurora A at centrosome during late G2 also contributes to the onset of mitosis (Dutertre et al., 2004; Tsai & Zheng, 2005). Depletion of Aurora A has been known to inhibit centrosome maturation and separation by affecting recruitment of proteins involved in microtubule nucleation/stabilisation. Recent discovery of interaction of *Transforming Acidic Coiled-Coil (TACC)* proteins with Aurora A could partly explains this mechanism involved in centrosome maturation, where Aurora A - phosphorylated D-TACC gets recruited to centrosome and forms complex with microtubule polymerase XMAP215 that further antagonises the activity of microtubule depolymerase called *Mitotic Centromere Associated Kinesin (MCAK)* promoting microtubule growth. (Berdnik & Knoblich, 2002; Hannak et al., 2001, Giet et al., 2002; Terada et al., 2003) Conte et al., 2003; Kinoshita et al., 2005). Overexpression of Aurora A causes abnormalities in G2 checkpoint while it can also override

the spindle checkpoint induced by chemotherapeutic agent paclitaxel (Taxol) that eventually make the cell inappropriately enter the anaphase even while the spindle is defective. This causes resistance to apoptosis induced by Taxol. Interestingly, Aurora A is an oncogene and is found overexpressed in several tumours. It has recently been reported that overexpression of Aurora A increases microtubule assembly rate. Increased microtubule assembly rate induces hyper-stabilisation of *kinetochore attached microtubules*, inducing *Chromosomal Instability (CIN*) in colorectal cancer cells (Ertych et al., 2014).

1.3.1.2. Aurora B

Aurora B is a chromosomal passenger protein that gets localised to centromeres from prophase till the metaphase-anaphase transition. Specifically, it is concentrated at the inner centromere during mitosis and later localises to the spindle midzone and cortex near the furrow ingression after anaphase. Aurora B closely interacts with *Inner Centromere Protein* (*INCENP)*, a founding member of CPC as well as Inhibitor of Apoptosis (IAP)- like protein *Survivin* (Adams, Maiato, et al., 2001). During prophase, Aurora B phosphorylates INCENP whereas this binding induces auto-phosphorylation of Aurora B that activates it via conformational change (Carmena et al., 2009; Sessa et al., 2005). In general, Aurora B plays an essential role in chromosome segregation, bipolar chromosomal assembly, chromosome condensation and cytokinesis (Dewar et al., 2004). Early studies in Drosophila melanogaster showed that depletion of Aurora B causes defects in chromosome congression, anaphase progression and cytokinesis (Adams, Maiato, et al., 2001; Giet & Glover, 2001). Recent studies have shown that Aurora activity inhibition using antibody injection caused defects in chromosome alignment, chromosome segregation and abrogated SAC (Kallio et al., 2002). Aurora B overexpression had been found in many cancers like colorectal cancer or thyroid carcinoma. But unlike Aurora A as described before, Aurora B is not an oncogene, but its overexpression causes metastasis (Adams, Eckley, et al., 2001; Katayama et al., 2003; Takahashi et al., 2000).

Overexpression of Aurora B 'kinase dead' mutant (Aur B K/R) in Normal Rat Kidney epithelial cells (NRK) causes chromosome congression defects by promoting unidirectional centromere movement and reduced chromosome velocity. Similar K/R mutant transfection in cells also leads to elongated spindles, all pointing out to disclose that Aurora B complexes interact with mitotic molecules that generate force via microtubules (Murata-Hori & Wang, 2002). Inhibition of Aurora B using small molecule inhibitors Hesperadin and ZM447439 gave more

evidence on the effects of Aurora B complex on microtubule dynamics in mammalian cells. Either of the inhibitor's treatment causes cells to override checkpoint arrest induced by taxol that stabilises microtubules and monastrol that causes monopolar spindles. On the other hand, small molecule inhibition of Aurora B did not affect checkpoint induction due to nocodazole treatment that causes destabilisation of microtubules. Considering that stabilised microtubules vs destabilised ones might activate different facets of checkpoint ie; one that monitors tension across sister centromeres vs one that monitors kinetochore microtubule occupancy respectively, these data of Aurora B inhibition strongly suggest that it plays a crucial role in correcting microtubule attachment errors specifically in the tension-sensing facet of the spindle checkpoint (Ditchfield et al., 2003; Hauf et al., 2003). Further discovery of how Aurora B is involved in tension sensing and checkpoint response came out when the Kinesin 13 family microtubule depolymerase MCAK turned out to be a substrate of Aurora B. It was recently discovered that Aurora B phosphorylation of MCAK induced a conformational change in the kinesin protein to an inactive form, thereby causing a compromise of its depolymerase activity. (Andrews et al., 2004; Ems-Mcclung et al., 2013; Ohi et al., 2004). Interestingly, Aurora B inhibition or expression of its kinase dead mutant blocked the localization of MCAK to the inner centromere and also loss of Centromere protein E (CenpE) and dynein important for chromosome congression from the kinetochore. Taken together, we can interpret that Aurora B phosphorylation of its substrates in a coordinated manner can affect the kinetochore-microtubule attachment/turnover. However, determining the exact mechanism of how Aurora B complex is involved in kinetochore-microtubule attachment, the kinetochore microtubule tension sensing by SAC and regulation of error correction by MCAK or other microtubule associated proteins remains to be a challenge for the future.

1.4. Microtubules

The cell cycle involves dramatic and dynamic rearrangement of the cell from interphase until cytokinesis. This is largely possible due to the organised networking and regulation of one of the major cellular cytoskeletons – the *Microtubules* that constitute the fundamental structural components of cell cycle machinery (Inoué & Salmon, 1995; Petry, 2016). Microtubules are hollow polymers composed of a and b-tubulin heterodimers that polymerize in a head-to-tail fashion to form a polar protofilament (Amos & Klug, 1974; Weisenberg et al., 1968). Lateral association of 11 to 13 such protofilaments forms a microtubule, which is approximately 25

mm in diameter (Desai & Mitchison, 1997). The surface of microtubules is largely negative due to the negatively charged glutamate rich C-terminal of tubulin. Microtubules are polar structures showing a dynamic fast growing plus end where the b-tubulin, an efficient GTPase is exposed and a stable slow growing minus end exposing a-tubulin that can weakly hydrolyse GTP (Allen & Borisy, 1974). Together, both the ends simultaneously incorporate tubulin dimers causing a net growth of microtubules called *polymerization* and rapidly remove tubulin dimers that causes shrinkage called *catastrophe*. This simultaneous growth and shrinkage events and rapid transition between the two was first observed by Tim Mitchison and Marc Kirchner in 1984 and called it the *dynamic instability* (Mitchison & Kirschner, 1984, 1988); Figure 3). This property of microtubules is important for various cellular functions during mitosis like chromosome separation, remodelling of spatial organisation of cytoskeleton etc. (Cassimeris et al., 1988; Gildersleeve et al., 1992; Mitchison & Kirschner, 1984; Sammak & Borisy, 1988).

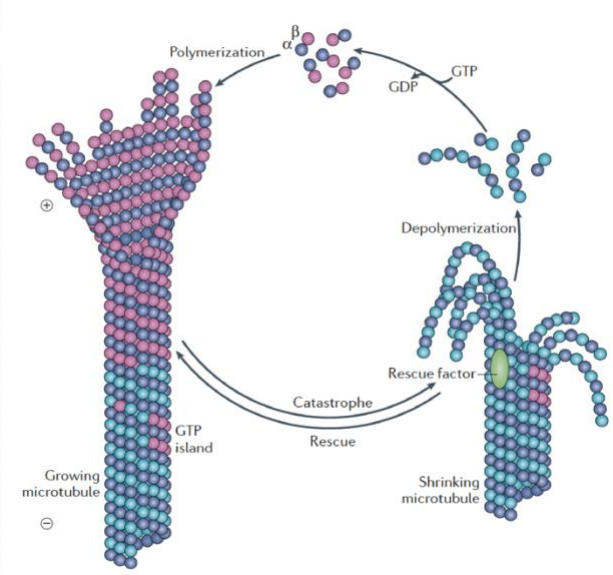

Figure 3. The cycle of tubulin assembly and disassembly

The GTP-bound tubulin dimer (purple) incorporates into the growing end (+) of microtubule. This process is called polymerization. GTP-bound β-tubulins on the plus end are termed a GTP-cap, which stabilizes the microtubule. Once the GTPs bound to β-tubulins are hydrolyzed (lightly blue), the tubulin dimers are removed from the plus end and undergo depolymerization/catastrophe, resulting in rapid shrinkage of the microtubule. When a rescue factor (e.g. a protein) approaches or new GTP bound tubulin dimers are added on the plus end, the microtubule stops shrinking and repolymerizes again. The cycle between microtubule growth and catastrophe is termed "dynamic instability". Figure is adapted from Akhmanova and Steinmetz, 2015.

Dynamic instability is thought to be an intrinsic property of the microtubules since purified tubulin can form microtubules by themselves even though in a concentration and temperature dependent manner (Kirschner & Mitchison, 1986; van der Vaart et al., 2009). Under ambient conditions for microtubule assembly, the polymerization of microtubules dominates *in vitro* at a rate determined by the concentration of free tubulin. Whereas, the catastrophe is much rapid and stochastic and doesn't depend upon the initial tubulin concentration. During catastrophe, the depolymerizing microtubules may or may not get rescued and resume growth. The major parameters used to characterise microtubule dynamics are the polymerization rate, the depolymerization rate, the catastrophe frequency and the rescue frequency (Brouhard, 2015; Desai & Mitchison, 1997). Despite being energetically expensive, the dynamic instability of microtubules is an evolutionarily conserved process, in tune with its important biological functions.

1.4.1. Microtubules and the mitotic spindle

During mitosis, it is important that the chromosomes are congressed and segregated properly without errors. This is achieved through the dynamic remodelling of microtubules to form a prominent bipolar structure called the *mitotic spindle*. In cells, the microtubule minus end is anchored to the Microtubule Organization Centre (MTOC) and one of the major MTOC consists the centrosome, where the nucleation of microtubules occurs and this later coordinates with chromatin-based microtubule nucleation as well as microtubule-based microtubule nucleation to form the bipolar mitotic spindle (Kapoor, 2017; Prosser & Pelletier, 2017)

The mitotic spindle assembly leads to formation of an antiparallel microtubule array that is composed of three major categories of microtubules namely, the *kinetochore microtubules (k-MTs),* the *astral microtubules* and the *non-kinetochore microtubules (nK-MTs)* or the *interpolar microtubules* (Howard & Hyman, 2003). Interpolar microtubules traditionally have their minus end embedded to the centrosomes and plus end overlap and crosslink with other interpolar microtubules plus ends. These microtubules are necessary for maintaining spindle shape and size during prometaphase and metaphase (Sharp et al., 2000). Astral microtubules have their minus ends embedded at the spindle poles and their plus ends are free to interact with the cell cortex. Astral microtubules are required for proper orientation of the spindle, which is important for defining the subsequent axis for formation of the cleavage furrow (Stevermann &

Liakopoulos, 2012). Third types of microtubules, k-MTs, have their plus ends bound to kinetochores. These k-MTs form discrete bundles of 20-25 k-MTs, which are further cross-linked and stabilised by formation of inter-microtubule bridges (Hepler et al., 1970; McDonald et al., 1992; Rieder, 1981, 2005; Witt et al., 1981). In vertebrate cells, such a bundle of k-MTs is known as a K-fiber. The K-fiber reaches the centrosome and needs to be stably anchored to kinetochores for proper chromosome alignment and segregation.

A plethora of proteins act on the spindle in order to regulate the dynamics of the microtubules within it. These proteins include Spindle Assembly Factors (SAFs) that associate with microtubules and recruit further regulatory proteins including Microtubule Associated Proteins (MAPs) that mainly control the microtubule kinetics via direct interactions.

1.4.2. Microtubules and the Kinetochore

The kinetochore is a highly conserved complex of proteins which appears as a trilaminar plate in vertebrates through thin-section transmission electron microscopy. It comprises of an electron dense inner kinetochore that forms the interphase with chromatin, an outer kinetochore with comparable electron density which acts as the platform for spindle microtubule interaction and an electron lucent central kinetochore (Dong et al., 2007; Santaguida & Musacchio, 2009). The inner kinetochore contains evolutionarily conserved and structurally unique set of proteins collectively known as the Constitutive Centromere-Associated Network. They associate with the centromeric DNA and provide the major structural framework for the assembly of kinetochore layers along with orchestration of the recruitment of key outer kinetochore proteins (Basilico et al., 2014; I. M. Cheeseman & Desai, 2008; Foltz et al., 2006; McClelland et al., 2007; Okada et al., 2006; Weir et al., 2016). The outer kinetochore that forms the interphase for *end on* attachments of microtubule plus ends has a nine-subunit-mega-complex that encompass three subcomplexes, namely KNL1, Mis12 and Ndc80 or the KMN network (Cheeseman & Desai, 2008; Foley & Kapoor, 2013; Przewloka et al., 2011; Screpanti et al., 2011; Janke et al., 2001; Wigge & Kilmartin, 2001).

The kinetochore is known to be involved in two fundamental feedback mechanisms. Broadly, one mechanism distinguishes the correct and incorrect kinetochore-microtubules while the second mechanism coordinates this information of kinetochore-microtubule attachment to cell cycle progression via SAC (Kelly & Funabiki, 2009; Musacchio & Salmon, 2007; Peters, 2006; Pinsky & Biggins, 2005).

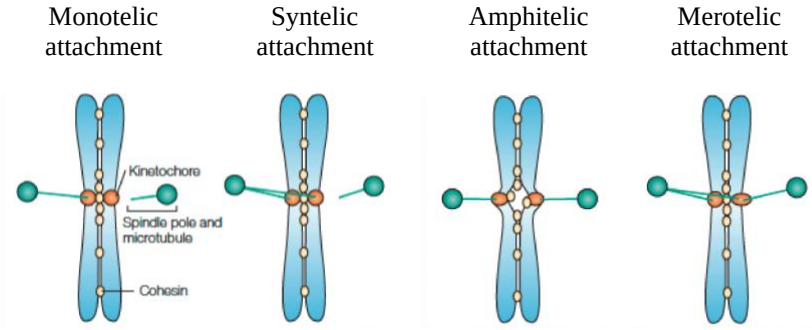

Figure 4. Types of the kinetochore-microtubule attachment

(A) Initial Monotelic Binding: Characterized by a solitary kinetochore forming a connection with microtubules projecting from a single spindle pole. (B) Syntelic Configuration: This occurs when kinetochores on the same chromosome erroneously attach to microtubules stemming from the same spindle pole. (C) Bipolar Amphitelic Association: In this correct attachment scenario, sister kinetochores are bound to microtubules emanating from opposing spindle poles, ensuring accurate chromosome segregation. (D) Complex Merotelic Coupling: A single kinetochore aberrantly associates with microtubules originating from both spindle poles, potentially leading to chromosome mis-segregation. Figure is adapted from Tanaka et al., 2005

Mature end-on attachments are required for chromosome bi-orientation and satisfaction of spindle assembly checkpoint. The search and capture of chromosomes in order to establish proper end on attachments occur concurrently with spindle assembly. The initial attachments of chromosomes are mostly to the microtubule lattice and later on stable end-on attachments are achieved with the help of KMN network. But the stochastic process of search and capture mechanism often causes sporadic kinetochore-microtubule mal-attachments during prometaphase. When kinetochore of one of the sister chromatids bind to the microtubule coming from one spindle pole while the other kinetochore doesn't bind to any microtubule at all, it constitutes a *monotelic* attachment (Rieder et al., 1995). *Syntelic* attachment is another mal-attachment, where both kinetochores of the sister chromatids attach to microtubules emanating from the same pole. Another form of mal-attachment, is the *merotelic* attachment where kinetochore of one sister chromatid bind to a pole while the other kinetochore binds to microtubules from both the spindle poles simultaneously (Cimini et al., 2003). Only the correct attachments persist stably, while the incorrect and labile attachments eventually get corrected. The mal-attachments specifically merotelic and syntelic attachments are efficiently corrected by an error correction machinery to *amphitelic* attachments, where the kinetochore of each sister chromatid binds to microtubules emanating from respective spindle poles

(Figure 4). Amphitelic attachments lead to generation of tension due to pulling forces exerted at the KTs by depolymerizing KT MTs and the resistance created due to the presence of cohesin. This tension results in labile-to-stable transition of amphitelic KT-MT attachments. In presence of unattached KTs, the SAC is activated and transmits a *wait* signal that ultimately leads to a mitotic arrest due to formation of a mitosis inhibitory complex called the *mitotic checkpoint complex (MCC)*. The MCC is a ternary complex composed of *Cdc20, Mad2, Bub3* and B*ubR1* that prevents premature anaphase onset by inhibiting the *anaphase promoting complex (APC/C)* (Lara-Gonzalez & Taylor, 2012). Once all the sister chromatids display amphitelic attachments, via a series of complex steps the MCC is disassembled, leading to release of Cdc20 and this subsequently associates with APC/C and activates the APC/C (Lara-Gonzalez & Taylor, 2012; Musacchio & Desai, 2017). Activated APC/C then catalyses the degradation of the Cdk1 regulatory subunit cyclin B, leading to a drop in Cdk1 activity. This releases separase from the inhibitory act of securin after which, separase is free to cleave cohesin thereby, allowing separation of sister chromatids and initiating anaphase. The major component of KMN that is involved in k-MT attachment is Ndc80, which has a weak microtubule binding affinity that synergistically increases on association with Mis12 and KNL1.

1.5. Microtubule Associated Proteins

Microtubules exhibit a complex assembly dynamic across the cell cycle that is regulated at a spatial and temporal level according to the demands of the cell. The microtubule polymer hence portrays many turnover mechanisms and polymer stabilities in order to participate in various cellular processes which is primarily possible due to the action of a broad class of microtubule/tubulin – interacting proteins, called the Microtubule Associated Proteins (MAPs). Some of the initial MAPs that were discovered as part of tubulin purification from brain extracts via microtubule assembly-disassembly cycles were *MAP1, MAP2* and *Tau* that contributed to microtubule assembly. MAPs are broadly categorised according to their mode of action into different types such as the *nucleating MAPs* that helps kick off the microtubule polymerization process by providing a platform for nucleation, the *microtubule motors/motile MAPs* that generate force and movement, the destabilising *MAPs* that can break microtubules and cause depolymerization, the stabilising *MAPs* that can reduce microtubule catastrophe and depolymerization rate and the *end binding proteins* that can associate with plus/minus end of

microtubules (Akhmanova & Steinmetz, 2008, 2015; Bhabha et al., 2016; Hirokawa, 1998; McNally & Roll-Mecak, 2018; Roostalu & Surrey, 2017). Action of MAPs on microtubules are further controlled by various regulatory mechanisms some of the key ones being protein expression level mediation, post-translational modifications like phosphorylation, dimerization or oligomerization, competition/antagonism between MAPs and intracellular localization.

Although microtubules can be formed from purified tubulin *in vitro* and show dynamic properties, the polymerization rate and stability are significantly different from that of physiological conditions. In a cytoplasmic environment, the polymerization is almost five to ten-fold more than the in vitro scenario, while the catastrophe occurs in much more controlled manner than *in vitro* frequency. One of the factors that lead to the accelerated microtubule growth rates in cells are the members of *XMAP215* family of stabilising MAPs that was first identified in *Xenopus laevis* egg extracts. The most conserved feature of XMAP215 family are the N-terminal TOG domains that can bind tubulins. The human ortholog of XMAP215, called *ch-TOG*, contains five TOG domains. Ch-TOG localises to the kinetochores, spindles and poles during mitosis (Charrasse et al., 1998; Popov et al., 2001). Another MAP that plays a part along with Ch-TOG in its function, is the Transforming Acid Coiled-coil Containing Protein 3 (TACC3) that exhibits plus end tracking in a Ch-TOG dependent manner. The recruitment and association of TACC3 to Ch-TOG in spindles occur in Aurora A dependent manner as described in the earlier section. Depletion of TACC3 in *Drosophila* S2 leads to disruption in the interphase microtubule network (Giet et al., 2002; Gutiérrez-Caballero et al., 2015). *End Binding (EB)* proteins are highly conserved plus tip interacting proteins (+TIPs) that autonomously track the growing plus ends of microtubules and stabilise them (Akhmanova & Steinmetz, 2008). In mammals, there are mainly three members of this family, namely the *EB1*, *EB2* and *EB3*, all of which serve both overlapping and non-redundant functions (Nehlig et al., 2017). It has been reported that depletion of EB1 in *Drosophila* reduces spindle size and leads to shorter astral microtubules during mitosis. *In vitro* reconstitution experiments using EB1 and microtubules showed that EB1 increases both rescue and catastrophe frequencies indicating its role in altering microtubule end structure (Bieling et al., 2007; Rogers et al., 2002; Vitre et al., 2008). Apart from these above-mentioned, other MAPs that are relevant for this project are described in detail below.

1.5.1. Kinesin 13 family of motor proteins

Kinesins are microtubule-associated motor proteins that utilise ATP hydrolysis to produce mechanical work. The kinesin superfamily of proteins also known as the KIFs generally move along the microtubules to translocate molecules or organelles, take part in sliding microtubules and regulate microtubule dynamics, specifically by their depolymerizing activity (Hirokawa et al., 2009; Peterman & Scholey, 2009). Unlike other kinesin family motor proteins that can depolymerize microtubules like Kinesin-8 or Kinesin-14, the Kinesin-13 family of motor proteins are unique depolymerizing enzymes that are non-motile in nature. They disassemble microtubules by targeting microtubule ends either directly or via diffusion along the microtubule lattice (Helenius et al., 2006; Wang et al., 2012). They were identified initially as motors involved in spindle function and their depletion or overexpression revealed their role as microtubule catastrophe factors and further their activity as microtubule depolymerases were discovered (Desai et al., 1999; Walczak et al., 1996; Wordeman & Mitchison, 1995).

Kinesin-13 proteins utilise diverse mechanisms to regulate microtubule dynamics. Their activities are regulated by post translational modifications like phosphorylation, differential localization or interaction with binding partners. Structurally, they are homodimeric proteins that constitute a motor domain with microtubules as well as ATP binding sites at the middle region of the protein (Hirokawa, 1998; Miki et al., 2001). The N-terminal domain is generally involved in subcellular localization while the C-terminal is often important for functional regulation and dimerization (Maney et al., 2001; Miki et al., 2001). In humans and mice, four key Kinesin-13 family motor proteins are known, namely, the *Kif2A, Kif2B, Kif2C/Mitotic Centromere Associated Kinesin (MCAK)* and *Kif24*.

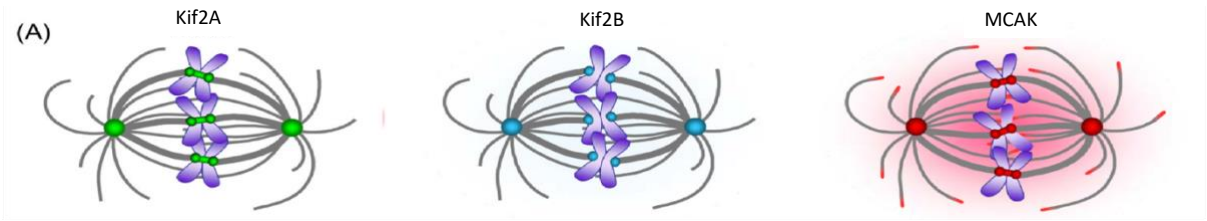

Figure 5. Localization of Kinesin-13s in mitosis

This diagram illustrates the spatial distribution of vertebrate Kinesin-13 family members during cell division. The localization patterns of Kif2A (highlighted in green), Kif2B (accented in teal), and MCAK (depicted in red) are shown, with each having a presence at spindle poles and kinetochore or centromeric regions. The figure is adapted from Ems Mc Clung et al, 2010.

Kif2A mainly localises to the spindle pole and depletion of this protein causes formation of monopolar spindles instead of bipolar ones. Kif2A is thus known to be involved in bipolar spindle assembly and chromosome movement as well. Kif2A primarily acts on the minus end of microtubules, affecting their poleward flux and thereby contributing to poleward chromosome movement during anaphase (Ganem et al., 2005; Ganem & Compton, 2004). Kif2A is seen enriched in spindle midzone during anaphase controlling the microtubule length and it is also known to be involved in spindle scaling of Xenopus laevis (Uehara et al., 2013; Wilbur & Heald, 2013).

Kif2B, although being expressed low in somatic cells, is a key player during mitosis. Kif2B is seen to have an enriched expression in testis while its overexpression in somatic cells causes its localization to kinetochores and centromeres (Manning et al., 2007). There it was revealed to be playing part in bipolar spindle assembly and kinetochore-microtubule error correction. Kif2B depleting through RNAi causes defects in cytokinesis and anaphase onset due to monopolar spindle formation (Bakhoum, Genovese, et al., 2009; Bakhoum, Thompson, et al., 2009; Hood et al., 2012; Manning et al., 2007).

Kif2C/MCAK is known to be the most potent microtubule depolymerase and a well characterised one in the Kinesin-13 family of motor proteins, which will be discussed in detail below.

1.5.1.2. Kif2C/MCAK

Mitotic centromere-associated kinesin (MCAK), a prominent member of the Kinesin-13 family, emerges as an efficient microtubule depolymerase with multifaceted roles during cell division (Andrews et al., 2004; Lan et al., 2004; Sanhaji et al., 2014; Wordeman & Mitchison, 1995). Intriguingly, MCAK localizes predominantly to centrosomes, centromeres, astral microtubules, and the spindle midbody, positioning itself strategically to influence various aspects of mitosis.

Functionally, MCAK plays a pivotal role in chromosome congression, spindle assembly, kinetochore-microtubule attachment, and general chromosome segregation during mitosis. Beyond mitosis, MCAK extends its influence to cytoskeletal remodeling during cell migration and invasion (Braun et al., 2014; Eichenlaub-Ritter, 2015). Additionally, MCAK participates in the regulation of meiotic events, contributing to meiotic spindle assembly in Xenopus laevis,

spindle pole limitation in Caenorhabditis elegans oocytes, and SAC (Spindle Assembly Checkpoint) silencing in mammalian oocytes (Connolly et al., 2015; Holmfeldt et al., 2005; Sun & Kim, 2012).

Structural insights into MCAK: Structurally, MCAK exhibits a modular organization comprising an N-terminal domain, a positively charged neck region, a central catalytic domain with conserved microtubule and ATP binding sites, and a C-terminal domain (Wordemann, 2005). Notably, MCAK forms dimers in solution, enhancing its depolymerization efficiency and specificity for microtubule ends(Cooper et al., 2010; Hertzer et al., 2006; Maney et al., 2001).

Role of the N-terminal domain: The N-terminal domain of MCAK, although not essential for in vitro microtubule depolymerization, assumes significance in subcellular localization. It is indispensable for recruiting MCAK to kinetochores, where it interacts with centromere-tethered Shugoshin 2 (Sgo2), contributing to inner kinetochore stretching and chromosome alignment. This recruitment, reliant on Aurora B activity, underscores the nuanced regulatory mechanisms governing MCAK function (Burns et al., 2014).

Moreover, the N terminus associates with End Binding (EB) proteins, facilitating microtubule end tracking. Aurora B-mediated phosphorylation of the N-terminal domain inhibits microtubule depolymerization in vitro in the absence of EB proteins. Deuterium exchange mass spectrometry implicates the N-terminal domain in kinesin force generation during depolymerization (McHugh et al., 2019).

Critical role of the motor domain and neck region: The motor domain, along with the neck region, constitutes the catalytic core crucial for depolymerization activity. Alterations in the neck region, driven by post-translational modifications like phosphorylation or site-directed mutagenesis, dramatically impact MCAK's enzymatic activity both *in vitro* and *in vivo* (Cooper et al., 2010; Ovechkina et al., 2002). The neck, oriented vertically towards the microtubule surface, is predicted to form a coiled coil, enhancing MCAK's delivery to microtubule ends and catalyzing its association with microtubules (Cooper et al., 2010).

Motor domain: Driving microtubule depolymerization: The central or motor domain of MCAK, although necessary, is not sufficient for depolymerization under physiological conditions. It induces a depolymerization-competent curved conformation in the microtubule protofilament, driving the depolymerization activity. X-ray crystallographic studies highlight the convex shape of the motor domain's microtubule-binding region, complementing the concave curvature of microtubule protofilament ends (Burns et al., 2015).

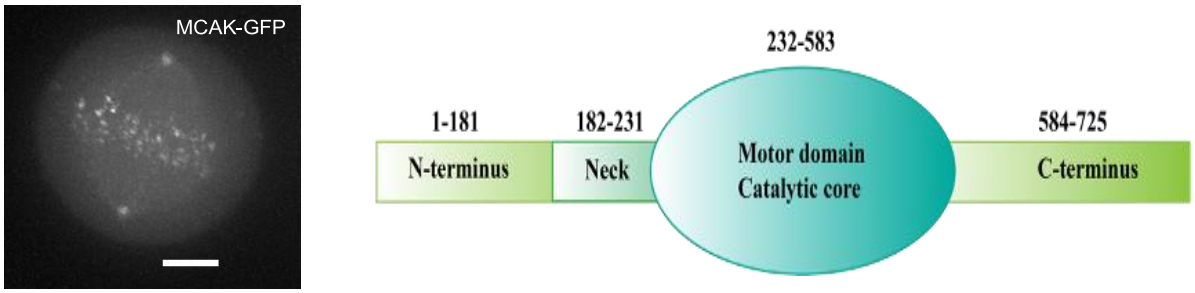

Figure 6. Intracellular Positioning and Molecular Structure of MCAK

A. An *in vivo* fluorescence microscopy image of MCAK-GFP in a metaphase Hela cell, depicting its accumulation at the centrosomes, kinetochores, and microtubules within the spindle. A scale marker indicating 5 micrometers is included. **B.** Conceptual diagram of the MCAK protein domains. The N-terminal region, encompassing amino acids 1-181, includes an SxIP motif essential for kinetochore association. The intervening neck domain, amino acids 182-231, combined with the motor domain, amino acids 232-583, is crucial for microtubule disassembly. The motor domain also engages with microtubules. Finally, the C-terminal section, amino acids 584-725, consists of the dimerization domain and regulates the depolymerization function of MCAK

Regulation of MCAK activity: The regulatory mechanisms governing MCAK are intricate and involve various levels of control exerted by phosphorylation through a multitude of mitotic kinases which can have both positive and negative effects on its functionality (Andrews et al., 2004; Ems-Mcclung et al., 2013; Lan et al., 2004; Sanhaji et al., 2014; Tanenbaum et al., 2011; Zhang et al., 2007). Phosphorylation, particularly by Aurora B kinase, significantly impacts MCAK's structural conformation during its catalytic cycle and its interaction with microtubules (Ems-Mcclung et al., 2013).

Advances in total internal reflection fluorescence (TIRF) microscopy have provided valuable insights into MCAK's function. These studies highlight the role of the neck region in catalyzing MCAK's association with microtubules and underscore its importance in the spatial and temporal regulation of MCAK at the microtubule ends (Talapatra et al., 2015; Zong et al.,

2016). The neck region, known for its susceptibility to post-translational modifications, now emerges as a pivotal element in MCAK's dynamic interaction with microtubules.

MCAK's activity involves transitioning between active and inactive conformations, binding to the microtubule lattice, diffusing on the lattice, and ultimately catalyzing the removal of tubulin dimers in an ATP-bound state (Friel & Howard, 2011; Ritter et al., 2016). Its ATP turnover cycle, marked by regulated ADP exchange and ATP cleavages, is essential for the protein's enzymatic function. In contrast to translocating kinesins, ATP cleavage, rather than product release, is the rate-limiting step for ATP turnover by MCAK. Microtubule ends enhance the ATPase activity, promoting the exchange of ADP for ATP, which fine-tunes MCAK for its depolymerizing role: lattice-stimulated ATP cleavage induces a weakly bound nucleotide state, facilitating MCAK's diffusion to microtubule ends, where it becomes tightly bound and promotes depolymerization (Figure 7).

While specific regulatory influences such as GTSE1 will be discussed later, it is important to note that the regulatory network of MCAK likely involves interactions with a spectrum of microtubule-associated proteins. These proteins may exert control by modulating the ATPase cycle, affecting MCAK's conformational states, or directly altering its microtubule binding and disassembly actions. This suggests a complex regulatory environment that precisely orchestrates MCAK's role in microtubule dynamics during critical cellular processes such as mitosis.

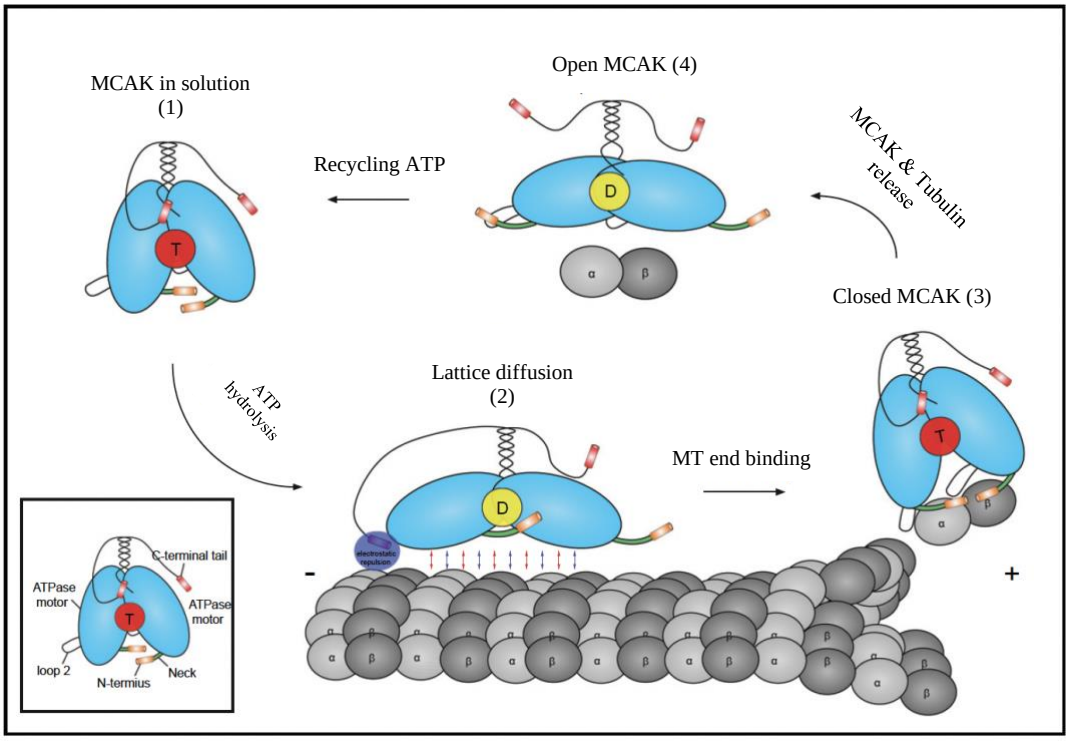

Figure 7. Simplified working model for MCAK's functional cycle

The schematic captures the conformational states of MCAK in its cycle of interaction with microtubules. Initially, MCAK adopts a compact structure as its C-terminal (CT) tail folds upon the motor domains (State 1). Binding to microtubules, potentially facilitated by Plk1-mediated phosphorylation, induces a structural shift to an extended 'open' configuration, allowing for MCAK's movement along the microtubule (State 2). The CT tail's repositioning, driven by electrostatic repulsion with tubulin's E-hook, aids in MCAK's progression to the microtubule ends. At the microtubule terminus, a specific interaction with tubulin dimers via MCAK's KVD motif triggers the depolymerization activity (State 3). Subsequent ATP hydrolysis results in the release of a tubulin dimer and reverts MCAK to its extended state, ready for another cycle (State 4). The design of the working model is adapted from Ritter et al., 2015.

In summary, the functional intricacies and the structural diversity of MCAK highlight its vital role in controlling microtubule dynamics, indicating that it is a key regulator of cellular division processes. The elucidation of these complex regulatory mechanisms, including the potential influence of microtubule-associated proteins, remains a significant area of research within cell biology.

1.5.2. GTSE1

In the realm of mitotic regulation, *G2 and S-phase expressed 1 (GTSE1)* emerges as a protein of paramount importance, constituting the central focus of this Ph.D. endeavor. Recognized for its overexpression in various tumors, GTSE1's correlation with metastasis and tumor grade underscores its potential significance as a regulatory hub in cellular dynamics (Scolz et al., 2012).

GTSE1's multifaceted nature unfolds during the cell cycle, where it exhibits distinct roles in interphase and mitosis. As an intrinsically disordered protein exclusive to vertebrates, GTSE1 dynamically interacts with microtubules (MTs) in a manner that aligns with the cellular context. Notably, during interphase, GTSE1 orchestrates its presence at the growing MT ends through interactions with EB1 via SxIP motifs. This MT tip tracking activity, crucial for cell migration, complements GTSE1's direct interaction with the MT lattice independently of EB1 (Jiang et al., 2012; Scolz et al., 2012).

Mitosis marks a peak in GTSE1 expression and its hyperphosphorylation, suggesting a distinctive role during this phase. Intriguingly, GTSE1's MT lattice binding and plus-end tracking cease at the prophase-to-prometaphase transition, resuming at anaphase onset. This shift is intricately tied to the regulatory influence of Cyclin-dependent kinase 1 (Cdk1), as GTSE1-MT association is abolished in a Cdk1-dependent manner during mitosis, while GTSE1 persists in its association with the mitotic spindle and spindle poles (Rondelet et al., 2020; Scolz et al., 2012).

Recent studies shed light on the orchestration of GTSE1's mitotic localization through the *TACC3-Ch-Tog-Clathrin* complex. This complex, involving microtubule-stabilizing proteins TACC3 and Clathrin assembly lymphoid myeloid leukemia (Ch-Tog), alongside Clathrin, contributes to spindle stability and K-fiber formation. The interdependence of TACC3, Clathrin, and GTSE1 in spindle localization underscores the intricacies of their collaborative actions during mitosis (L. P. Cheeseman et al., 2013; Hubner et al., 2010; Nixon et al., 2015).

The five conserved clathrin-binding motifs within GTSE1's C-terminal region further substantiate its involvement in the TACC3-Ch-Tog-Clathrin complex. Our recent findings illuminate the direct interaction between GTSE1 and Clathrin, with GTSE1's spindle recruitment hinging on its integration into this complex. Perturbations, such as TACC3 or Clathrin depletion, not only disrupt GTSE1 localization but also contribute to delays in chromosome alignment and significant microtubule destabilization during mitosis (Rondelet et al., 2020).

A central aspect of GTSE1's role in mitosis, as delineated by Bendre et al., 2016 (Bendre et al., 2016), is its regulatory impact on MCAK, a potent microtubule depolymerase. GTSE1 tunes microtubule stability for chromosome alignment and segregation by inhibiting the microtubule depolymerase MCAK. This regulation is crucial for maintaining the balance between microtubule stability and dynamics necessary for accurate chromosome alignment and segregation. The study revealed that depletion of GTSE1 leads to heightened MCAK activity, resulting in microtubule instability and defects in spindle positioning and chromosome alignment. Interestingly, this destabilization, while detrimental to some aspects of cell division, may also enhance the correction of improper microtubule-kinetochore attachments, reducing chromosome segregation errors in certain cancer cell lines.

Moreover, the study provides a insights GTSE1's role in mediating chromosome stability through its inhibition of MCAK.

Despite these compelling insights, the exact functional nuances of GTSE1 during mitosis remain enigmatic, urging further investigations to unravel the intricacies of its contributions to cellular dynamics. The fine-tuning of microtubule dynamics by GTSE1 is posited as a potential target for cancer therapies aimed at modulating microtubule behaviour. The elucidation of GTSE1's influence on MCAK highlights a novel regulatory pathway that cells may exploit to achieve the precise balance of microtubule stability required for chromosome alignment and segregation, offering new insights into the mechanisms underlying chromosomal stability in the context of mitosis and cancer. The integrated findings presented here provide a foundation for understanding GTSE1's multifaceted role, paving the way for deeper explorations into its regulatory mechanisms and potential therapeutic implications.

1.6 Aim of this study

The overarching goal of this Ph.D. thesis is to deepen our understanding of the intricate molecular interplay between GTSE1 and Mitotic Centromere-Associated Kinesin (MCAK), elucidating their roles in mitotic regulation. The study builds upon previously identified facts surrounding GTSE1, a protein known for its impact on microtubule (MT) stability during mitosis.

The first objective of the study delved into the necessity of Aurora kinase phosphorylation of GTSE1 for its interaction with MCAK. Recognizing the intrinsically disordered nature of GTSE1, the study sought to understand how phosphorylation during mitosis enhances its binding affinity to MCAK, differentiating it from the G2/S phase. This was pivotal in identifying the phosphorylation-dependent nature of the GTSE1-MCAK interaction.

Subsequently, the study aimed to pinpoint the specific regions within GTSE1 and MCAK that are critical for their interaction. By narrowing down the interacting domains to the N-termini of both proteins, the research shed light on the molecular basis for their binding. This not only contributed structural insights but also suggested functional implications regarding GTSE1's potential modulation of MCAK's activity at microtubule ends and kinetochores.

A key aspect of the research was to ascertain the role of specific phosphorylation sites on GTSE1 in its interaction with MCAK. Emphasis was placed on the phosphorylation of a singular residue, Threonine 165, by Aurora kinases. This residue emerged as a critical determinant for the interaction, underpinning the precise control mechanisms that govern the GTSE1-MCAK interplay. The role of Aurora kinases in this phosphorylation process, particularly Aurora B, was carefully examined to discern its specific contributions to the regulation of GTSE1-MCAK interactions within the cellular milieu.

The study also ventured into the realm of *in vivo* analysis by expressing a GTSE1 variant, harbouring a mutation at the Threonine 165 site, within cells. This approach facilitated the examination of GTSE1-MCAK interactions within a living cellular context, offering insights

into the potential redundancy and alternative phosphorylation mechanisms that might preserve this interaction even when the primary phosphorylation site is mutated.

In addition to in vitro studies, the research addressed the broader implications of GTSE1-MCAK interactions in the regulation of mitotic spindle dynamics and chromosome alignment. The intent was to connect the dots between the molecular interactions and the larger picture of chromosome segregation fidelity during cell division.

Lastly, the study sought to move beyond the interaction of GTSE1 with the microtubule lattice, aiming to dissect the direct influence of phosphorylated GTSE1 on MCAK's activity. This involved an intricate investigation into how GTSE1, particularly when phosphorylated, could regulate MCAK’s depolymerization activity independent of its ability to bind microtubules. By differentiating the effects of GTSE1 on MCAK's ATPase and depolymerization activities, this objective was designed to reveal new dimensions of GTSE1's regulatory roles and suggest potential avenues for therapeutic intervention targeting the GTSE1-MCAK axis.

Collectively, these objectives aimed to provide a comprehensive picture of the role of GTSE1 in the regulation of MCAK, with the potential to uncover novel therapeutic targets for the regulation of mitosis and, by extension, for the treatment of diseases characterized by mitotic dysregulation, such as cancer.

2. Materials and Methods

2.1 Chemicals and Solutions

Table 1. List of chemicals and solutions

Chemical name	Compositions	Company
Agarose		Carl Roth GmbH, Karlsruhe, Germany
Ammonium persulfate (APS)		Max-Planck-Institute, Dortmund, Germany
Ampicillin sodium salt		GERBU Biotechnik GmbH; Heidelberg; Germany
Blasticidine		Invitrogen, California, U.S.A
Bradford Solution		Bio-Rad Laboratories GmbH, Munich, Germany
BRB80 Buffer	80 mM Pipes-KOH pH 6.9 1 mM EGTA 1mM $MgCl_2$ 150 mM KCl	Sigma-Aldrich GmbH, Steinheim, Germany Thermo Fisher Scientific, Waltham, U.S.A J.T Baker Chemicals, Center Valley, USA Avantor Performance Materials (J.T. Baker), Center Valley, U.S.A.

Buffer A	50 mM HEPES pH 7.5	Sigma-Aldrich GmbH, Seelze, Germany
	300 mM NaCl	VWR Chemicals, Darmstadt, Germany
	5% Glycerol	GERBU Biotechnik GmbH, Heidelberg, Germany
	2 mM TCEP	Biosynth AG; Staad; Switzerland
Cell Lysis Buffer	50 mM HEPES pH7.2	Sigma-Aldrich GmbH, Seelze, Germany
	50 mM Na_2HPO_4,	Avantor Performance Materials (J.T. Baker), Center Valley, U.S.A
	150 mM NaCl	VWR Chemicals, Darmstadt, Germany
	10% Glycerol	GERBU Biotechnik GmbH, Heidelberg, Germany
	1% Triton X-100	Thermo Fisher Scientific, Waltham, U.S.A
	1 mM EGTA	Thermo Fisher Scientific, Waltham, U.S.A
	1.5 mM $MgCl_2$	J.T Baker Chemicals, Center Valley, USA

CO_2 Independent Medium		Thermo Fisher Scientific (Gibco), Waltham, U.S.A.
Coomassie Brilliant Blue staining solution	10% Acetic acid 2.5% Coomassie G250	Sigma-Aldrich GmbH, Hamburg, Germany Serva GmbH, Heidelberg, Germany
Destaining solution for ProQ Diamond staining	20% Acetonitrile 50 mM Sodium acetate	Fisher Scientific, UK Sigma-Aldrich GmbH, Steinheim, Germany
Dimethyl sulfoxide (DMSO)		SERVA Electrophoresis GmbH, Heidelberg, Germany
Dithiothreitol (DTT)		SERVA Electrophoresis GmbH, Heidelberg, Germany
DNA Loading Buffer (6x)	0.4% Orange G 30% Glycerol 10 mM Tris-HCl 25 mM Ethylenediaminetetraacetic acid (EDTA)	Sigma Aldrich, Hamburg, Germany GERBU Biotechnik GmbH, Heidelberg, Germany Carl Roth, Karlsruhe, Germany GERBU Biotechnik GmbH, Heidelberg, Germany
Dulbecco's Modified Eagle's Medium (DMEM)		PAN Biotech, Aidenbach, Germany
Dynabeads Protein G magnetic beads		Invitrogen GmbH, Karlsruhe, Germany
Dynein Lysis Buffer	50 mM HEPES pH7.2	Sigma-Aldrich GmbH, Seelze,

		Germany
	150 mM NaCl	VWR Chemicals, Darmstadt, Germany
	5% glycerol	GERBU Biotechnik GmbH, Heidelberg, Germany
	1% Triton X-100	Thermo Fisher Scientific, Waltham, U.S.A
ECL prime Western blotting detection reagent		GE Healthcare, Freiburg, Germany
Effectene transfection reagent		QIAGEN GmbH, Hilden, Germany
Ethanol		Sigma-Aldrich GmbH, Seelze, Germany
Fetal Bovine Serum		Thermo Fisher Scientific (Gibco), Waltham U.S.A.
Fixing solution for ProQ Diamond staining	50% Methanol	Sigma-Aldrich GmbH, Steinheim, Germany
	10% Acetic acid	Sigma-Aldrich GmbH, Steinheim, Germany
FuGENE® HD Transfection Reagent		Promega GmbH, Mannheim, Germany
GeneRuler 1 kb Plus DNA		Fermentas, Hennigsdorf, Germany
GSH Amintra Glutathione Resin		Amintra, Cambridge, UK
GST-Binding buffer	25 mM HEPES pH 7.5	Sigma-Aldrich GmbH, Seelze, Germany
	300 mM NaCl	VWR Chemicals, Darmstadt, Germany

	1 mM EDTA	GERBU Biotechnik GmbH, Heidelberg, Germany
	5% Glycerol	GERBU Biotechnik GmbH, Heidelberg, Germany
	1% Triton X-100	Thermo Fisher Scientific, Waltham, U.S.A
HEPES		Sigma-Aldrich GmbH, Seelze, Germany
Isopropyl β-D-1-thiogalactopyranosid (IPTG)		Carl Roth, Karlsruhe, Germany
Imidazole		Merck Millipore, Darmstadt, Germany
Kanamycin		GERBU Biotechnik GmbH; Heidelberg; Germany
L-Glutamine		Thermo Fisher Scientific, Waltham, U.S.A.
Laemmli SDS Sample loading buffer (5X)	4% Sodium dodecyl sulfate (SDS)	Sigma-Aldrich GmbH, Steinheim, Germany
	10% Glycerol	GERBU Biotechnik GmbH, Heidelberg, Germany
	1% 2-Beta mercaptoethanol	Thermo Fisher Scientific, Waltham, U.S.A
	0.02% Bromophenol Blue	Sigma Aldrich, Hamburg, Germany
	50 mM Tris-HCl	Carl Roth GmbH, Karlsruhe,

		Germany
Lipofectamine 2000 Reagent		Invitrogen GmbH, Karlsruhe, Germany
Luria-Bertani medium (LB medium)	1% Peptone 0.5% Yeast extract 0.5% NaCl	Sigma Aldrich, Hamburg, Germany GERBU Biotechnik GmbH, Heidelberg, Germany VWR Chemicals, Darmstadt, Germany
Methanol		Sigma-Aldrich GmbH, Steinheim, Germany
Midori Green DNA Stain		Nippon Genetics Europe GmbH, Düren, Germany
Milk powder		Carl Roth, Karlsruhe, Germany
MLN8054		Sigma-Aldrich GmbH, Seelze, Germany
Nickel-NTA-Superose Beads		GE Healthcare, Freiburg, Germany
BioTrace Nitrocellulose Membrane		Pall Life Sciences, Pensacola, Florida, USA
OptiMEM		Invitrogen GmbH, Karlsruhe, Germany
Oligofectamine		Invitrogen GmbH, Karlsruhe, Germany
Paraformaldehyde (PFA, 16%)		Thermo Scientific, Rockford, USA
Penicillin Streptomycin		Serva Electrophoresis GmbH, Heidelberg, Germany

Pelleting Buffer	80mM PIPES pH 6.8 1mM EGTA 1mM $MgCl_2$ 70mM KCl	Sigma-Aldrich GmbH, Steinheim, Germany Thermo Fisher Scientific, Waltham, U.S.A J.T Baker Chemicals, Center Valley, USA Avantor Performance Materials (J.T. Baker), Center Valley, U.S.A.
Phosphate buffered saline (PBS)	137 mM Sodium chloride 2.7 mM Potassium chloride 10 mM Di-Sodium hydrogen phosphate dihydrate 2 mM Potassium dihydrogen-phophate (0.2 g/l)	VWR Chemicals, Darmstadt, Germany J.T.Baker Chemicals, Center Valley, USA Merck Millipore, Darmstadt, Germany AppliChem GmbH, Darmstadt, Germany
Potassium chloride (KCl)		Avantor Performance Materials (J.T. Baker), Center Valley, U.S.A.
Precision Plus Protein unstained standards		Bio-Rad, Munich, Germany
Precision Plus Protein prestained standards		Bio-Rad, Munich, Germany
ProLong® Gold antifade mounting solution with DAPI		Molecular Probes, Life technology

ProQ Diamond Phosphoproetin gel stain		Invitrogen, Molecular probes, Eugene, Oregon, USA
Protease Inhibitor mix (500X)		Serva GmbH, Heidelberg, Germany
Pull-down buffer	25 mM HEPES pH 6.9 150 mM NaCl 1 mM ATP	Sigma-Aldrich GmbH, Seelze, Germany VWR Chemicals, Darmstadt, Germany Sigma-Aldrich GmbH, Steinheim, Germany
Pull-down wash buffer	25 mM HEPES pH 7.0 300 mM NaCl 5% Glycerol 0.1% Triton X-100 1mM TCEP	Sigma-Aldrich GmbH, Seelze, Germany VWR Chemicals, Darmstadt, Germany GERBU Biotechnik GmbH, Heidelberg, Germany Thermo Fisher Scientific, Waltham, U.S.A Biosynth AG; Staad; Switzerland
Sf-900 III medium	25 mM Tris-HCl 200 mM Glycin 3.5 mM SDS	Carl Roth, Karlsruhe, Germany Sigma Aldrich, Hamburg, Germany Carl Roth, Karlsruhe, Germany

Size Exclusion Chromatography (SEC) buffer	20 mM HEPES pH 6.9 150 mM NaCl 5% Glycerol 1mM TCEP 10 µM ATP	Sigma-Aldrich GmbH, Seelze, Germany VWR Chemicals, Darmstadt, Germany GERBU Biotechnik GmbH, Heidelberg, Germany Biosynth AG, Switzerland Sigma-Aldrich GmbH, Steinheim, Germany
Terrific Broth (TB)	1.2% tryptone 2.4% yeast extract 0.5% glycerol	Sigma Aldrich, Hamburg, Germany GERBU Biotechnik GmbH, Heidelberg, Germany GERBU Biotechnik GmbH, Heidelberg, Germa
TCEP		Biosynth AG, Switzerland
Tetramethylethylenediamine (TEMED)		SERVA Electrophoresis GmbH, Heidelberg, Germany
Tertracycline		Sigma-Aldrich GmbH, Steinheim, Germany
Thymidine		Sigma-Aldrich GmbH, Steinheim, Germany
Triton X-100		Thermo Fisher Scientific, Waltham, U.S.A.
Trypsin-EDTA		PAN-Biotech GmbH, Aidenbach, Germany

Tween-20		SERVA Electrophoresis GmbH, Heidelberg, Germany
Wash buffer for pulldowns	20 mM HEPES 500 mM NaCl 5% Glycerol 0.1% Triton X-100 1mM TCEP	Sigma-Aldrich GmbH, Seelze, Germany VWR Chemicals, Darmstadt, Germany GERBU Biotechnik GmbH, Heidelberg, Germany Thermo Fisher Scientific, Waltham, U.S.A Biosynth AG, Switzerland
Western transfer buffer	25 mM Tris 190 mM Glycin 10 % Methanol	Carl Roth, Karlsruhe, Germany Carl Roth, Karlsruhe, Germany Sigma Aldrich, Hamburg, Germany
β-Mercaptoethanol		Serva Electrophoresis GmbH, Heidelberg, Germany

2.2 Instruments and devices

Table 2. List of instruments and devices

Device	Model	Company
-80° freezer	MDF-U5386S	SANYO Electric Co., Ltd.; Moriguchi, Japan
Cell Counter	Countess	Invitrogen GmbH, Karlsruhe, Germany

Cell Counter	Scepter Handheld Automated Cell counter 2.0	Merck Chemicals GmbH; Darmstadt; Germany
Centrifuge	Mini Spin plus	Eppendorf GmbH; Wesseling-Berzdorf; Germany
Centrifuge	5418	Eppendorf GmbH; Hamburg Germany
Centrifuge	5417 R	Eppendorf GmbH; Wesseling-Berzdorf; Germany
Centrifuge	5804 R	Eppendorf GmbH; Wesseling-Berzdorf; Germany
Centrifuge	Avanti J-20 XP	Beckman and Coulter GmbH; Krefeld, Germany
Centrifuge	Allegra J-30 I New	Beckmann and Coulter GmbH; Engelsdorf, Germany
Centrifuge (high speed)	Avanti J-30 I Old	Beckman and Coulter GmbH; Krefeld, Germany
Cryogenic Freezer	MDF-1156-PE Ultra Low Temperature Freezer	Panasonic Biomedical Sales Europe B.V
DNA Electrophoresis Unit	CRHU10, Min-Plus Horizontal	Carl Roth, Karlsruhe, Germany
Electrophoresis power supply	Power SourceTM 300V	VWR International GmbH; Langenfeld; Germany
Flake ice machine	AF 100	Scotsman Ice Systems; Milan; Italy
Fluorescence Microscope	EVOS® FL Imaging System	Life Technologies; Thermo Fisher Scientific, Waltham, U.S.A.
Freezer -20 °C	LGex 3410 MediLine	Liebherr-Elektronik GmbH; Lindau; Deutschland

Freezer -20 °C	LGUex 1500 MediLine	Liebherr-Elektronik GmbH; Lindau; Deutschland
Fridge 4 °C	LKexv 1800	Liebherr-Elektronik GmbH; Lindau; Deutschland
Fridge 4 °C	LKUexv 1610 MediLine	Liebherr-Elektronik GmbH; Lindau; Deutschland
Imaging System	ChemiDoc MP	Bio-Rad Laboratories GmbH, Munich, Germany
Incubator	Heraeus B6030	Thermo Electron LED GmbH; Langenselbold Germany
Incubator CO_2-DH Autoflow	NU-5500	NuAir
ibidi Imaging chamber	15µ-Slide 8 well	iBidi, Martinsried, Germany
ibidi Imaging chamber	µ-Dish 35 mm dish	iBidi, Martinsried, Germany
Incubator shaker	Multitron Standard	Infors HAT AG; Bottmingen; Switzerland
Incubator shaker	Minitron	Infors HAT AG; Bottmingen; Switzerland
Mini Rocker Shaker	MR1	BioSan
PCR cycler	T3000 Thermocylcer	Biometra GmbH; Göttingen; Germany
Photometer	NanoDrop 2000	Thermo Electron LED GmbH; Langenselbold Germany
Photometer	Biophotometer 6131	Eppendorf GmbH; Wesseling-Berzdorf; Germany
SDS Page Electrophoresis Unit	Mini Protean Tetra Cell	Biorad, China
Scale	BL150 S	Sartorius
Scale	PE 3600	Mettler

See-saw rocker	SSL4	Bibby Scientific Limited; Staffordshire; UK

Sonicator	Sonifier 450	Branson Ultraschall- Emerson Technologies GmbH; Dietzenbach; Germany
Sterile bench	Herasafe™ KS	Thermo Electron LED GmbH; Langenselbold Germany
Sterile Bench	NU-437 (Nuaire)	Ibs tecnomara GmbH; Fernwald; Germany
Thermostat-Metal	Techne Dri-Block D13.3	Germany
Thermostat	BT 100	Kleinfeld Labortechnik, Germany
Thermostat	MBT 250	ETG-Ilmenau; Illmenau; Germany
Thermomixer	Thermomixer comfort	Eppendorf GmbH; Wesseling-Berzdorf; Germany
Thermomixer	Thermomixer 5436	Eppendorf GmbH; Wesseling-Berzdorf; Germany
Ultracentrifuge Optimal TL	TL361547	Beckman Coulter
Vortex	Vortex-Genie 2	Scientific Industries, Inc; New York; U.S.A.
Water bath	WNB7	Memmert (Shanghai) Trading Co. Ltd; Shanghai City; China
Waterbath	TW8	Julabo
Western Blot electrophoresis chamber	Mini Protean II ™	Biorad, Italy

2.3. Cloning and Plasmids

Table 3. List of plasmid constructs, vectors and primers

Construct name	Vector	Primers (5'-3')
pFG-GTSE1-FL	pFastBac with GST (pFG)	Fwd – AAAGGATCCGAAGGAGGCGGCGGCCGCG Rev – AAAGAATTCTTAGAACTTGAGGAGTGGGG
pFG-GTSE1 1-460	pFastBacwith GST (pFG)	Fwd – AAAGGATCCGAAGGAGGCGGCGGCCGCG Rev – AAAGAATTCTTATGTCTTGGAATTTAGAC
pFG-GTSE1 381-739	pFastBacwith GST (pFG)	Fwd – AAAGGATCCCTGCGGCCAGCTCTGCCTGC Rev – AAAGAATTCTTAGAACTTGAGGAGTGGG
pFH-MCAK FL	pFastBac with His (pFH)	MCAK Fwd – ACCTGTATTTTCAGGGCGCCATGGGATCCGCCATGGACTCG TCGCTTCAGGCCC MCAK Rev – GACTAGTGAGCTCGTCGACGTAGGCCTTTGAATTCTCACTG GGGCCGTTTCTTGCTGC pFH Vector Fwd- AAGCAGCAAGAAACGGCCCCAGTGAGAATTCAA AGGCCTACGTCGACGAGCTCACTAGTC pFH Vector Rev – GGGCCTGAAGCGACGAGTCCATGGCGGATCCCATGGCGCC CTGAAAATACAGGT
GST-GTSE1 1-460	pGEX-6p1	GTSE1 fwd – CCCCTGGGATCCCCGGAATTCCCGGAAGGAGGCGGCGGCCG CGA Vector_Rev – TCGCGGCCGCCGCCTCCTTCCGGGAATTCCGGGGATCCCAG GGG Vector Fwd– CGGCGAGATTCCTGTCTAAATTCCAAGACATAAGTCGACTC GAGCGGCCGCATCG GTSE1 rev – CGATGCGGCCGCTCGAGTCGACTTATGTCTTGGAATTTAGA

		CAGGAATCTCGCCG
GST-GTSE1 463-739	pGEX-6p1	Fwd – GGATCCATGCCTACTCCTACAAATCAA Rev – GTCGACGAACTTGAGGAGTGGGGAA
GST-GTSE1 135-195	pGEX-6p1	Fwd - CCCTGCCCAGCTCTGGTGCCTAAGTCGACTCGAGCGGCCGCATC Rev - CTCCTGTATGAATCTTTCCGGGAATTCCGGGGATCCCAGGGGCC
GTSE1 150-250	pGEX-6p1	GTSE1 fwd – CCCCTGGGATCCCCGGAATTCCCGAAAGAAAAGGAAATGAAGAAA Vector rev - TTTCTTCATTTCCTTTTCTTTCGGGAATTCCGGGGATCCCAGGGG GTSE1 rev – CGATGCGGCCGCTCGAGTCGACTTACCCAGGGATGCTTCTTCCTCTAACAGA Vector fw – TCTGTTAGAGGAAGAAGCATCCCTGGGTAAGTCGACTCGAGCGGCCGCATCG
GTSE1 160-260	pGEX-6p1	GTSE1 fwd – CCCCTGGGATCCCCGGAATTCCCGTCTCTTAAAAGGGAGACATACTA Vector rev - TAGTATGTCTCCCTTTTAAGAGACGGGAATTCCGGGGATCCCAGGGG GTSE1 rev – CACGATGCGGCCGCTCGAGTCGACTTATGGAATCTCTTTCTTGGGCTTCTCCGCA Vector fw - TGCGGAGAAGCCCAAGAAAGAGATTCCATAAGTCGACTCGAGCGGCCGCATCGTG
GTSE1 1-360	pGEX-6p1	GTSE1 Rev – CGATGCGGCCGCTCGAGTCGACTTAAGGAATACTTGCAAATTCACTTGATTTAGCTTTGC

		Vector Fwd – GCAAAGCTAAATCAAGTGAATTTGCAAGTATTCCTTAAGTC GACTCGAGCGGCCGCATCG
GTSE1 1-260	pGEX-6p1	GTSE1 Rev - CGATGCGGCCGCTCGAGTCGACTTATGGAATCTCTTTCTTGG GCTTCTCCGCAGC Vector_Fwd – GCTGCGGAGAAGCCCAAGAAAGAGATTCCATAAGTCGACTC GAGCGGCCGCATCG
GTSE1 1-160	pGEX-6p1	GTSE1 Rev – CGATGCGGCCGCTCGAGTCGACTTAAGACGTGGGGCTTTTC TTCATTTCCTTTTCTTTC Vector_Fwd - GAAAGAAAAGGAAATGAAGAAAAGCCCCACGTCTTAAGTC GACTCGAGCGGCCGCATCG
GTSE1 250-400	pGEX-6p1	GTSE1 Fwd – CCCCTGGGATCCCCGGAATTCCCGGGGGCTGCGGAGAAGCC CAAGAAAG VectorRev – CTTTCTTGGGCTTCTCCGCAGCCCCCGGGAATTCCGGGGATC CCAGGGG GTSE1 Rev – CGATGCGGCCGCTCGAGTCGACTTAGACCCGCTTGGCCTGC CAGGAG VectorFwd - CTCCTGGCAGGCCAAGCGGGTCTAAGTCGACTCGAGCGGCC GCATCG
GTSE1 50-200	pGEX-6p1	GTSE1 Fwd – CCCCTGGGATCCCCGGAATTCCCGGATGATGAAGTCTTCTTC GGACCCTTTGGAC VectorRev – GTCCAAAGGGTCCGAAGAAGACTTCATCATCCGGGAATTCC GGGGATCCCAGGGG GTSE1 Rev – CGATGCGGCCGCTCGAGTCGACTTAGGTGAGGCGGGCCTGG GCAC

		VectorFwd – GTGCCCAGGCCCGCCTCACCTAAGTCGACTCGAGCGGCCGCATCG
GTSE1 380-739	pGEX-6p1	GTSE1 Fwd – CCCCTGGGATCCCCGGAATTCCCGCTGCGGCCAGCTCTGCCTGCAG VectorRev – CTGCAGGCAGAGCTGGCCGCAGCGGGAATTCCGGGGATCCCAGGGG GTSE1 Rev – CGATGCGGCCGCTCGAGTCGACTTAGAACTTGAGGAGTGGGGAATCCACGTTC VectorFwd – GAACGTGGATTCCCCACTCCTCAAGTTCTAAGTCGACTCGAGCGGCCGCATCG

2.3.1. Cloning using restriction enzymes

a. Polymerase Chain Reaction

PCR is a powerful molecular biology technique that allows us to modify genes and clone the gene of interest. The principle of PCR is to generate multiple copies of the gene of interest using a high fidelity DNA polymerase.

In this study three different DNA polymerases namely, Q5 DNA polymerase, Flash Phusion, and Taq polymerase were used depending on their purpose and availability. Q5 polymerase and Flash Phusion polymerase are high fidelity polymerases and were used for error free amplification of genes. Taq polymerase was used for confirming the results after cloning. Following are the standard procedures that were used for PCR amplification.

Table 4. Standard PCR reaction using Q5 polymerase

Component	Volume for 50 µL PCR reaction
Q5 2x Master Mix (contains dNTPs, Polymerase)	25 µL
10 µM Primer Mix	5 µL (2.5 µL Forward + 2.5 µL Reverse)
DNA	~ 10 – 100 ng

ddH_2O	X µL

Table 5. Standard program used for PCR amplification

Step	Temperature	Time	
Denaturation	98 °C	45 s	
	98 °C	10 s	30x
Annealing	52 °C – 65 °C	30 s	
Elongation	72 °C	3 -5 min	
	72 °C	3 – 5 min	
Pause	4 °C	~	

b. Restriction digestion and agarose gel purification

For cloning using restriction digestion enzymes, the amplified insert and vector DNA were digested with 2 Units of respective enzyme, 2X restriction digestion buffer and ddH_2O as per requirement. The restriction digestion was performed overnight at 37 °C and agarose gel electrophoresis was used to confirm the size of the digested insert and vector. The principle of agarose gel electrophoresis is to separate DNA fragments according to their size. Agarose gels were prepared by dissolving 0.8 or 1% agarose in 1X TAE buffer and 1:25000 Midori Green DNA stain was added to this solution. GeneRuler 1 kb plus DNA ladder was used as a reference for dsDNA molecular weight. Samples were prepared by adding 1/10 volume of Orange G DNA loading dye. Electrophoresis was performed in 1X TAE buffer for 20 min at 120 V. The insert and vector were purified using QIAgen gel extraction kit according to instructions mentioned in the user manual.

Table 6. List of restriction digestion enzymes used for cloning

Restriction enzyme	Company
*Dpn*I	New England Bio Labs Inc., New England, U.S.A.
High Fidelity *EcoR*I	New England Bio Labs Inc., New England,

	U.S.A.
High Fidelity *BamH*I	New England Bio Labs Inc., New England, U.S.A.
Sal1	New England Bio Labs Inc., New England, U.S.A.

GST tagged GTSE1 FL,GTSE1 1-460 and GTSE1 463-739 constructs were generated by cloning these constructs in pGEX-6p1 bacterial expression vector using *BamH1* and *Sal1* restriction enzymes. For expression of GST tagged GTSE1 in insect cells, *GTSE1-FL, GTSE1 1-460* and *GTSE1 381- 739* were cloned into pMultiBAC vector (pFG) using *BamH1* and *EcoR1* restriction enzymes.Myc-tagged *MCAK-FL, MCAK 1-181, MCAK 1-231, MCAK 182-583, MCAK 232-583* and *MCAK 584-725* were cloned in pcDNA4/TO/mycHisA mammalian expression vector using *BamH1* and *EcoR1* restriction enzymes.

c. Ligation

The appropriately digested insert and vector were recombined using T4 DNA ligase. Ligation was performed for 6-7 h at room temperature using the following scheme:

Table 7. Standard scheme used for ligation

Component	Volume for 10 □L ligation reaction
Vector:Insert	1:3
T4 DNA Ligase	2 µL
T4 Ligase Buffer	2 µL
ddH_2O	X µL

d. Transformation

Recombinant DNA was transformed into competent *E.coli* bacterial cells using heat shock method. Bacterial cells were incubated with recombinant DNA for 30 min on ice followed by incubation at 42^0C for 50 sec and then immediately transferred on ice for 5 min. These cells

were then supplemented with fresh LB medium and incubated at 37^0C for 1 h before plating on LB agar plates containing the appropriate antibiotic.

Table 8. List of competent *Escherichia coli (E.coli)* cells used for transformation

Bacteria	Strain	Company
E. coli	Rosetta 2(DE3)	Max-Planck Institute, DPF, Dortmund, Germany.
E. coli	OmniMax (chemically competent cells)	Max-Planck Institute, DPF, Dortmund, Germany.
E. coli	Top10 (chemically competent cells)	Thermo Fisher Scientific (Gibco), Waltham, USA
E. coli	Max Efficiency DH10Bac™ Chemically competent cells (EMBACY)	Thermo Fisher Scientific (Gibco), Waltham, USA

2.3.2. Site-directed mutagenesis

Mutations were generated by site-direct mutagenesis using Q5 2X Master Mix. Wild-type plasmids were used as templates for DNA amplification. The PCR products were digested by DpnI for 2 hour and then performed transformation.

Table 9. List of mutants, vectors and primers

Construct name	Original template	Primers (5'-3')
GTSE1 T165A	pGEX-6p-1 GTSE1 1-460	Fwd - GCATACTACCTGTCAGACAGCCCCTTGCT Rev - TCTGACAGGTAGTATGCCTCCCTTTTAAG
GTSE1 S186A,S187A,S192A S193A	pGEX-6p-1 GTSE1 1-460	Fwd - GCCGCCCCGGCCCTGCCCGCCGCTGGTGCCCAGGCCCGCC Rev - AGCGGCGGGCAGGGCCGGGGCGGCGGCCAAGAGCCGAGG

GTSE1 T200A	pGEX-6p-1 GTSE1 1-460	Fwd - GCCCGGGCGCCGGGGCCTCCGCACTCTGCT Rev - CGGCGCCCGGGCGAGGCGGGCCTGGGCACC
GTSE1 S208A	pGEX-6p-1 GTSE1 1-460	Fwd - CCGCACGCTGCTCATGCTTTGCCCAGGGAA Rev - CAAAGCATGAGCAGCGTGCGGAGGCCCCGG
GTSE1 S216A,T218A,S223A	pGEX-6p-1 GTSE1 1-460	Fwd - GCATGCGCTGCTCATGCTGCAGCTCAGGCAGCGACTCAGA Rev - AGCTGCAGCATGAGCAGCGCATGCTTCCCTGGGCAAAGCA
GTSE1 S247A	pGEX-6p-1 GTSE1 1-460	Fwd - GCCATCCCTGGGGCTGCGGAGAAGCCCAAG Rev - GGCTCTTCCTCTAACAGAGGCCGCTCGAGG

2.3.3. Gibson Assembly

Gibson assembly is a technique used to seamlessly clone several genes in a vector (Gibson et al., 2009). It is a one step *in vitro* recombination that uses a combination of a 5' exonuclease, a DNA polymerase, and a DNA ligase. The 5' exonuclease creates 3' overhangs that are repaired by a DNA polymerase and a DNA ligase catalyzes the formation of phosphodiester bonds and ligates the DNA. The insert and vector both were PCR amplified using respective primer pairs and purified using agarose gel extraction. A mixture of vector and insert with a ratio of 1:3 respectively (100ng total DNA concentration) was mixed with the Gibson master mix and incubated at 50^0C for 1 h. Bacterial cells were transformed using 10 µL of this Gibson assembly reaction mix.

2.3.4. Plasmid extraction

Plasmids were extracted using the following kits according to manufacturer's protocol.

Table 10. List of kits used for plasmid/BAC extraction

Kit Name	Company
Zymoclean Gel DNA Recovery Kit	Zymo Research Corporation, Irvine, U.S.A.
GeneJET Plasmid Miniprep Kit	Thermo Scientific, Baltics, U.S.A
QiaQuick PCR Purification Kit	Qiagen, Hilden, Germany

Wizard SV Gel and PCR Clean-up system	Qiagen, Hilden, Germany

2.3.5. Preparation of bacterial glycerol stocks

Glycerol stocks of the bacterial cells containing recombinant DNA were prepared by mixing 400 µL of bacterial cell culture with 600 µL of 50% sterile glycerol. The mixture was frozen at -80^{0}C.

2.4. Cell culture and cell lines

All cell lines were grown in DMEM media containing 10% fetal bovine serum, 2 mM L-Glutamine, 100U/mL Penicillin and 0.1mg/mL streptomycin (PAN Biotech) at 37^{0}C in 5% CO_2.

Table 11. List of mammalian cell lines

Cell line	Species	Antibiotic resistance	Transgene	Cell line number
U2OS wt	Human	-	-	A00002
U2OS GTSE1-GFP siR3 212	Human	G418 (200 µg/µL)	GTSE1-LAP harboring resistance to RNAi #3	A00252

U2OS cells stably expressing RNAi-resistant GTSE1 wild-type transgenes were described previously (Scolz et al., 2012). HCT116 p53$^{-/-}$ and U2OS-PA-GFP-tubulin cells were kind gifts from Duane Compton. U2OS cells expressing NFLAP-GTSE1, MCAK-LAP and mH2A.Z-mCherry were generated by transfecting the respective BACs using Effectene transfection reagent according to manufacturer's protocol, and selecting for stable transfectants and were obtained from Antony Hyman. HCT116 and HCT116 p53$^{-/-}$ cells grown in 6 cm dishes were transfected with 1.5 µg of hGTSE1-GFP-T2A-BSD cDNA using5 µL of Lipofectamine 2000 according to manufacturer's protocol. Stable line populations were selected on BSD (4 µg/mL), and individual clones isolated. HCT116 and HCT116 p53$^{-/-}$control clones were isolated after treating the cells with Lipofectamine 2000 in absence of DNA.

2.5. Maintaining mammalian cell stocks

Mammalian cells are stored at -150^{0}C for long-term. Cell grown in 15 cm dishes were harvested by centrifugation at 1500 rpm for 5 min at room temperature. The cell pellet was resuspended in 10 mL freezing media (90% FBS an 10% DMSO) and distributed in cryo- vials and frozen in cryo-freezers for 2 days at -80^{0}C and then transferred to -150^{0}C.

Approximately 35,000-40,000 cells were added to prewarmed media in 24-well plates or 8-well imaging chambers. Transfection complexes containing 2.5 µL oligofectamine and siRNA were prepared and incubated at room temperature for 20 min and added immediately afterwards to the cells. Media was changed after 6–8 h. All experiments were performed 48 hours after siRNA transfection.

2.6. Antibodies

Table 12. List of primary and secondary antibodies

Primary antibody	Directed to	Made in	Dilution		Clone number and Company
			WB	IF	
DM1α (anti-alpha tubulin)	Human	Mouse Monoclonal	1:10,000	1:400	Sigma Aldrich
Anti-GTSE1 3753	Human	Rabbit	1:30,000	1:1000	MPI CBG, Dresden (Scolz et al., 2012)
Anti-CREST (human nuclear antibodies to nuclear antigens–centromere autoantibody)	Human	Human	-	1:500	CS1058; Europa Bioproducts Ltd.
Anti-EGFP	Human	Goat	1:10,000	1:5000	MPI CBG, Dresden (Poser et al., 2008)
Anti-MCAK	Human	Mouse	1:800	1.50	Clone 1G2; Abnova Corporation

Anti-CEP135	Human	Rabbit	-	1:5000	MPI CBG, Dresden (Bird and Hyman, 2008)
Anti-End Binding Protein 1 (EB1)	Human	Rat			Absea Biotechnology, Clone KT-51
Anti-alpha tubulin	Human	Rat		1:500	Santa Cruz Biotechnlogy, YL1/2
Anti-Aurora B	Human	Rabbit	1:1000	1:1000	Abcam #2254
Texas Red (594) dye-conjugated AffinityPure	Mouse	Donkey	-	1:500	Jackson ImmunoResearch Europe Ltd., UK
Texas Red (594) dye-conjugated AffinityPure	Rabbit	Donkey		1:500	Bethyl Laboratories, Inc. Montgomery, USA
Texas Red (594) dye-conjugated AffinityPure	Rat	Donkey		1:500	Bethyl Laboratories, Inc. Montgomery, USA
Texas Red (594) dye-conjugated AffinityPure	Human	Donkey		1:500	Jackson ImmunoResearch Laboratories
Alexa 488-conjugated AffinityPure	Mouse	Donkey		1:500	Bethyl Laboratories, Inc. Montgomery, USA
Alexa 488-conjugated AffinityPure	Rabbit	Donkey	-	1:500	Bethyl Laboratories, Inc. Montgomery, USA
Alexa 488-conjugated AffinityPure	Rat	Donkey		1:500	Bethyl Laboratories, Inc. Montgomery, USA

Cy5-conjugated AffinityPure	Human	Donkey		1:500	Jackson ImmunoResearch Laboratories
HRP-conjugated	Mouse	Goat	1:5000	-	GE/Amersham
HRP-conjugated	Rabbit	Donkey	1:5000	-	GE/Amersham
HRP-conjugated	Goat	Donkey	1:5000	-	GE/Amersham

2.7. Immunofluorescence

2.7.1. Fixing using Methanol

Cells on coverslips were fixed using −20 °C methanol for 10 min and then blocked with 0.2% fish skin gelatin (FSG) in PBS for 15 min. Cells were incubated with primary antibodies in 0.2% FSG in PBS for 1 h at 37 °C in a humidified chamber. They were then washed for 30 min with 0.2% FSG, and the same process was repeated with secondary antibodies. Coverslips were mounted with ProLong gold containing DAPI.

2.7.2. Fixing using Paraformaldehyde (PFA)

Cells grown on coverslips were washed once with PBS and then incubated with PFA for 10 min at room temperature. Cells were washed three times with PBS and then incubated with 0.1% Triton X-100 for 5 min followed by washing with PBS. The cells were then stained using the same procedure as mentioned above.

2.7.3. Microscopy and live cell imaging

Images used for quantifying chromosomal misalignment and lagging chromosomes in metaphase were acquired using the 60 /1.4 NA Plan-Apochromat Oil Objective (Zeiss) on the DeltaVision Imaging System (GE Healthcare) equipped with an sCMOS camera (PCO edge 5.5). Serial Zstacks of 0.25 µm thickness were acquired and then deconvolved using SoftWoRx 6.1.1 software. All other images for quantifying inner spindle intensity, microtubule lengths in prometaphase, spindle length and spindle tilt were taken using the 3i Marianas™ spinning disk confocal system (Intelligent Imaging Innovations Inc.) equipped with Axio Observer Z1 microscope (Zeiss), Plan-Apochromat 60 /1.4 NA Oil Objective, M27 with DIC III Prism (Zeiss), Orca Flash 4.0 sCMOS Camera (Hamamatsu Photonics) and controlled by Slidebook Software 6.0 (Intelligent Imaging Innovations Inc.). For live cell imaging, media was changed to CO2 independent media (Gibco) 12 h prior to imaging. Live cell image sequences were

acquired at 1 min intervals for 12 h in 2 µm serial Z sections using a 40x 1.42 NA UPlanFL-N objective (Olympus) at 37 °C.

2.7.4. Image quantification and data analysis

Image quantification was performed on unmodified 16-bit z-series images using Fiji and Imaris 7.6.4 32-bit software (Bitplane). On Imaris, all images were opened and analysed in the 'Surpass' mode in the software.

2.8. Immunoprecipitation

Cells were arrested in prometaphase using 10 µMS-trityl-L-Cysteine (STLC; Sigma Aldrich) for 16 hours and collected using mitotic shake off. They were then pelleted down by centrifuging at 1000 rpm for 5 min and then washed with PBS supplemented with 10 µM MG-132 (Calbiochem). After centrifugation, the cells were resuspended in complete DMEM medium supplemented with 10 µM MG-132 and incubated in an incubator maintained at 37^0C and 5% CO2 for 90 min to allow the cells to reach metaphase. Mitotic cells were harvested using mitotic shake-off and lysed using cell lysis buffer followed by centrifugation at 13,000 rpm for 10 min at 4^0C in order to clear the lysate. A part of the supernatant (100 uL) was taken as "input" and 1-2 ug of the indicated antibody was added to the remaining supernatant and incubated for 2 h at 4^0C with rotation. Dynabeads coupled to protein G wereadded to the extracts and incubated for 4 h at 4^0C. The beads were washed three times with1 mL of cell lysis buffer each and once with 1X PBS and then resuspended in hot Laemmli buffer to be analyzed by Western blotting. To study the interdependence of GTSE1-MCAK interaction on phosphorylation the cell lysates were treated with either a phosphatase inhibitor (PPI) to prevent removal of any phosphorylation or with λ-phosphatase to obtain theabove proteins in the dephosphorylated state.

2.9. RNA interference

The use of dsRNA for 'genetic interference' is now one of the most popular methods for physiological gene silencing. It relies on the formation of a DICER silencing complex between a short oligonucleotide sequence and the mRNA of the protein it targets followed by subsequent cleavage and degradation of the mRNA by the silencing complex.

For depleting endogenous GTSE1, U2OS cells, reverse transfection using 80 nM of silencer RNA (siRNA) for GTSE1 was performed using Oligofectamine (Invitrogen). Briefly, transfection complexes consisting of siRNA and Oligofectamine was prepared by mixing 2.5 µL Oligofectamine with siRNA in OptiMEM (Invitrogen) at room temperature for 20 min. This was added to roughly 35,000-40,000 cells in prewarmed medium in 24-well plates (Sarstedt) containing glass coverslips or 8-well imaging chambers (ibidi), and the volume made up to 500 µL. The cells were left in the humidified incubator at 37 ◦C for 8 hours after which the media was replaced. All experiments were performed 48 hours after transfection. Table 11 shows the details of siRNA oligonucleotides used in this study.

Table 13. Sequences of silencer RNA (siRNA)

Name	Sequence	Working concentration	Company
GTSE1	5‖-GAUUCAUACAGGAGUCAAA-3‖	80 nM	Ambion
MCAK	5‖-GAUCCAACGCAGUAAUGGU-3‖	12 nM	Ambion
Kif2A #2	5’-CUACACAACUUGAAGCUAU-3’	50 nM	Sigma-Aldrich
Silencer	-		Ambion

2.10. Sodium dodecyl sulfate (SDS) electrophoresis

SDS electrophoresis separates proteins according to their molecular weights. Proteins are denatured using Laemmli buffer, which contains a negatively charged detergent SDS that coats the polypeptide chains. Due to this the proteins obtain a net negative charge. These negatively charged proteins move with different speeds towards the anode. The speed at which they move depends on the molecular weight of proteins and the percentage of acrylamide in the gel. Smaller proteins move faster through the pores towards the anode, whereas, the motion of larger proteins is retarded due tothe small pore size of the acrylamide gel. SDS PAGE gels were run using SDS-PAGErunning buffer at 100-120 V for 1.5-2 h.

2.11. Coomassie Brilliant Blue Staining

After separating proteins by SDS-PAGE, they were visualized by staining the gel with the protein stain Coomassie Brilliant Blue R-250 (CBB). The staining solution consists of 0.05% (w/v) CBB in an acid-methanol mixture, which fixes the proteins in the gel to prevent it from

being washed out while the gel is staining. The gels were stained with CBB for an hour and then destained by providing repeated washes with water followed by boiling.

2.12. Western blot

Proteins separated on SDS-page gels were further processed for Western blot analysis.Western blotting is employed to detect specific proteins of interest using specific antibodies. Proteins from SDS-PAGE gels were transferred onto nitrocellulose membrane using Western transfer buffer at 300 mA for 3 h at 4^0C. The membrane was blocked with 5 % skimmedmilk in 1X PBS containing 0.1% Tween20 (PBS-T) and incubated with primary antibodies overnight at 4^0C. The membrane was then washed three times for 10 min each using PBS-T followed by incubation with appropriate secondary antibodies for 1 h at room temperature. The membrane was washed three times for 15 min each with PBS-T. Protein signals were detected using enhanced chemiluminescence.

2.13. Purification of proteins

2.13.1. Proteins purification from insect cells

A full-length human GTSE1 cDNA sequence was cloned into pFL- MultiBac vectors, and baculovirus- generated hGTSE1-FL protein was expressed in Tnao38 insect cells at 27°C for 48 h. The cells were harvested by centrifugation at 1,800 rpm for 15 min in a Sorvall RC 3BP Plus centrifuge (Thermo Fisher Scientific). The cell pellet was either stored at −80°C or processed immediately. The cell pellet from 1-liter culture was resuspended in 100 ml ice-cold buffer A (50 mM Hepes, pH 8.0, 300 mM NaCl, 5% glycerol, 2 mM Tris(2-carboxyethyl)phosphine, and protease inhibitors [Serva]) lysed by sonication and clarified by centrifuging at 29,000 rpm for 50 min at 4°C. The cell lysate was incubated with 1 ml glutathione resin (Amintra) for 1 hr at 4°C. The resin beads were loaded on gravity flow columns and washed with 150 ml buffer A at 4°C. hGTSE1 was cleaved from the beads using GST Precision (Max Planck Institute of Molecular Physiology) over- night at 4°C. The protein was eluted and concentrated using Amicon concentrators. The protein was further purified by size exclusion in a Superdex 200 10/300 column (GE Healthcare) using gel filtration buffer (30 mM Hepes, pH 8, 300 mM NaCl, 5% glycerol, and 2 mM Tris(2-carboxyethyl)phosphine). The peak fractions were collected and concentrated in Amicon concentrators. MCAK-His6 was

expressed in Tnao38 cells and purified by a sequence of nickel affinity, and size-exclusion chromatography in Buffer A using same protocol of lysis as above.

2.13.2. Proteins purification from bacteria

Genes of interest were cloned into pGEX-6p-1 or pET28(A)+ vectors and expressed in Rosetta. Bacteria were grown in TB medium until they reached an O.D600 of 0.8 and added 1 mM IPTG overnight at 20 °C for protein expression. The bacterial cells were pelleted by centrifugation at 6000 rpm for 10 min at room temperature. Cells were resuspended in GST binding buffer (25 mM HEPES pH 7.5, 300 mM NaCl, 1 mM EDTA, 5% glycerol, 1% Triton X-100, DNase) with 1 mM PMSF, lysed by sonication and cleared by centrifugation at 30,000 rpm for 30 min at 4 °C. The supernatant after the centrifugation was incubated with Glutathione resin (Amintra) for 4~8 hour at 4 °C. The beads were washed with GST binding buffer and the purified protein was used for experiments.

2.14. In vitro proteins phosphorylation and pull down

Proteins of interest were phosphorylated by Aurora A, Aurora B, Plk1 or Cdk1 using a molar ratio 1:100 (kinase: protein) overnight on ice in the buffer further supplemented with 10 mM MgCl2, 1 mM sodium orthovanadate and 2 mM ATP. For the pulldown, 3 μM of the prey (phosphorylated or unphosphorylated protein) was mixed with 1 μM of the GST-tagged protein or the 'bait' and 5 μL of GSH beads in a total volume of 25 μL of the kinase buffer (20 mM HEPES pH 7.8, 150 mM NaCl, 5% (v/v) glycerol). A sample (25%) was taken out as input before incubating the protein mixture on ice for 1 hour for the pulldown. Following this, the beads were washed thrice with 250 μL of wash buffer (20 mM HEPES pH 7.0, 500 mM NaCl, 5% (v/v) glycerol, 0.1% (v/v) Triton X-100, 1 mM TCEP)at 1900 rpm for 3 min at 4 ◦C and then denatured by adding 20 μL 1× SDS-loading buffer before loading the samples on SDS gels.

2.15. Phosphorylation of GTSE1

GST-GTSE1- (FL, 1-460, 381-739, 1-160, 1-260, 50-200, 250-400), GTSE1-FL, GST-GTSE1-T165A and GST-GTSE1 135-195 purified from bacterial and/or insect cells were phosphorylated by kineses like Aurora A, Aurora B, Cdk1 or Plk1 as per experimental

requirements. The phosphorylation was done using a 1:80 (kinase: protein) ratio overnight on ice in pull-down buffer further supplemented with 10 mM $MgCl_2$ and 2 mM ATP. The phosphorylation reaction was stopped by adding 5 uM RO-3306 (Cdk1 inhibitor), 500 nM MLN8054 (Aurora A inhibitor), 500nM ZM447439 (Aurora B inhibitor) for 10 min on ice. The proteins were then either used for GST pull-down or for gel filtration.

2.16. ProQ Diamond staining

Phosphorylation of GTSE1 was confirmed using ProQ diamond staining. Equimolar concentrations (2 μM) of all proteins phosphorylated and unphosphorylated were resolved on a SDS PAGE gel. The gels were incubated with fixing solution overnight following which they were washed three times with water to remove all traces of fixing solution. Next the gelswere incubated with ProQ Diamond phospho-specific stain for 90 min with shaking in dark. Gels were destained thrice for 30 min each with destaining solution followed by washingwith water for 10 min thrice. All the steps were performed at room temperature. The signalfor ProQ was detected using the BioRad developer. The gel was then stained with Coomassie brilliant blue (CBB) to confirm equal protein loading.

2.17. GST-Pull-down experiments

In vitro GST pull-downs were performed by incubating 3μM of the 'prey' (phosphorylated or unphosphorylated protein) with 1μM of GST tagged protein or the 'bait' and 10μL of GSH beads in a total volume of 40μL of pull down buffer. A sample (25%) was taken out as input before incubating the protein mixture on ice for 1 hour for the pulldown. Following this, the beads were washed thrice with 250μL of pulldown wash buffer at 1900 rpm for 3 min at 4^0C and then denatured by adding 10μL 5x SDS-loading buffer before loading the samples on SDS gels.

2.18. Cross-linking Mass Spectrometry (MS)

MS for identification of interaction regions of GTSE1 and MCAK and phosphorylation status of GTSE1 T165 wa sperformed by Dr. Tanja Bange. GST-GTSE1 1-460 was phosphorylated by Aurora A and the phosphorylated protein was incubated along with MCAK for 1 hour at room temperature for binding to occur.

2.19. Microtubule Cosedimentation Assay

GMPCPP stabilized MTs were prepared by incubating 20μM MTs in BRB80 buffer with 1 mM GMPCPP at 37^0C for 30 min. For the experiment, 1μM MTs were mixed with 500nM protein (unphosphorylated or phosphorylated) and the volume made up to 40μL with pelleting buffer. The MT:protein mixture was incubated at room temperature for 1 hour followed by carefully layering it over 100μL cushion buffer (BRB80 buffer supplemented with 60% (v/v) glycerol) in ultracentrifuge tubes. The ultracentrifuge tubves were centrifuged at 90000 rpm for 10 min at 25^0C in a TLA-120.1 rotor. Of the supernatant, 36μL consisting of unpolymerized tubulin was collected in a tube and boiled after addition of 9μL of 5x SDS-loading buffer to it. The leftover solution was discarded and the pellet was boiled in 45μL 1x SDS-loading buffer. The supernatant and pellet fractions were separated by SDS-PAGE and stained with CBB for analysis.

2.20. ATP/NADH coupled assay for MCAK ATPase activity measurement

The required concentration of MCAK or GTSE1 or both are added to make a total 100 μl volume along with the ATPase reaction buffer (25 mM Hepes pH 7.5, 150 mM NaCl, 2.5% glycerol, 10 mM BME and 1 mM MgCl2.) supplemented with 1mM ATP and a regeneration system (3 mM PEP, 20 U/ml PK), 20 U/ml LDH and NADH to give an A340 of 0.5-2.0. Absorbance data are collected using a microplate spectrophotometer. The rate of ATP hydrolysis is calculated from the equation:

$$ATPase\ rate\ [min^{-1}] = -\frac{dA_{340}}{dt}\left[\frac{OD}{min}\right] \times K_{path}^{-1} \times\ moles^{-1}\ ATPase\ dt$$

where K_{path} is the molar absorption coefficient for NADH for a given optical path length.

2.21. Total internal reflection fluorescence microscopy assays for microtubule dynamics and MCAK activity

2.21.1. Tubulin preparation

Tubulin purification was performed according to a standard method (Gavriljuk et al, 2021). Pig brains were lysed in depolymerization Buffer (50 mM MES pH 6.6, 1 mM CaCl2) in the ratio

of 1.5 buffer/brain (l/kg). The lysate was centrifuged for 60 min (4 °C) at 28,000 × g in SLA-1500 (Sorvall/Thermo Fisher Scientific). The supernatant was collected, supplemented with: PIPES, ATP and GTP to the final concentration of 333, 1.5, and 0.50 mM, respectively, and incubated for 60 min at 37 °C. The polymerized supernatant was centrifuged for 30 min (37 °C) at 200,000 × g in Type 45 TI (Beckman Coulter, Krefeld, Germany). The pellets were resuspended in depolymerization Buffer on ice. The depolymerized solution was centrifuged for 20 min (4 °C) at 140,000 × g in Type 45 TI (Beckman Coulter, Krefeld, Germany). After repeating polymerization and depolymerization steps, purified tubulin concentration was adjusted to the of 200 μM with BRB80 (80 mM PIPES pH 6.8, 1 mM MgCl2, 1 mM EGTA) and stored at −150 °C after flash freezing in liquid nitrogen.

2.21.2. Tubulin labelling

Tubulin was labelled with NHS-Alexa568, −488 or −647 (Thermo Fisher Scientific) or EZ-link NHS-biotin (Thermo Fisher Scientific) according to a standard procedure (Hyman et al, 1991). Typically, 50 mg of tubulin were labelled with a 7.5-fold molar excess of dye assuming 70% tubulin recovery after the initial polymerization step. Following deviations from the published procedure were made: the dye was added in two steps, each followed by a 15 min incubation, totaling 40 μl DMSO in 1 ml buffer. The reaction was not specifically stopped, and all ultracentrifugation steps were performed at an increased speed of 400,000 Å~ g in an MLA-80 rotor (Beckman Coulter, Krefeld, Germany). Labelled tubulin was adjusted to 200 μM with BRB80 and stored at −150 °C.

2.21.3. Total Internal Reflection Fluorescence

Glass slides and coverslips functionalised with biotin were used to create microfluidic flow chambers, as per the established protocols on TIRF (Gell al, 2010, Beiling et al, 2009, Methods in Cell Biology). Tubulin purified from porcine brains were labelled independently with Alexa fluor 568 NHS dye and biotin respectively. A mix of labelled and unlabelled tubulin along with biotin tubulin was polymerised using non-hydrolysable GTP analogue GMPCPP to generate non-dynamic stable MT seeds. These stabilized seeds, in turn made to adhere into neutravidin coated flow chambers, were used as a base to polymerize a mix of labelled and unlabelled free tubulin (15uM or 12uM) to generate fluorescently visualizable dynamic MTs.

2.22. Microtubule Depolymerisation asaay

Microtubules were polymerized by incubating tubulin with GMPCPP at a concentration of 1 mM at 37°C for 30 minutes to create stabilized MTs. This initial polymerization step allowed for the microtubules to form and elongate. Following stabilization, the reaction mixture was prepared by adding 2 μM tubulin to a buffered solution containing MCAK at a final concentration of 200 nM. To this, varying concentrations of GTSE1 were introduced. The buffer used for the reaction was BRB80, a common microtubule-stabilizing buffer composed of 80 mM PIPES at pH 6.8, 1 mM EGTA, and 1 mM MgCl2. This was supplemented with 70 mM KCl and 1.5 mM ATP to provide the necessary ionic strength and energy source for enzymatic activities. Additionally, 10 μM taxol was included to maintain microtubule stability throughout the assay. The reaction mixture was then incubated at room temperature for 60 minutes to allow sufficient time for the interactions between MCAK, GTSE1, and the microtubules to occur. After incubation, the mixture was carefully layered onto a glycerol cushion buffer consisting of 80 mM PIPES, 1 mM EGTA, 1 mM MgCl2, and 50% glycerol to facilitate separation of bound from unbound proteins. Centrifugation was carried out at a high speed of 90,000 rpm for 10 minutes at a controlled temperature of 25°C using a TLA-120.1 rotor. This step enabled the sedimentation of the microtubules along with any proteins that were bound to them, resulting in two distinct fractions: the supernatant containing unbound proteins and the pellet comprising the microtubules and any associated proteins. To analyze the composition of these fractions, SDS-PAGE was performed. The separated proteins were then visualized by staining with Coomassie Brilliant Blue, which binds to the protein molecules and provides a colorimetric method for detection. The intensity of the staining correlates with the amount of protein present, allowing for qualitative and quantitative assessments of the protein interactions in the assay.

3. Results

3.1 Aurora kinase phosphorylation of GTSE1 is necessary for its interaction with MCAK.

GTSE1 is an intrinsically disordered protein that gets hyperphosphorylated during mitosis. From previous studies on GTSE1, it was learned that GTSE1 efficiently binds to MCAK during mitosis, but not during G2/S phase (Figure 8 a). Both these observations together raised the possibility that GTSE1-MCAK interaction is phosphorylation dependent.

In order to investigate the importance of this hyperphosphorylation of GTSE1 on its interaction with MCAK, we phosphorylated GST-GTSE1 full length protein using various mitosis-specific kinases like Aurora A, Aurora B, Cdk1, Plk1 or a combination of all. The phosphorylation was done by incubating GST-GTSE1 full-length with the kinases along with 2mM ATP and 10mM $MgCl_2$ overnight at 4^0C. The phosphorylated GTSE1 was further used to implement GST-pulldown by incubating it with GST beads for 2 hours at 4^0C. The kinases were washed from phosphorylation mix after GTSE1was attached to beads. Input samples with proteins before interaction were collected after addition of MCAK. The rest of GST-GTSE1 bound beads were thereafter incubated with MCAK for one hour in room temperature for the GTSE1-MCAK interaction to take place followed by final wash of GST pull down. GST alone was used as a negative control that won't bind MCAK. The proteins in the input and pulldown were analyzed using western blot. Interestingly, Aurora kinase (A and B or mix with both) phosphorylated GTSE1 could efficiently pull down MCAK while Cdk1 or Plk1 phosphorylated GTSE1 couldn't. This showed that Aurora kinase A or B phosphorylation was necessary for GTSE1 to interact with MCAK *in vitro* (Figure 8 b).

Next, we wanted to check if this was true within cells as well. To confirm Aurora kinase phosphorylation dependency in cells, U2OS wild type cells were first arrested in mitosis using S-trityl-L-cysteine (STLC) and later synchronized in metaphase using proteosome inhibitor MG132 along with Aurora A inhibitor MLN084 or Aurora B inhibitor ZM447439 to inhibit the respective kinases. These synchronized cells were lysed to extract proteins and prepared for Co-immunoprecipitation (Co-IP) assay. Endogenous GTSE1 was immunoprecipitated from U2OS wild type cells using anti-GTSE1 antibody while anti-GFP antibody was used as a negative control. Input samples and co-IP extracts were then analyzed by western blot (Figure

8 c). As shown in Figure, endogenous GTSE1 in U2OS wild type cells treated only with MG132 bind and pulldown MCAK. Upon both Aurora kinase A and B inhibition, there is a decrease in binding of MCAK with the endogenous GTSE1 which is in consensus with the *in vitro* results. Whereas, the anti-GFP IP could not pull down endogenous GTSE1 or MCAK as expected. Interestingly, Aurora B inhibition has a stronger effect on GTSE1-MCAK interaction as there is less binding of MCAK to endogenous GTSE1 seen for ZM44739 treated U2OS cells. This could mean that Aurora B phosphorylation has better influence on GTSE1-MCAK interaction in cells.

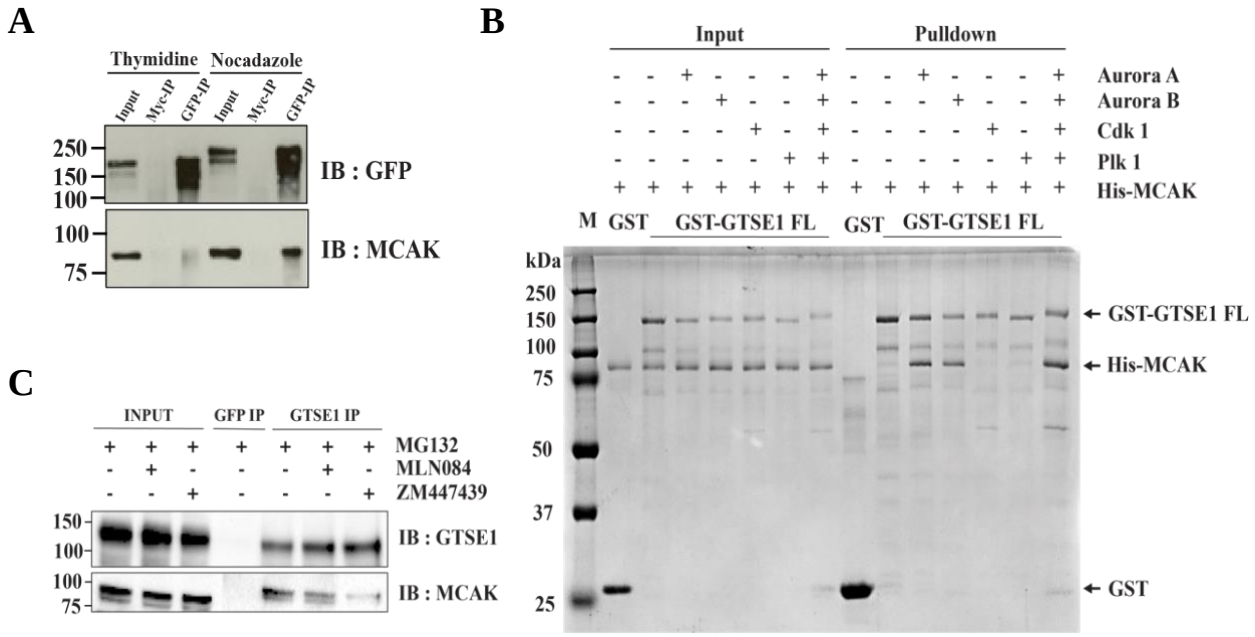

Figure 8. Phosphorylation of GTSE1 by aurora kinase is necessary for its interaction with MCAK

A. Western blots of cell extracts immunoprecipitated to check if interaction between GTSE1 with MCAK was mitosis specific. U2OS cells stably expressing GTSE1-LAP (U2OS$^{WT(212)}$) were either arrested in mitosis with nocodazole or in G2/S phase transition using a single thymidine block. Co-IPs were done in presence of phosphatase inhibitor (PPI) to prevent loss of any phosphorylations. Protein extracts were immunoprecipitated using either 9E10 anti-myc antibody as control antibody or anti-GFP antibody. Input and immunoprecipitated fractions were processed for SDS-PAGE followed by Western blot andprobed with anti-GFP and anti-MCAK antibody. GTSE1-GFP could efficiently pull down endogenous MCAK during mitosis. **B.** Coomassie Blue stained gel of a GST pulldown assay using purified full length GST-GTSE1 and His-MCAK. GST-GTSE1 was phosphorylated using different mitotic kinases Aurora A, Aurora B, Cdk1, Plk1 and an equimolar mix of Aurora A and B and was used a bait to pull down His-MCAK. **C.** Immunoblots of cell lysates and IPs of GFP and GTSE1 in U2OS wt cells synchronised using MG132 stained. IBs are stained sepearately for GTSE1 and MCAK. Synchronised cells were treated

with either Aurora A inhibitor MLN084 or Aurora B inhibitor ZM447439 to check the effect of respective kinase inhibition on GTSE1-MCAK interaction withing cells.

3.2 GTSE1 N-terminus interacts with the N-terminal domain of MCAK.

After identifying the importance of Aurora kinase phosphorylation on GTSE1-MCAK interaction, we wanted to narrow down the region on GTSE1 and MCAK that is crucial for their interaction to investigate more on the molecular mechanism of GTSE1-MCAK interplay. To determine more structural details of GTSE1-MCAK interaction, we next tried to narrow down the interaction region of GTSE1 and MCAK. For this, Aurora A phosphorylated GTSE1 fragments namely; GST-GTSE1 1-160, GST-GTSE1 1-260, GST-GTSE1 1-460 and GST-GTSE1 381-739 were used to pull down full length His tagged MCAK. These constructs

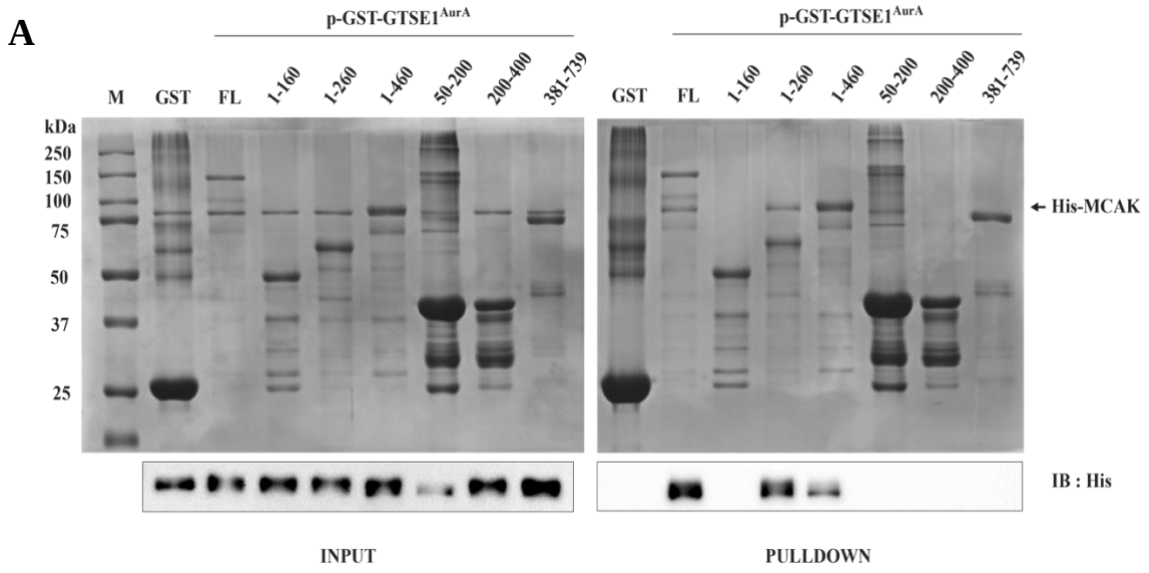

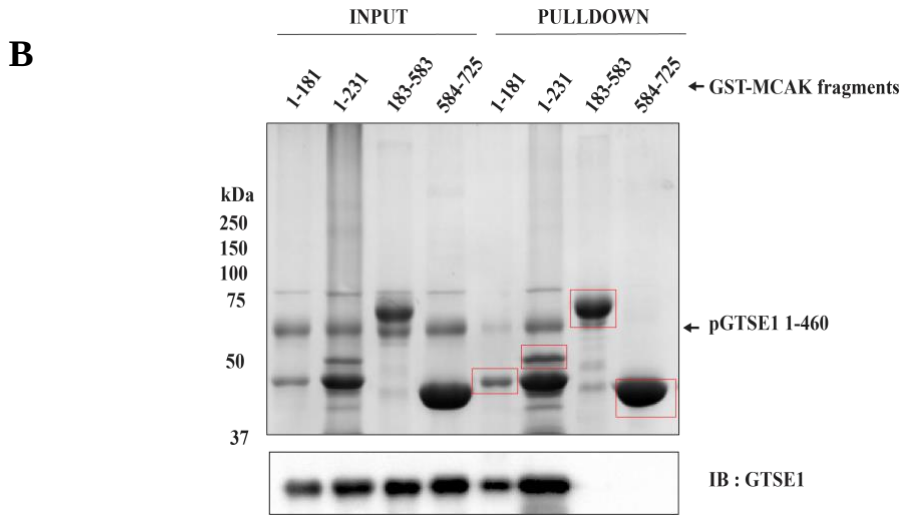

Figure 9. GTSE1 N Terminus interacts with the N terminal of MCAK

A. Coomassie Blue stained gel of a GST pulldown assay using Aurora A-phosphorylated purified GST-GTSE1 fragments: 1-160, 1-260, 1-460, 50-200, 200-400, 381-739 as bait to pull down His-MCAK. Immunoblot stained for Histidine was also used to detect presence of MCAK in the pulldowns. **B.** Coomassie Blue stained gel of a GST pulldown assay using GTSE 1-460 and GST-MCAK fragments: 1-181, 1-231, 183-583, 584-725. GTSE1 was phosphorylated by Aurora A and pulled down using GST-MCAK fragments as bait. Immunoblot stained for GTSE1 was also used to detect it' s presence in the pulldowns.

for the fragments were designed, expressed and purified earlier in the lab by one of the previous students. Pull down samples were loaded in a 10% SDS gel to see the interaction, if any. The samples were also used to develop blots to confirm pull down of MCAK by anti-his antibody (Figure 9 a). The pull-down assay results show that MCAK interacts predominantly with the N terminus of GTSE1 (1-460) with more specific region of interaction possibly lying between residues 160 and 381. Similar GST pull-down assay was also done using GST tagged MCAK fragments to pull down Aurora A phosphorylated GTSE1 N terminus (1-460). GTSE1 N terminus was pulled down by the N terminal fragment (1-181) of MCAK (Figure 9 b) and together these pull-down assays suggested that GTSE1-MCAK interaction occurred through their respective N termini. It is known that MCAK localizes to the inner kinetochore via its N-terminus and regulates proper KT-MT attachments through depolymerization of mal-attached MTs (Maney et al., 1998, Wordemann et al., 1999, Walkzak et al., 2002). Studies have also suggested that MCAK N-terminus has amino acid residues important for its binding to tubulin specifically at MT ends (Moore et al., 2005, McHugh et al., 2019). Remarkably, this unwraps new likelihoods of how GTSE1 might be affecting MCAK activity in a cellular context by interacting with the N-terminus of MCAK. It is possible that either GTSE1 might have a role in interfering with kinetochore localization of MCAK and/or it disrupts MCAK function by preventing its binding to MT ends. Further work needs to be done in terms of *in vivo* localization experiments of MCAK and GTSE1 (bound/unbound), and *in vitro* MT binding assays preferentially on dynamic MTs, to explore these possibilities in detail.

3.3.1 Phosphorylation of a single site on GTSE1 by Aurora kinases is important for its interaction with MCAK *in vitro*

Combining the knowledge that phosphorylation is necessary for interaction between GTSE1 and MCAK and the interaction occurs at GTSE1 N-terminus, we checked onto the Aurora A

phosphorylation sites on GTSE1 N terminus region that bound to MCAK. Combining this information with the sequence alignment data to identify the most conserved residues of GTSE1 among vertebrates, a set of Serine/Threonine residues on GTSE1 were sequentially mutated (independently or as combination) to create GTSE1 phospho-null mutant protein fragments. These fragments either with or without phosphorylation by Aurora A, were used to further pull down His-MCAK protein to check interaction (Figure 10 a). Surprisingly, one of the fragments, with a single mutation done on 165th Threonine residue of GTSE1 (T165) into Alanine, was no longer able to interact with MCAK even after phosphorylation of other residues with Aurora A (Figure 10 b, 10 c). In order to check whether T165 could be phosphorylated by Aurora kinase B as well or not, same pull-down assay was done with/without Aurora B phosphorylation of the GTSE1 T165A fragment (Figure 10 d). Results revealed that both Aurora A or Aurora B could phosphorylate GTSE1 T165 and this phosphorylation indeed was necessary for GTSE1-MCAK interaction. Hence, we could conclude that T165 phosphorylation by Aurora kinase is necessary for GTSE1 to interact with MCAK. As the recruitment of GTSE1 to spindle during mitosis involves Clathrin– TACC3 complex formation in the presence of Aurora A, it is interesting to consider whether this presence of Aurora A in spindle is also relevant for the GTSE1-MCAK interaction to occur inside the cells. While at the same time, in the kinetochores, Aurora B plays a much relevant role in the error correction process which raises the possibility that it can also play a role in

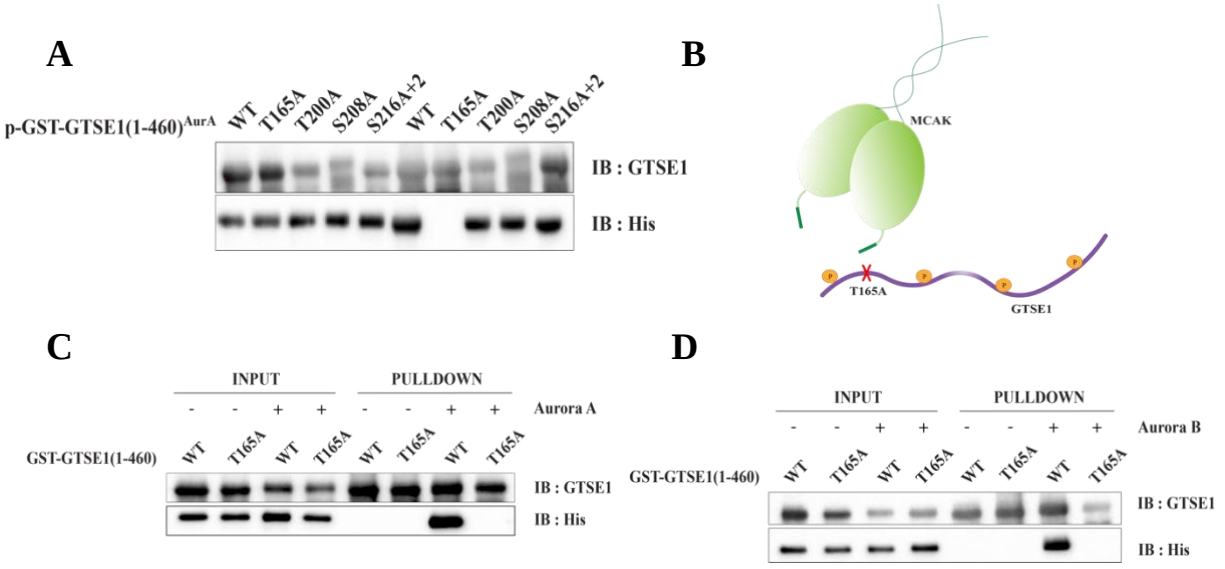

Figure 10. Phosphorylation of T165 of GTSE1 by aurora kinase promote its interaction with MCAK

A. Immunoblots of GST-pulldown assay using phosphorylated GST-GTSE1N terminus wt and different phospho-null mutations: T165A, T200A, S208A & S216A+2 that were used as bait to pull

down His-MCAK. Blots were stained using His to detect the pulled-down MCAK. **B.** Illustrative image of T16A phospho-null mutation disrupting GTSE1-MCAK interaction. **C.** Immunoblots of GST pull-down assay using either unphosphorylated or Aurora A phosphorylated GST-GTSE1 wt and GST-GTSE1 T165A mutant as bait to pull down His-MCAK. **D.** Immunoblots of GST pull-down assay using either unphosphorylated or Aurora B phosphorylated GST-GTSE1 wt and GST-GTSE1 T165A mutant as bait to pull down His-MCAK.

GTSE1-MCAK interaction if any near the kinetochore region. In an attempt to specifically identify the Aurora kinase responsible for the T165 phosphorylation, we tried to use a commercially synthesised phospho-specific antibody targeted to T165, so that along with analysing the localization of phosphorylated GTSE1, we could also check the effect of Aurora A or B inhibition in the localization of T165 phosphorylated GTSE1. Unfortunately, for further experiments down this lane, we have been unable to reliably detect a signal in cell extracts, potentially due to other post translation modifications being present nearby T165.

3.3.2 Redundant pathways and *in vivo* insights into GTSE1-MCAK interaction

Even though *in vitro* interaction studies and assays can provide relevant information on how complex regulatory mechanisms work, it is crucial to understand that things are more diverse and complicated within a living cell environment. Hence, it is important to investigate how the GTSE1-MCAK system behaves *in vivo* within cells. The effect of the GTSE1 T165A mutation, where it cannot bind to MCAK or possibly not inhibit it, can be understood by expressing this mutant protein at endogenous levels in U2OS wild-type cells using Bacterial Artificial Chromosome (BAC) transgene. The T165A mutation was introduced into a BAC already containing the GFP-tagged GTSE1 gene with si-RNA resistance by recombineering (Figure 11 a). The mutant GTSE1 carrying BAC was purified and introduced into the U2OS cell line using a non-liposomal lipid reagent (effectene) based transfection. The positively transfected clonal cell colonies were checked for homogenous expression level of the mutant GFP-GTSE1 through live cell imaging. To check whether the transgene level of protein expression was similar to endogenous, cell lysates from the clones were loaded onto a 10% SDS gel and immunoblotted for GTSE1. Clones with the expression level of GFP-GTSE1 T165A comparable to the level of endogenous wild-type GTSE1 within the cells were considered as the best GFP-GTSE1 T165A clones. Clones with the best expression of GFP-GTSE1 T165A at the endogenous level were selected for further studies. Initially, the ability of GTSE1 T165A

to interact with MCAK within cells was tested using Co-Immunoprecipitation assays. For this, both U2OS cell lines with GTSE1 wild-type transgene and another with mutated GTSE1 T165A were synchronized at metaphase by MG132 and depleted of the endogenous GTSE1 by RNAi. The cells were later lysed and checked for MCAK interaction using Co-IP of GTSE1. It was observed that there was a slight reduction in GTSE1-MCAK interaction in cell lines with GTSE1 T165A (11 b). The slight reduction indicates that in cells, there must be redundant pathways by which GTSE1-MCAK interaction is protected or that multiple phosphorylation of amino acid residues by Aurora kinases or other mitotic kinases might be promoting GTSE1-MCAK interaction.

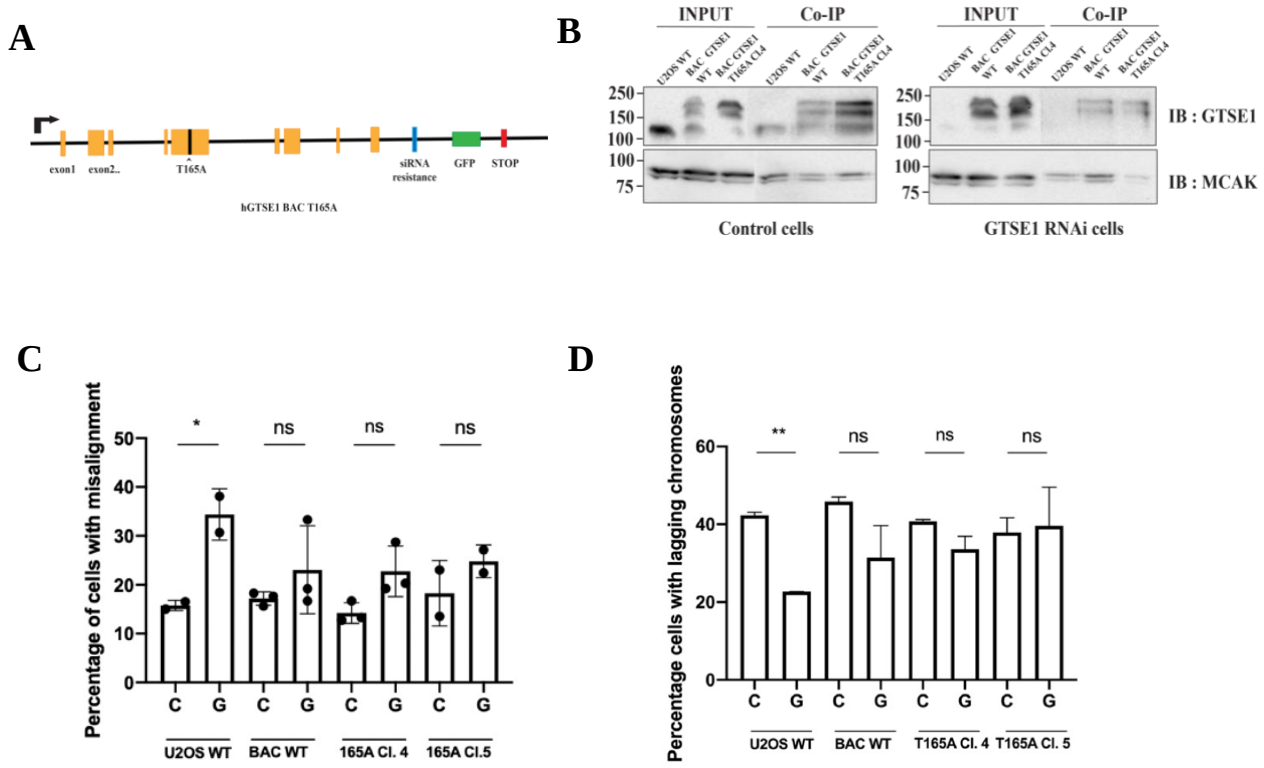

Figure 11. GTSE1 T165A in cells show slight reduction in its interaction with MCAK

A. Schematic representation of hGTSE1 BAC with GTSE1 mutated at T165 **B.** Immunoblots of cell lysates used to Co-IP MCAK from GTSE1 in U2OS wt cells, U2OS cells with GTSE1 wt BAC and GTSE1 T165A BAC (Cl.4). Left panel shows control cells that still has endogenous GTSE1 present, right panel shows cells depleted of endogenous GTSE1 after RNAi. IBs are stained separately for GTSE1 and MCAK. **C.** Bar graph showing quantification of percent cells with misaligned chromosomes during metaphase after treatment with control and GTSE1 RNAi in U2OS wt cells, U2OS cells with wt GTSE1 trangene, and two different U2OS cell lines with T165A GTSE1 trasgene. (n>100 cells per experiment, data is

from 3 independent experiments) **D.** Bar graph showing quantification of percent cells with lagging chromosomes during anaphase after treatment with control and GTSE1 RNAi in U2OS wt cells, U2OS cells with wt GTSE1 trangene, and two different U2OS cell lines with T165A GTSE1 trasgene. (n>100 cells per experiment, data is from 3 independent experiments).

The exploration of GTSE1-MCAK interaction not only uncovered its phosphorylation-dependent intricacies, notably focusing on the critical T165 residue but also delved into its *in vivo* behavior, enriching our understanding. Previous studies established that GTSE1 plays a crucial role in maintaining genome stability by orchestrating precise microtubule (MT) dynamics, essential for chromosome alignment and segregation, through its interaction with MCAK (Bendre et al., 2016). Building on this knowledge, our investigation dissected the phosphorylation dynamics critical for GTSE1-MCAK interaction. Introducing the GTSE1 T165A mutant at endogenous levels in U2OS cells provided a platform for *in vivo* analyses. Co-Immunoprecipitation assays unveiled a subtle reduction in GTSE1-MCAK interaction in T165A mutants, suggesting the potential existence of redundant pathways or alternative phosphorylation events governing this interaction within cells. Surprisingly, the analysis of mitotic phenotypes in T165A clones, including chromosome alignment and segregation, did not manifest significant changes compared to wild-type GTSE1 cells (Figure 11 c, d). This unexpected observation raises intriguing questions about the nuanced regulatory mechanisms that govern GTSE1-MCAK interaction within the cellular context. Considering the multifaceted nature of cellular processes, future investigations, encompassing analyses of astral microtubule density and spindle positioning, promise a holistic understanding of GTSE1-MCAK dynamics during mitosis.

The current study, building upon earlier findings, underscores the necessity for comprehensive *in vivo* investigations to unravel the intricacies of this critical cellular interaction fully. The collective insights not only contribute to deciphering the regulatory landscape of GTSE1-MCAK but also provide a foundation for future explorations into the broader networks governing kinesin 13 family proteins. As we navigate the molecular complexities governing cellular division, the journey ahead holds the potential not only for a deeper comprehension of these intricate processes but also for implications in therapeutic interventions targeting these regulatory pathways.

3.4 Cross Linking Mass-Spectrometry of GTSE1-MCAK

In order to have a closer look at the GTSE1-MCAK interaction at amino-acid residue level, Aurora A phosphorylated GTSE1 (1-460) was cross linked with MCAK using DSBU. DSBU (disuccinimidyl dibutyric urea), or BuUrBU, is a mass-spectrometry (MS) cleavable that contains an amine-reactive Nhydroxysuccinimide (NHS) ester at each end of an 11-atom spacer arm. The cross-linker facilitates analysis of protein structure and complex interactions using mass spectrometry. Network maps of cross linked amino acids, for both intra-molecular interactions within GTSE1/MCAK and inter-molecular interactions between GTSE1 and MCAK were plotted to analyse the corresponding interactions. While there were no relevant intra molecular interactions detected within GTSE1 itself, intra-molecular interactions were

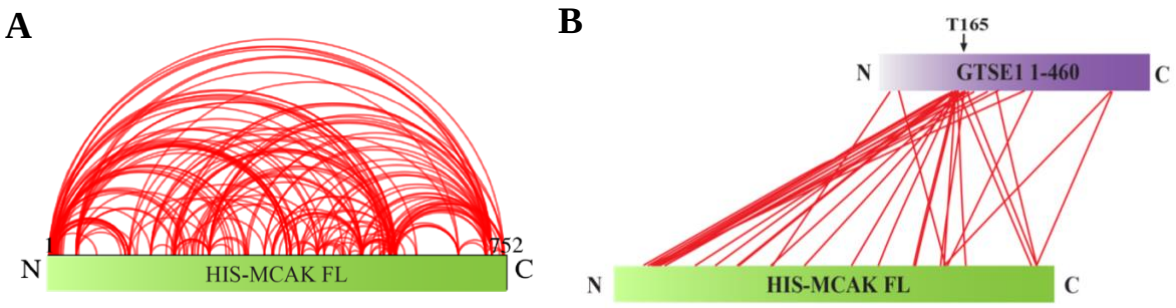

Figure 12. Cross linking mass spectrometry of GTSE1-MCAK

A. Intra cross links within full length MCAK which is similar to finding in Mc Hugh et al; 2019. **B.** Inter cross links between GTSE1 N terminus and full length MCAK. There are more cross links from MCAK N terminus to the region near T165 of GTSE1.

detected within MCAK (Figure 12 a), confirming its existence as an actively folded dimer, and in accordance with previous findings mentioned in literatures.

Analysing the cross-linked amino acid residues between GTSE1 and MCAK confirmed that it is indeed the extreme N terminus of MCAK that interacts with GTSE1 N terminus as most of the cross-linked amino acid residues were on the N termini of GTSE1 and MCAK (Figure 12 b). Since the requirement of T165 phosphorylation for GTSE1-MCAK interaction was already established, we checked whether this residue showed phosphorylation in the sample submitted, and as expected T165 showed prominent phosphorylation by Aurora A. Noteworthy, the lysine (K162) and tyrosine(Y166) residues nearest to the T165 residue also showed abundant cross

links to MCAK N terminus, specifically to the 52nd lysine, a well-conserved residue across vertebrates and other kinesin 13 family members in MCAK. These further hints that the apart from the necessity of phosphorylation by Aurora A at T165, the nearby region of the residues might also be important for the interaction. Apart from this, the 125th lysine (K125) residue on GTSE1 also showed frequent crosslinks with MCAK amino acid residues. It would be interesting to check in future, whether the region near to K125 on GTSE1 alone has a direct interaction to MCAK *in vitro*.

3.5 Understanding MCAK interplay on dynamic microtubules *in vitro*: Total Internal Reflection Fluorescence (TIRF) microscopy assays.

The multifaceted journey of MCAK in depolymerizing microtubules (MTs), involving pivotal stages such as transitioning between active and inactive conformations, binding to the MT lattice, diffusion on the lattice, and the ultimate removal of tubulin dimers in an ATP-bound state (Figure 13 a, Friel & Howard 2011, Ritter et al 2016), lays the foundation for the complex regulatory influence of GTSE1. This intricate interplay beckons a comprehensive exploration into how GTSE1 might be inhibiting MCAK across this spectrum of functions.

The significance of unravelling the inhibitory action of GTSE1 on MCAK gains prominence, especially considering its impact on dynamic MTs *in vitro*, offering a representation close to the intricacies of MT behaviour within a living cell. Total Internal Reflection Fluorescence (TIRF) microscopy assays stand as a powerful tool to delve into this nuanced interaction. Through meticulous examination of MCAK on dynamically growing MTs, the study aims to decipher the diverse possibilities of GTSE1's influence on MCAK activity.

Dynamic MTs were systematically generated for varying concentrations of free tubulin, providing a platform to analyze growth rates and catastrophe frequencies, crucial parameters for understanding MT dynamics. Following established protocols (Gell et al., 2010), microtubule dynamics assays were conducted using 12µM free tubulin. The addition of 2nM MCAK into the flow chambers alongside 12µM free tubulin allowed for the assessment of resulting changes in MT dynamics due to MCAK's depolymerization activity. Kymographs, generated using ImageJ, facilitated the quantification of growth rates and catastrophe frequencies of dynamic MTs, offering valuable insights into the intricate interplay between GTSE1 and MCAK (Figure 3.5b).

Notably, the observed growth rate of 24.10 ± 1.42 nm/s^{-1} for 15µM tubulin alone, coupled with a catastrophe frequency of 0.0053 ± 0.002 s^{-1} (Figure 13 b), aligned seamlessly with existing data. Introduction of 2nM MCAK revealed no significant difference in growth rate (23.08 ± 2.04 nm/s^{-1}), yet a subtle but significant increase in catastrophe frequency (0.0069 ± 0.002 s^{-1}), indicative of MCAK's functional and active role in depolymerizing MTs. Titrating MCAK onto dynamic MTs further heightened catastrophe frequency without notably impacting growth rates (Figure 13 c). It's crucial to acknowledge that additional experiments to introduce GTSE1 into these analyses did not materialize in this phase of the study. This research gap underscores the need for future investigations to comprehensively explore GTSE1's impact on the dynamic interplay with MCAK, providing a more holistic understanding of the regulatory mechanisms governing microtubule dynamics during mitosis.

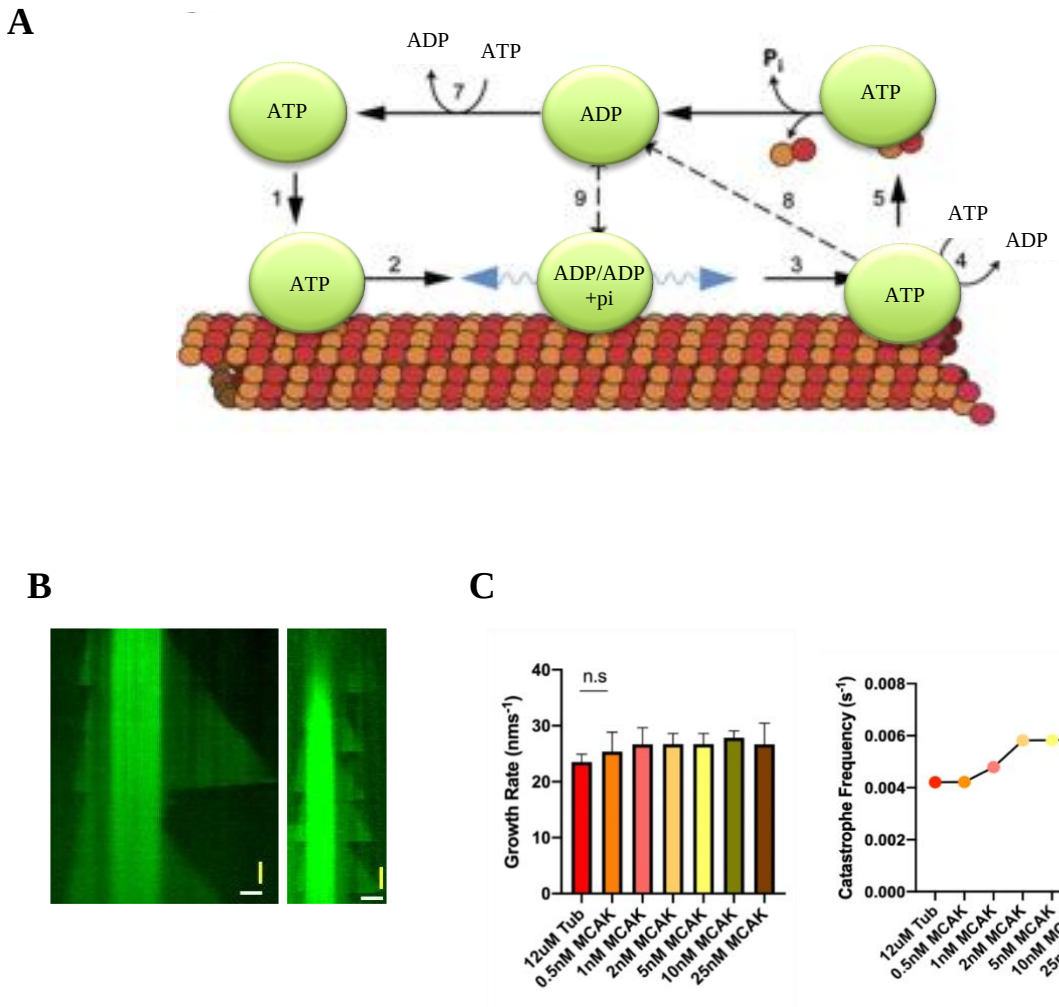

Figure 13. Understanding microtubule dynamics *via* TIRF microscopy

A. Mechanism of microtubule depolymerization by MCAK (1) The ATP hydrolysis by MCAK, a crucial step, is hindered in the absence of tubulin or microtubules, resulting in the approach of MCAK to the microtubule while in an ATP-bound form. (2) Once bound, MCAK grips the microtubule lattice; however, the lattice's stimulation of ATP hydrolysis transitions MCAK to a state of reduced lattice affinity, allowing for diffusion. (3) MCAK's diffusion culminates at the microtubule end, (4) where it undergoes a nucleotide exchange, reaffirming its ATP-bound state and ensuring a robust interaction at the microtubule terminus. (5) A strong bond forms between ATP-charged MCAK and a tubulin subunit, facilitating microtubule disassembly. (6) A subsequent round of ATP hydrolysis disengages MCAK from the tubulin, facilitating its release. (7) In an ATP-rich milieu, MCAK recharges with ATP, resuming its active conformation. (8) MCAK's ATPase action may persist on the microtubule without tubulin detachment. (9) Finally, MCAK might dissociate from the microtubule prematurely or revert to a weakly associated state following ATP hydrolysis at the microtubule end, ready for another cycle. This figure has been adapted from Friel & Howard, 2011. **B.** Kymographs representing the growth and shrinkage of dynamic MTs grown in the presence of 15µM free tubulin only (left) and 2nM MCAK over 15µM tubulin (right). Scale, X axis: Scale bar, X-axis: 2µm; Y-axis: 1 min. **C**. Bar graph showing growth rate of dynamic MTs at various concentration of MCAK over 12uM tubulin concentration(left), plot showing catastrophe frequency of dynamic MTs at increasing concentrations of MCAK over 12uM tubulin concentration (right).

3.6 GTSE1 inhibits MCAK differentially in phosphorylated and unphosphorylated conditions

3.6.1 Unphosphorylated GTSE1 prevents MCAK ATPase activity

MCAK has a systematized ATP turnover cycle with controlled ADP exchange and ATP cleavages, which is important for its enzymatic activity (Friel and Howard, 2011). Hence, one of the possible ways in which MCAK could be functionally regulated at a molecular level is by perturbing this ATPase activity cycle. To assess whether GTSE1 has a direct effect on MCAK ATPase activity, we performed NADH coupled ATPase activity to measure ATP consumption per minute per enzyme MCAK on both free tubulin dimers and GMPCPP stabilized microtubules. MCAK showed both MT lattice induced, and free tubulin dimer induced ATPase activity (Figure 14 a), in consensus with previous studies (Hunter et al, 2003, Patel et al, 2016). Upon addition of GTSE1 along with MCAK, there is a decrease in ATPase and this decrease becomes more evident with increasing amount of GTSE1 (Figure 14 b). As GTSE1 can directly bind to stabilized MT lattice, this could be preventing MCAK to have lattice induced or end induced ATPase activity, hence reducing the overall ATP cleavage. However as non-phosphorylated GTSE1 cannot bind to MCAK, the inhibition of ATPase

activity cannot be attributed to GTSE1 directly inhibiting MCAK through an interaction. Rather, GTSE1 *in vitro* physically prevents MCAK from acting on MTs. To investigate if Aurora kinase phosphorylated GTSE1 which has reduced affinity for MTs and also that directly bind to MCAK affect the ATPase activity, the same assay was carried out with Aurora A phosphorylated GTSE1. Surprisingly, there doesn't seem to be a reduction in MCAK ATPase activity, on contrary there seems to be an increase that could be attributed to the basal contaminant effect of the kinase it (Figure 14 c). Further experiments need to be done over more conditions to conclude the exact effect of phosphorylated GTSE1 over MCAK ATPase activity.

3.6.2 Aurora kinase phosphorylated GTSE1 prevents efficient MCAK depolymerisation *in vitro*.

Our investigation into the intricate interplay between GTSE1 and MCAK revealed intriguing complexities, particularly in the context of phosphorylation dynamics. Initial observations indicated that while unphosphorylated GTSE1 physically obstructs MCAK's action on microtubules, phosphorylated GTSE1 seemed ineffectual in modulating MCAK's ATPase activity. This paradox prompted a more nuanced exploration to disentangle the dual binding capacity of phosphorylated GTSE1 to both MCAK and microtubules, potentially introducing a competitive interaction that could obscure the true impact of phosphorylation on MCAK activity. To disentangle these interactions, we undertook the essential step of segregating the functions of phosphorylated GTSE1 in binding to microtubules and MCAK. For this purpose, a minimal peptide region of GTSE1 encompassing the crucial T165 residue was synthesized. The 60-residue region spanning positions 135 to 195 of GTSE1 emerged as the most stable protein for purification, setting the stage for a detailed investigation. Initial assessments involved confirming its binding ability with MCAK through a GST pulldown experiment, affirming that even in the phosphorylated state, GTSE1 (135-195) maintained its affinity for MCAK (Figure 14 d). However, the plot thickened when we conducted a co-sedimentation assay of this GTSE1 peptide with 2μM microtubules. Intriguingly, the results unveiled a transformation in its binding capabilities—while phosphorylated GTSE1 (135-195) retained its association with MCAK, it exhibited an inability to bind to microtubules (Figure 14 e). Hence this fragment could be crucial in further experiments to understand the GTSE1-MCAK interplay.

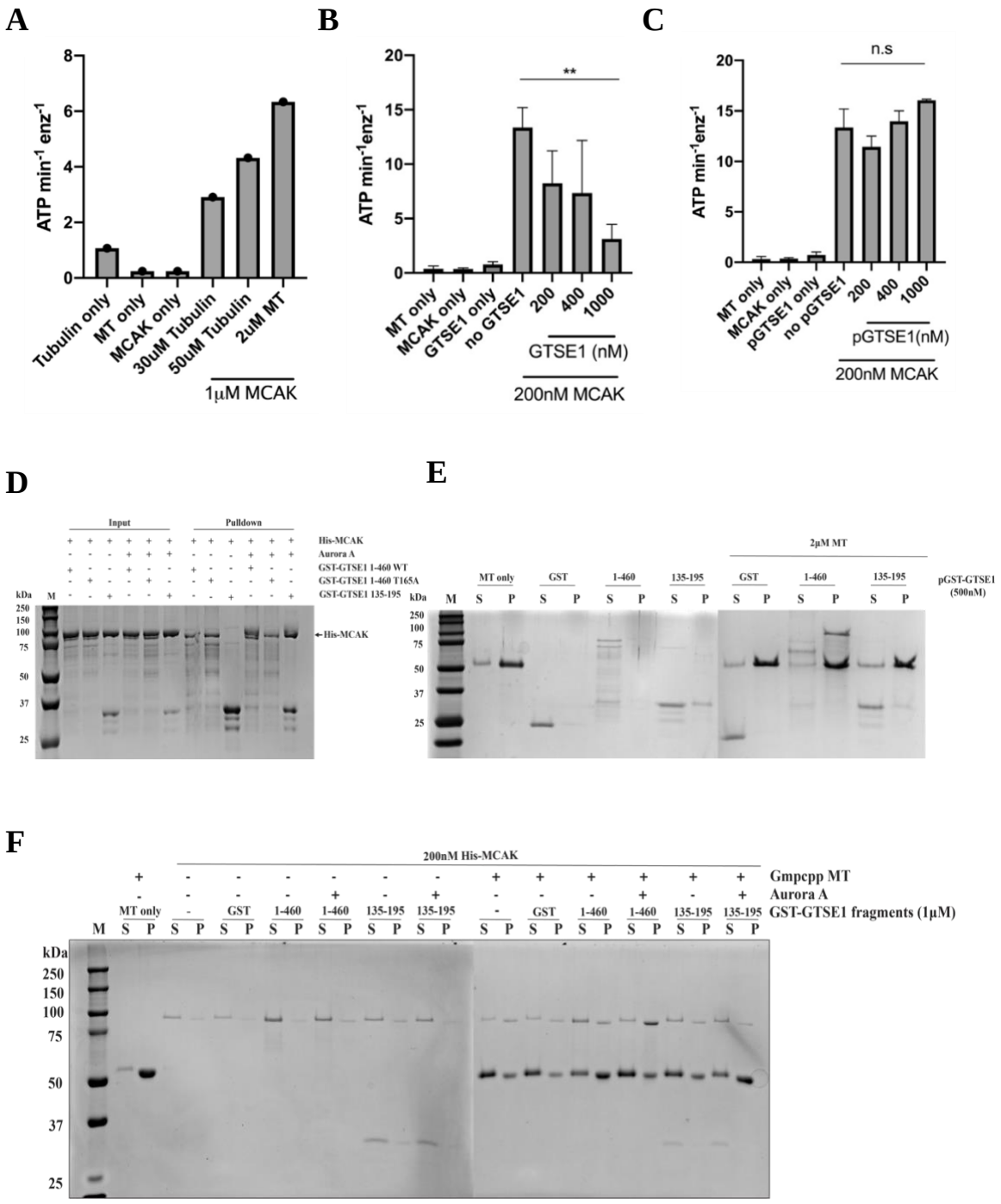

Figure 14. GTSE1 inhibits MCAK differentially in phosphorylated and unphosphorylated conditions

A. Bar graph showing ATP activity (measure by ATP consumption per minute per dimer enzyme) of 200nM MCAK with free tubulin dimer (20uM) or GMPCPP stabilized MTs (2uM) as substrate. **B.** Bar graph showing ATPase activity of 200nM MCAK alone or in the presence of increasing concentration of non-phosphorylated GTSE1 over 2uM GMPCPP stabilized MTs. **C.** Bar graph showing ATPase activity of 200nM MCAK alone or in the presence of increasing concentration of Aurora A phosphorylated GTSE1 over 2uM GMPCPP stabilized MTs. **D.** Coomassie stained gel showing GST pulldown assay using phosphorylated or unphosphorylated GST-GTSE1 1-460 wt, T165A and GST-GTSE1 135-195 as baits to

pull down His-MCAK. **E.** Coomassie stained gel showing microtubule co-sedimentation assay using 2μM MT as lattice to check binding of Aurora A phosphorylated GTSE1 1-460 and GTSE1 135-195 onto MTs. The supernatant (s) phase had any protein that doesn't bind the MT lattice while pellet (p) phase has the MT polymer and the bound protein, if any. **F.** Coomassie stained gel showing MT depolymerisation assay using 2μM MT as polymer lattice to check its depolymerisation over 1 hour time in the presence of MCAK alone and MCAK along with phosphorylated or unphosphorylated GTSE1 1-460 and GTSE1 135-195. More proportion of tubulin in the supernatant implies higher depolymerisation efficiency of MCAK while more proportion of tubulin in the pellet phase implies depolymerisation efficiency of MCAK was compromised leading MTs to remain as polymers in the pellet.

To dissect the intricacies of GTSE1's influence on MCAK-mediated microtubule depolymerization, we conducted detailed depolymerisation assay using GMPCPP-stabilized microtubules. Incubating these microtubules with MCAK for an hour significantly heightened microtubule depolymerization, resulting in a substantial accumulation of tubulin dimers in the supernatant phase. Subsequent addition of unphosphorylated GTSE1 N terminus to this microtubule-MCAK mixture during incubation exerted a remarkable effect—microtubule depolymerization was noticeably impeded, causing a predominant shift of tubulin dimers into the pellet phase (Figure 14 f). This outcome aligns with our expectations, mirroring the inhibitory action observed in the ATPase assay. The physical binding of GTSE1 to microtubules essentially acted as a barrier, preventing MCAK from efficiently depolymerizing microtubules. In contrast, introducing Aurora A phosphorylated GTSE1 N terminus into the microtubule-MCAK mixture yielded a distinct result. The phosphorylated GTSE1 fragment failed to significantly inhibit MCAK depolymerization activity, and a substantial portion of tubulin dimers remained in the supernatant (Figure 14 f). Notably, akin to the ATPase assay, directly inferring the impact of GTSE1 phosphorylation on MCAK activity based on this result is challenging. This complexity arises from the concurrent binding of GTSE1 to both microtubules and MCAK, necessitating a more refined approach. To address this challenge, we performed a depolymerization assay specifically focusing on GTSE1's individual functio ns—binding to microtubules versus MCAK using GTSE1 135-195 fragment. The surprising outcome of this refined assay shed light on the nuanced interplay between GTSE1 and MCAK.

Phosphorylated GTSE1 135-195, separated from its microtubule-binding function, remarkably prevented MCAK depolymerization activity. This unexpected result underscores the nuanced influence of the GTSE1 N terminus region on MCAK, revealing that phosphorylated GTSE1-MCAK interaction profoundly affects MCAK depolymerization activity (Figure 14 f). This

ground-breaking discovery suggests that while full-length GTSE1 may engage redundant pathways, the minimal region of GTSE1 binding to MCAK is a potent regulator of MCAK depolymerization activity. The intricate interplay between phosphorylated GTSE1 and MCAK not only advances our understanding of microtubule dynamics during mitosis but also points toward future avenues of research for a more holistic exploration of their multifaceted relationship. This pivotal finding deepens our comprehension of GTSE1-MCAK interplay and underscores the need for further investigations to comprehensively understand the regulatory mechanisms governing microtubule dynamics during mitosis.

The revelation that unphosphorylated GTSE1 impedes MCAK ATPase activity through physical hindrance on microtubules emphasise the intricate mechanisms orchestrating mitotic events. Furthermore, the unexpected inhibitory effect of phosphorylated GTSE1 on MCAK depolymerization activity sheds light on the multifaceted roles played by distinct regions of GTSE1. While these findings mark significant strides in deciphering GTSE1-MCAK interaction, it is crucial to acknowledge the complexity of these regulatory pathways. Our results, coupled with the insights from earlier studies, underscore the need for more exhaustive investigations. The interplay between GTSE1 and MCAK is undoubtedly a pivotal regulator of microtubule dynamics, yet the full extent of its implications remains a terrain ripe for exploration.

5. Discussion

The findings presented in this thesis shed light on the intricate regulatory mechanisms governing the activity of MCAK during mitosis, with a particular focus on its interaction with GTSE1. The overarching goal of this investigation was to unravel the molecular intricacies that underlie the regulation of MCAK and, consequently, influence the dynamics of the microtubule network during cell division.

One of the central revelations from this study is the essential role played by Aurora kinase-dependent phosphorylation in facilitating the interaction between GTSE1 and MCAK. Through a meticulous series of *in vitro* experiments, it was demonstrated that Aurora A or Aurora B phosphorylation of GTSE1 is necessary for the efficient binding of GTSE1 to MCAK (Figure 15 a). The phosphorylation of GTSE1 by Aurora kinases represents a critical regulatory event that dictates its interaction with MCAK, an essential player in mitotic microtubule dynamics. Our findings demonstrate that during mitosis, GTSE1 undergoes hyperphosphorylation, enabling its efficient binding to MCAK, which is notably absent during the G2/S phase. This phosphorylation-dependent binding suggests a temporal precision in the regulatory mechanisms that control mitosis, highlighting the role of phosphorylation as a key modulator of protein interactions.

In vitro experimentation has established the necessity of Aurora kinase activity for the interaction between GTSE1 and MCAK. Both Aurora A and Aurora B kinases are capable of mediating this phosphorylation, with a pronounced effect noted in the presence of Aurora B. This specificity emphasizes the distinct roles that different kinase subtypes play in the spatial-temporal regulation of mitotic events.

Structural investigations into the GTSE1-MCAK interaction unveiled the critical involvement of the N-terminus of both proteins. Specifically, the N-terminus of GTSE1 was found to predominantly interact with the N-terminal domain of MCAK. This structural revelation aligns with the known localization of MCAK to the inner kinetochore via its N-terminus. The newfound understanding of this interaction prompts further exploration into how GTSE1, by interacting with the N-terminus of MCAK, may influence its cellular functions, potentially

disrupting MCAK's binding to microtubule ends or interfering with kinetochore localization. The application of cross-linking mass spectrometry provided a closer look at the amino acid residue-level interactions between GTSE1 and MCAK. The results confirmed that the extreme N-terminus of MCAK interacts with the N-terminus of GTSE1. Notably, the study highlighted the importance of T165 phosphorylation and neighbouring residues for this interaction. Furthermore, the investigation into the functional consequences of GTSE1-MCAK interaction revealed that GTSE1, particularly when bound to the microtubule lattice, inhibits MCAK ATPase activity, suggesting a potential regulatory mechanism.

Zooming in on the phosphorylation sites of GTSE1, a specific residue, T165, emerged as a critical molecular switch governing the interaction between GTSE1 and MCAK. Through mutational analyses, it was revealed that phosphorylation at T165 by Aurora kinases is indispensable for the GTSE1-MCAK interaction (Figure 15b). This insight opens avenues for understanding how the recruitment of GTSE1 to the spindle during mitosis, involving Clathrin–TACC3 complex formation and Aurora A presence, might correlate with the GTSE1-MCAK interaction. Moreover, the T165 site's phosphorylation presents an interesting nexus for exploring the role of Aurora kinases in the spindle checkpoint and error correction mechanisms at the kinetochore.

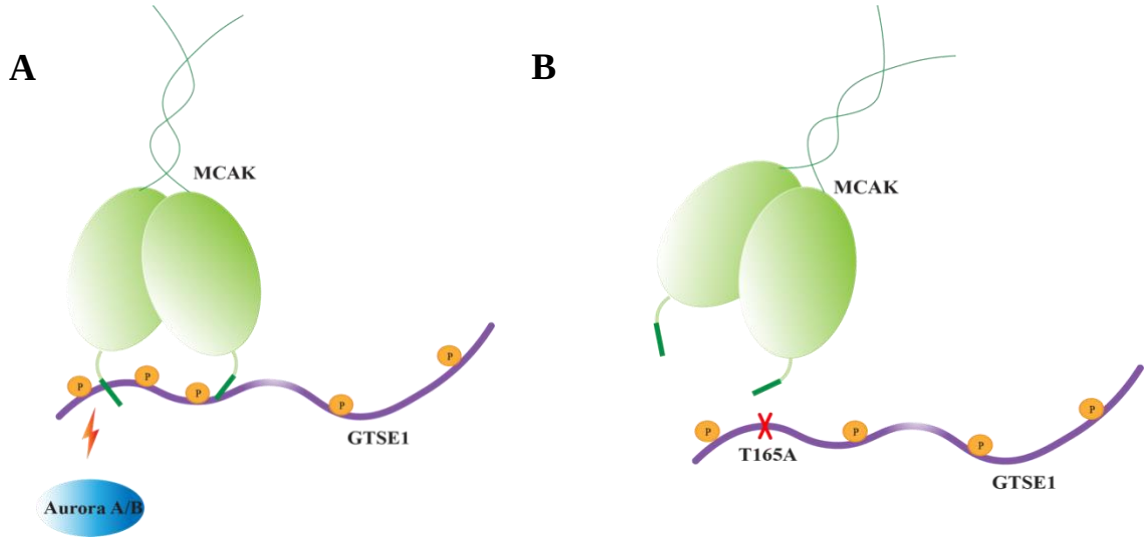

Figure 15. Importance of phosphorylation in GTSE1-MCAK interaction

A. Schematic model showing Aurora A/B kinase phosphorylation of GTSE1 promoting its interaction with MCAK **B.** Schematic model showing T165A mutated GTSE1 disrupting its interaction with MCAK.

Examining the GTSE1 T165A mutation within living cells revealed nuanced insights into the regulatory dynamics of GTSE1-MCAK interaction. The mutation, disrupting GTSE1's binding to MCAK, was expressed at endogenous levels in U2OS cells using a Bacterial Artificial Chromosome (BAC) transgene. Co-Immunoprecipitation assays demonstrated a slight reduction in GTSE1-MCAK interaction in cells with the T165A mutation, implying potential redundant pathways or alternative phosphorylation events. These findings reveal the complexity of cellular regulatory networks, providing a more intricate understanding of how GTSE1 engages with MCAK *in vivo*.

Looking forward, the outlined results pave the way for a deeper exploration of the regulatory landscape surrounding MCAK and its interplay with GTSE1. The proposed use of Total Internal Reflection Fluorescence (TIRF) microscopy assays promises to provide valuable insights into the inhibitory action of GTSE1 on MCAK activity on dynamic microtubules. This avenue of research holds the potential to quantify growth rates and catastrophe frequencies, offering a nuanced understanding of the dynamic interplay between GTSE1 and MCAK *in vitro*.

Regulatory complexity in mitotic dynamics: Phosphorylation dependent modulation of MCAK by GTSE1

The final findings of this study underline the dualistic influence of GTSE1 on MCAK activity, contingent upon its phosphorylation status, presenting a compelling narrative on the modulation of mitotic progression. GTSE1, in its unphosphorylated state, exhibits a pronounced inhibitory effect on MCAK’s ATPase activity, not through direct interaction with MCAK but rather by physically hindering its access to microtubules, thus impeding its depolymerization function. This physical obstruction underscores the fundamental role of spatial organization within the cell, dictating the functionality of mitotic proteins. Contrastingly, the phosphorylated form of GTSE1 delineates a more nuanced scenario. Initially observed to have no significant reduction in MCAK’s ATPase activity, further investigation reveals that this may be attributed to the concurrent binding affinity of phosphorylated GTSE1 for both MCAK and microtubules. This complex interplay necessitated a more focused approach, leading to the use of a synthesized peptide of GTSE1, which confirmed that phosphorylated GTSE1 selectively inhibits MCAK depolymerization without binding to the microtubules. This selective inhibition is pivotal, as it implies that post-translational

modifications of GTSE1 could fine-tune MCAK’s activity, thereby intricately controlling microtubule dynamics and stability during mitosis.

The study presents a comprehensive model elucidating this interaction, highlighting the differential impact of GTSE1's phosphorylation status on microtubule behaviour. In its unphosphorylated form, GTSE1 binds robustly to the microtubule lattice, forming a barrier that precludes MCAK from engaging with the microtubule ends, thereby thwarting its depolymerization activity. This suggests a crucial role for GTSE1 as a safeguard, maintaining microtubule integrity when necessary.

Conversely, the phosphorylated GTSE1 exhibits a reduced affinity for the microtubule lattice, attributable to post-translational modifications. This nuanced reduction does not abrogate the interaction entirely but modulates it, potentially allowing MCAK to maintain its depolymerization function in the presence of phosphorylated GTSE1. The findings reveal a competitive dynamic where phosphorylated GTSE1 and microtubules vie for MCAK binding, subtly altering its capacity to destabilize microtubules.

The employment of a GTSE1 peptide fragment, specifically the phosphorylated 135-195 region, further refines this model. This fragment demonstrates an exclusive interaction with MCAK's N-terminus, independent of microtubule binding. This direct interaction significantly inhibits MCAK's ability to disassemble microtubules, offering persuasive evidence that GTSE1's regulatory function on MCAK extends beyond mere lattice obstruction to include direct modulation of its enzymatic activity (Figure 16).

The proposed schematic model, incorporating these observations, offers a visual narrative that harmonizes the complexity of GTSE1-MCAK interactions with microtubule dynamics. It highlights the potential of phosphorylation as a decisive regulatory mechanism, where a single post-translational modification on GTSE1 can switch its role from a passive lattice occupant to an active modulator of MCAK, thereby influencing the delicate equilibrium of microtubule assembly and disassembly during cell division.

This finding enriches our current understanding and opens up avenues for targeted research to unravel the specific molecular determinants within the GTSE1 sequence that are responsible for these regulatory dynamics. These results contribute a significant piece to the puzzle of mitotic regulation, emphasizing the importance of protein modifications in the spatiotemporal

coordination of mitotic events. The discovery that GTSE1 can differentially regulate MCAK, depending on its phosphorylation state, provides a nuanced perspective on how cells may rapidly adapt to the needs of the mitotic phase, ensuring the agility and adaptability necessary for successful cell division. The insights derived from this study have far-reaching implications, not only deepening our understanding of the molecular choreography that dictates mitosis but also potentially informing therapeutic strategies. By delineating the exact molecular interactions and consequences of GTSE1's interaction with MCAK, we could envisage novel approaches to modulate this pathway in diseases where mitotic control is compromised, such as cancer.

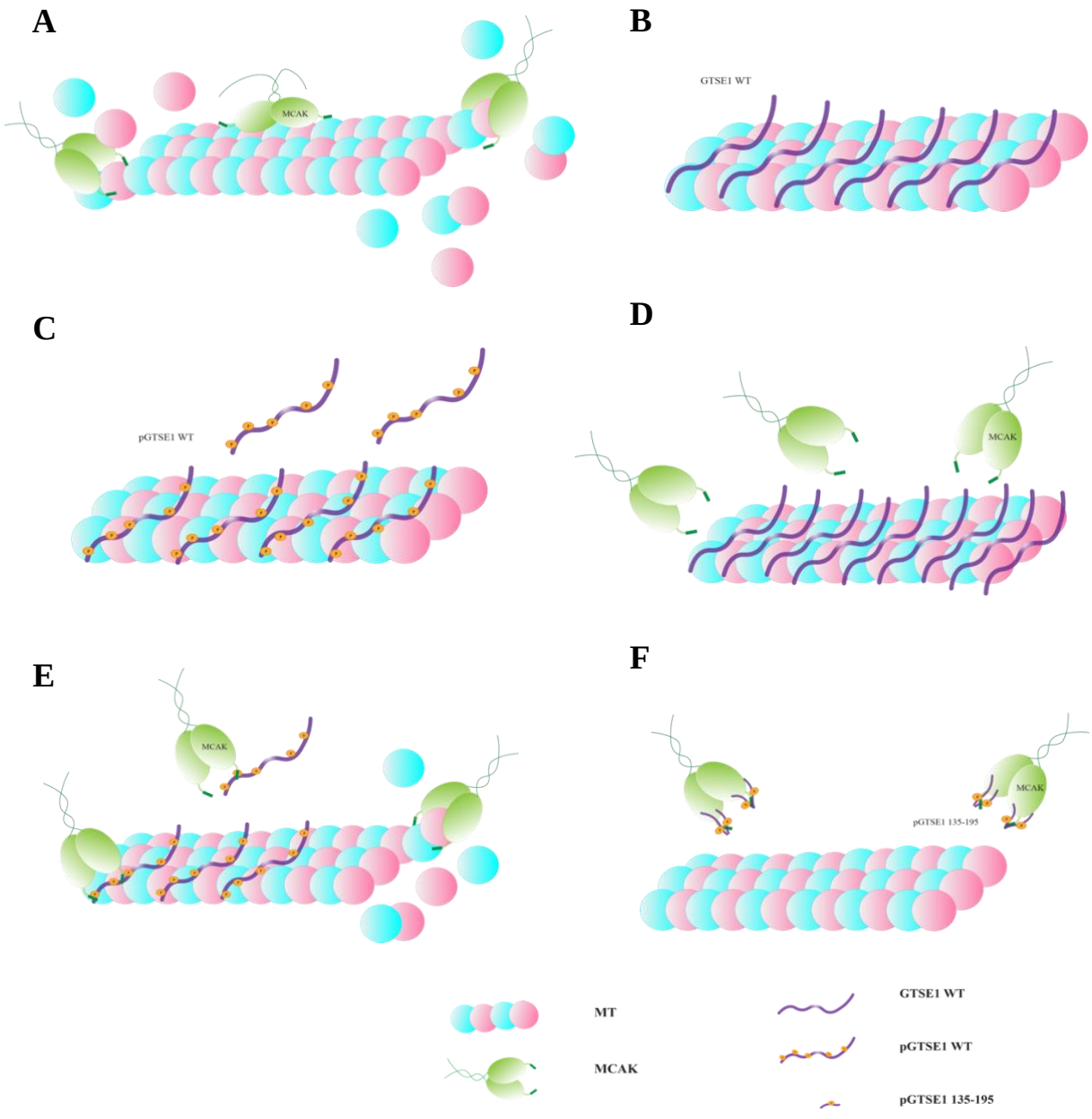

Figure 16. Phosphorylation-Dependent Regulation of Microtubule Dynamics by GTSE1-MCAK Interaction

A. MCAK-mediated Microtubule Depolymerization: MCAK binds along the microtubule lattice and diffuses towards the microtubule end, catalyzing the removal of tubulin dimers through its ATPase activity, leading to microtubule depolymerization. **B.** Unphosphorylated GTSE1 on Microtubule Lattice: GTSE1 in its unphosphorylated state binds strongly to the microtubule lattice, preventing access and subsequent depolymerization by MCAK. **C.** Phosphorylated GTSE1 on Microtubule Lattice: Phosphorylated GTSE1 shows diminished binding to the microtubule lattice due to post-translational modifications, subtly allowing MCAK activity. **D.** Unphosphorylated GTSE1 Inhibiting MCAK Activity: Unphosphorylated GTSE1 binds directly to the microtubule but not to MCAK, acting as a physical barrier to MCAK and thereby inhibiting microtubule depolymerization. **E.** Phosphorylated GTSE1 Competing with MCAK for Microtubule Binding: Phosphorylated GTSE1 binds both to MCAK and the microtubule lattice. Despite the reduced lattice binding, MCAK is still able to depolymerize microtubules, suggesting a competitive inhibition by GTSE1. **F.** Direct Inhibition of MCAK by Phosphorylated GTSE1 Fragment: The phosphorylated GTSE1 fragment (135-195) binds tightly to MCAK's N-terminus without associating with the microtubule lattice. This strong interaction prevents MCAK from depolymerizing microtubules, demonstrating that phosphorylated GTSE1 can inhibit MCAK activity through direct binding.

Furthermore, the project's scope extends beyond the confines of GTSE1-MCAK interaction to encompass a broader perspective on the regulation of kinesin 13 family proteins, including Kif2a or Kif2b, during cell division. Unravelling the regulatory intricacies of these proteins on a molecular level could significantly enhance our comprehension of microtubule dynamics and cellular division processes. In conclusion, this thesis has not only elucidated novel aspects of GTSE1-MCAK interaction but has also paved the way for future explorations into the broader regulatory networks governing kinesin 13 family proteins. The molecular insights gained from this study offer a foundation for unravelling the complex orchestration of events that dictate proper microtubule dynamics during mitosis. As we navigate the intricate web of molecular interactions, the journey ahead promises not only a deeper understanding of cellular division but also potential implications for therapeutic interventions targeting these regulatory pathways.

Summary

This thesis presents a comprehensive study of the regulatory mechanisms governing Mitotic Centromere-Associated Kinesin (MCAK) during mitosis, emphasizing the role of G2 and S phase-expressed 1 (GTSE1). The central focus of the research is to elucidate the molecular intricacies that control MCAK's function and consequently influence microtubule dynamics critical for cell division. The study reveals that Aurora kinase-mediated phosphorylation of GTSE1 is imperative for its interaction with MCAK. GTSE1, characterized as an intrinsically disordered protein, undergoes hyperphosphorylation during mitosis, enhancing its affinity for MCAK specifically in this phase and not during the G2/S phase. This phosphorylation-dependent interaction is demonstrated *in vitro* and corroborated within cellular contexts, highlighting the differential impacts of Aurora kinase subtypes on this interaction, with a more pronounced effect observed with Aurora B inhibition. Structural analysis indicates that the interaction between GTSE1 and MCAK primarily involves their N-terminal domains. The study postulates that this interaction may influence MCAK's localization to kinetochores and its microtubule depolymerization activity, which is critical for proper chromosome alignment and segregation. A pivotal discovery of the research is the identification of a single phosphorylation site on GTSE1, Threonine 165 (T165), as crucial for its binding to MCAK. Mutational analysis showed that the T165A mutant of GTSE1 fails to interact with MCAK, affirming the site's significance. Additionally, *in vivo* experiments using U2OS cells expressing the T165A mutant further support the indispensability of this phosphorylation for the GTSE1-MCAK interaction and discusses the existence of other potential pathways that might compensate for the disrupted interaction.

The study concludes that GTSE1's modulation of MCAK is distinctly influenced by its phosphorylation state, with unphosphorylated GTSE1 impeding MCAK's ATPase activity and the phosphorylated form affecting MCAK's depolymerization ability. These results not only enhance our understanding of the molecular dynamics at play during mitosis but also lay the groundwork for potential therapeutic interventions targeting the GTSE1-MCAK pathway, particularly in pathological conditions where mitotic control is deregulated, such as in cancer.

Zusammenfassung

In dieser Arbeit werden die Regulationsmechanismen von Mitotic Centromere-Associated Kinesin (MCAK) während der Mitose umfassend untersucht, wobei die Rolle von G2 und S Phase-expressed 1 (GTSE1) im Vordergrund steht. Das Hauptaugenmerk der Forschung liegt auf der Aufklärung der molekularen Feinheiten, die die Funktion von MCAK kontrollieren und folglich die für die Zellteilung kritische Mikrotubuli-Dynamik beeinflussen. Die Studie zeigt, dass die von der Aurora-Kinase vermittelte Phosphorylierung von GTSE1 für dessen Interaktion mit MCAK unerlässlich ist. GTSE1, das als intrinsisch ungeordnetes Protein charakterisiert wird, erfährt während der Mitose eine Hyperphosphorylierung, die seine Affinität für MCAK speziell in dieser Phase und nicht während der G2/S-Phase erhöht. Diese von der Phosphorylierung abhängige Interaktion wurde in vitro nachgewiesen und in zellulärem Kontext bestätigt, wobei die unterschiedlichen Auswirkungen der Aurora-Kinase-Subtypen auf diese Interaktion hervorgehoben wurden, wobei eine ausgeprägtere Wirkung bei der Hemmung von Aurora B beobachtet wurde. Die Strukturanalyse zeigt, dass die Interaktion zwischen GTSE1 und MCAK in erster Linie ihre N-terminalen Domänen betrifft. Die Studie geht davon aus, dass diese Interaktion die Lokalisierung von MCAK an den Kinetochoren und seine Aktivität zur Depolymerisation von Mikrotubuli beeinflussen kann, die für die korrekte Ausrichtung und Segregation von Chromosomen entscheidend ist. Eine zentrale Entdeckung der Forschung ist die Identifizierung einer einzigen Phosphorylierungsstelle auf GTSE1, Threonin 165 (T165), die für die Bindung an MCAK entscheidend ist. Eine Mutationsanalyse ergab, dass die T165A-Mutante von GTSE1 nicht mit MCAK interagiert, was die Bedeutung dieser Stelle bestätigt. In-vivo-Experimente mit U2OS-Zellen, die die T165A-Mutante exprimieren, untermauern die Unverzichtbarkeit dieser Phosphorylierung für die Interaktion zwischen GTSE1 und MCAK und erörtern die Existenz anderer möglicher Wege, die die gestörte Interaktion kompensieren könnten.

Die Studie kommt zu dem Schluss, dass die Modulation von MCAK durch GTSE1 deutlich von seinem Phosphorylierungszustand beeinflusst wird, wobei unphosphoryliertes GTSE1 die ATPase-Aktivität von MCAK behindert und die phosphorylierte Form die Depolymerisationsfähigkeit von MCAK beeinträchtigt. Diese Ergebnisse verbessern nicht nur unser Verständnis der molekularen Dynamik, die während der Mitose abläuft, sondern legen auch den Grundstein für potenzielle therapeutische Maßnahmen, die auf den GTSE1-MCAK-Signalweg abzielen, insbesondere bei pathologischen Zuständen, in denen die mitotische Kontrolle gestört ist, wie z. B. bei Krebs.

Bibliography

Adams, R. R., Eckley, D. M., Vagnarelli, P., Wheatley, S. P., Gerloff, D. L., Mackay, A. M., Svingen, P. A., Kaufmann, S. H., & Earnshaw, W. C. (2001). Human INCENP colocalizes with the Aurora-B/AIRK2 kinase on chromosomes and is overexpressed in tumour cells. *Chromosoma*, *110*(2). https://doi.org/10.1007/s004120100130

Adams, R. R., Maiato, H., Earnshaw, W. C., & Carmena, M. (2001). Essential roles of Drosophila inner centromere protein (INCENP) and aurora B in histone H3 phosphorylation, metaphase chromosome alignment, kinetochore disjunction, and chromosome segregation. *Journal of Cell Biology*, *153*(4). https://doi.org/10.1083/jcb.153.4.865

Akhmanova, A., & Steinmetz, M. O. (2008). Tracking the ends: A dynamic protein network controls the fate of microtubule tips. In *Nature Reviews Molecular Cell Biology* (Vol. 9, Issue 4). https://doi.org/10.1038/nrm2369

Akhmanova, A., & Steinmetz, M. O. (2015). Control of microtubule organization and dynamics: Two ends in the limelight. In *Nature Reviews Molecular Cell Biology* (Vol. 16, Issue 12). https://doi.org/10.1038/nrm4084

Alberts B, Johnson A, L. J. (2002). Molecular Biology of the Cell. *New York: Garland Science*, *4th edition.*

Allen, C., & Borisy, G. G. (1974). Structural polarity and directional growth of microtubules of Chlamydomonas flagella. *Journal of Molecular Biology*, *90*(2). https://doi.org/10.1016/0022-2836(74)90381-7

Amos, L. A., & Klug, A. (1974). Arrangement of subunits in flagellar microtubules. *Journal of Cell Science*, *14*(3). https://doi.org/10.1242/jcs.14.3.523

Andrews, P. D., Ovechkina, Y., Morrice, N., Wagenbach, M., Duncan, K., Wordeman, L., & Swedlow, J. R. (2004). Aurora B regulates MCAK at the mitotic centromere. *Developmental Cell*, *6*(2). https://doi.org/10.1016/S1534-5807(04)00025-5

Bakhoum, S. F., Genovese, G., & Compton, D. A. (2009). Deviant Kinetochore Microtubule Dynamics Underlie Chromosomal Instability. *Current Biology*, *19*(22). https://doi.org/10.1016/j.cub.2009.09.055

Bakhoum, S. F., Thompson, S. L., Manning, A. L., & Compton, D. A. (2009). Genome stability is ensured by temporal control of kinetochore-microtubule dynamics. *Nature Cell Biology*, *11*(1). https://doi.org/10.1038/ncb1809

Barr, F. A., Silljé, H. H. W., & Nigg, E. A. (2004). Polo-like kinases and the orchestration of cell division. In *Nature Reviews Molecular Cell Biology* (Vol. 5, Issue 6). https://doi.org/10.1038/nrm1401

Basilico, F., Maffini, S., Weir, J. R., Prumbaum, D., Rojas, A. M., Zimniak, T., De Antoni, A., Jeganathan, S., Voss, B., van Gerwen, S., Krenn, V., Massimiliano, L., Valencia, A., Vetter, I. R., Herzog, F., Raunser, S., Pasqualato, S., & Musacchio, A. (2014). The pseudo GTPase CENP-M drives human kinetochore assembly. *ELife*, *3*. https://doi.org/10.7554/elife.02978

Bendre, S., Rondelet, A., Hall, C., Schmidt, N., Lin, Y. C., Brouhard, G. J., & Bird, A. W. (2016). GTSE1 tunes microtubule stability for chromosome alignment and segregation by inhibiting the microtubule depolymerase MCAK. *Journal of Cell Biology*, *215*(5). https://doi.org/10.1083/jcb.201606081

Berdnik, D., & Knoblich, J. A. (2002). Drosophila Aurora-A is required for centrosome maturation and actin-dependent asymmetric protein localization during mitosis. *Current Biology*, *12*(8). https://doi.org/10.1016/S0960-9822(02)00766-2

Bhabha, G., Johnson, G. T., Schroeder, C. M., & Vale, R. D. (2016). How Dynein Moves Along Microtubules. In *Trends in Biochemical Sciences* (Vol. 41, Issue 1). https://doi.org/10.1016/j.tibs.2015.11.004

Bieling, P., Laan, L., Schek, H., Munteanu, E. L., Sandblad, L., Dogterom, M., Brunner, D., & Surrey, T. (2007). Reconstitution of a microtubule plus-end tracking system in vitro. *Nature*, *450*(7172). https://doi.org/10.1038/nature06386

Braun, A., Dang, K., Buslig, F., Baird, M. A., Davidson, M. W., Waterman, C. M., & Myers, K. A. (2014). Rac1 and Aurora A regulate MCAK to polarize microtubule growth in migrating endothelial cells. *Journal of Cell Biology*, *206*(1). https://doi.org/10.1083/jcb.201401063

Brouhard, G. J. (2015). Dynamic instability 30 years later: Complexities in microtubule growth and catastrophe. In *Molecular Biology of the Cell* (Vol. 26, Issue 7). https://doi.org/10.1091/mbc.E13-10-0594

Burns, K. M., Sarpe, V., Wagenbach, M., Wordeman, L., & Schriemer, D. C. (2015). HX-MS2 for high performance conformational analysis of complex protein states. *Protein Science*, *24*(8). https://doi.org/10.1002/pro.2707

Burns, K. M., Wagenbach, M., Wordeman, L., & Schriemer, D. C. (2014). Nucleotide exchange in dimeric MCAK induces longitudinal and lateral stress at microtubule ends to support depolymerization. *Structure*, *22*(8). https://doi.org/10.1016/j.str.2014.06.010

Carmena, M., Ruchaud, S., & Earnshaw, W. C. (2009). Making the Auroras glow: regulation of Aurora A and B kinase function by interacting proteins. In *Current Opinion in Cell Biology* (Vol. 21, Issue 6). https://doi.org/10.1016/j.ceb.2009.09.008

Cassimeris, L., Pryer, N. K., & Salmon, E. D. (1988). Real-time observations of microtubule dynamic instability in living cells. *Journal of Cell Biology*, *107*(6 I). https://doi.org/10.1083/jcb.107.6.2223

Charrasse, S., Schroeder, M., Gauthier-Rouviere, C., Ango, F., Cassimeris, L., Gard, D. L., & Larroque, C. (1998). The TOGp protein is a new human microtubule-associated protein homologous to the Xenopus XMAP215. *Journal of Cell Science*, *111*(10). https://doi.org/10.1242/jcs.111.10.1371

Cheeseman, I. M., & Desai, A. (2008). Molecular architecture of the kinetochore-microtubule interface. In *Nature Reviews Molecular Cell Biology* (Vol. 9, Issue 1). https://doi.org/10.1038/nrm2310

Cheeseman, L. P., Harry, E. F., McAinsh, A. D., Prior, I. A., & Royle, S. J. (2013). Specific removal of TACC3-ch-TOG-clathrin at metaphase deregulates kinetochore fiber tension. *Journal of Cell Science*, *126*(9). https://doi.org/10.1242/jcs.124834

Cimini, D., Moree, B., Canman, J. C., & Salmon, E. D. (2003). Merotelic kinetochore orientation occurs frequently during early mitosis in mammalian tissue cells and error correction is achieved by two different mechanisms. In *Journal of Cell Science* (Vol. 116, Issue 20). https://doi.org/10.1242/jcs.00716

Connolly, A. A., Sugioka, K., Chuang, C. H., Lowry, J. B., & Bowerman, B. (2015). KLP-7 acts through the Ndc80 complex to limit pole number in C. elegans oocyte meiotic spindle assembly. *Journal of Cell Biology*, *210*(6). https://doi.org/10.1083/jcb.201412010

Cooper, J. R., Wagenbach, M., Asbury, C. L., & Wordeman, L. (2010). Catalysis of the microtubule on-rate is the major parameter regulating the depolymerase activity of MCAK. *Nature Structural and Molecular Biology*, *17*(1). https://doi.org/10.1038/nsmb.1728

Desai, A., & Mitchison, T. J. (1997). Microtubule polymerization dynamics. In *Annual Review of Cell and Developmental Biology* (Vol. 13). https://doi.org/10.1146/annurev.cellbio.13.1.83

Desai, A., Verma, S., Mitchison, T. J., & Walczak, C. E. (1999). Kin I kinesins are microtubule-destabilizing enzymes. *Cell*, *96*(1). https://doi.org/10.1016/S0092-8674(00)80960-5

Dewar, H., Tanaka, K., Nasmyth, K., & Tanaka, T. U. (2004). Tension between two kinetochores suffices for their bi-orientation on the mitotic spindle. *Nature*, *428*(6978). https://doi.org/10.1038/nature02328

Ditchfield, C., Johnson, V. L., Tighe, A., Ellston, R., Haworth, C., Johnson, T., Mortlock, A., Keen, N., & Taylor, S. S. (2003). Aurora B couples chromosome alignment with anaphase by targeting BubR1, Mad2, and Cenp-E to kinetochores. *Journal of Cell Biology*, *161*(2). https://doi.org/10.1083/jcb.200208091

Dong, Y., Vanden Beldt, K. J., Meng, X., Khodjakov, A., & McEwen, B. F. (2007). The outer plate in vertebrate kinetochores is a flexible network with multiple microtubule interactions. *Nature Cell Biology*, *9*(5). https://doi.org/10.1038/ncb1576

Dutertre, S., Cazales, M., Quaranta, M., Froment, C., Trabut, V., Dozier, C., Mirey, G., Bouché, J. P., Theis-Febvre, N., Schmitt, E., Monsarrat, B., Prigent, C., & Ducommun, B. (2004). Phosphorylation of CDC25B by Aurora-A at the centrosome contributes to the G2-M transition. *Journal of Cell Science*, *117*(12). https://doi.org/10.1242/jcs.01108

Eichenlaub-Ritter, U. (2015). Microtubule dynamics and tumor invasion involving MCAK. *Cell Cycle*, *14*(21). https://doi.org/10.1080/15384101.2015.1093813

Ems-Mcclung, S. C., Hainline, S. G., Devare, J., Zong, H., Cai, S., Carnes, S. K., Shaw, S. L., & Walczak, C. E. (2013). Aurora B inhibits MCAK activity through a phosphoconformational switch that reduces microtubule association. *Current Biology*, *23*(24). https://doi.org/10.1016/j.cub.2013.10.054

Ertych, N., Stolz, A., Stenzinger, A., Weichert, W., Kaulfuß, S., Burfeind, P., Aigner, A., Wordeman, L., & Bastians, H. (2014). Increased microtubule assembly rates influence chromosomal instability in colorectal cancer cells. *Nature Cell Biology*, *16*(8). https://doi.org/10.1038/ncb2994

Eyers, P. A., Erikson, E., Chen, L. G., & Maller, J. L. (2003). A novel mechanism for activation of the protein kinase Aurora A. *Current Biology*, *13*(8). https://doi.org/10.1016/S0960-9822(03)00166-0

Foley, E. A., & Kapoor, T. M. (2013). Microtubule attachment and spindle assembly checkpoint signalling at the kinetochore. In *Nature Reviews Molecular Cell Biology* (Vol. 14, Issue 1). https://doi.org/10.1038/nrm3494

Foltz, D. R., Jansen, L. E. T., Black, B. E., Bailey, A. O., Yates, J. R., & Cleveland, D. W. (2006). The human CENP-A centromeric nucleosome-associated complex. *Nature Cell Biology*, *8*(5). https://doi.org/10.1038/ncb1397

Friel, C. T., & Howard, J. (2011). The kinesin-13 MCAK has an unconventional ATPase cycle adapted for microtubule depolymerization. *EMBO Journal*, *30*(19). https://doi.org/10.1038/emboj.2011.290

Ganem, N. J., & Compton, D. A. (2004). The KinI kinesin Kif2a is required for bipolar spindle assembly through a functional relationship with MCAK. *Journal of Cell Biology*, *166*(4). https://doi.org/10.1083/jcb.200404012

Ganem, N. J., Upton, K., & Compton, D. A. (2005). Efficient mitosis in human cells lacking poleward microtubule flux. *Current Biology*, *15*(20). https://doi.org/10.1016/j.cub.2005.08.065

Giet, R., & Glover, D. M. (2001). Drosophila aurora B kinase is required for histone H3 phosphorylation and condensin recruitment during chromosome condensation and to organize the central spindle during cytokinesis. *Journal of Cell Biology*, *152*(4). https://doi.org/10.1083/jcb.152.4.669

Giet, R., McLean, D., Descamps, S., Lee, M. J., Raff, J. W., Prigent, C., & Glover, D. M. (2002). Drosophila Aurora A kinase is required to localize D-TACC to centrosomes and to regulate astral microtubules. *Journal of Cell Biology*, *156*(3). https://doi.org/10.1083/jcb.200108135

Gildersleeve, R. F., Cross, A. R., Cullen, K. E., Fagen, A. P., & Williams, R. C. (1992). Microtubules grow and shorten at intrinsically variable rates. *Journal of Biological Chemistry*, *267*(12). https://doi.org/10.1016/s0021-9258(18)42399-x

Glover, D. M., Leibowitz, M. H., McLean, D. A., & Parry, H. (1995). Mutations in aurora prevent centrosome separation leading to the formation of monopolar spindles. *Cell*, *81*(1). https://doi.org/10.1016/0092-8674(95)90374-7

Gutiérrez-Caballero, C., Burgess, S. G., Bayliss, R., & Royle, S. J. (2015). TACC3-ch-TOG track the growing tips of microtubules independently of clathrin and Aurora-A phosphorylation. *Biology Open*, *4*(2). https://doi.org/10.1242/bio.201410843

Hannak, E., Kirkham, M., Hyman, A. A., & Oegema, K. (2001). Aurora-A kinase is required for centrosome maturation in Caenorhabditis elegans. *Journal of Cell Biology*, *155*(7). https://doi.org/10.1083/jcb.200108051

Hartwell, L. H. (1971). Genetic control of the cell division cycle in yeast. II. Genes controlling DNA replication and its initiation. *Journal of Molecular Biology*, *59*(1). https://doi.org/10.1016/0022-2836(71)90420-7

Hauf, S., Cole, R. W., LaTerra, S., Zimmer, C., Schnapp, G., Walter, R., Heckel, A., Van Meel, J., Rieder, C. L., & Peters, J. M. (2003). The small molecule Hesperadin reveals a role for Aurora B in correcting kinetochore-microtubule attachment and in maintaining the spindle assembly checkpoint. *Journal of Cell Biology*, *161*(2). https://doi.org/10.1083/jcb.200208092

Helenius, J., Brouhard, G., Kalaidzidis, Y., Diez, S., & Howard, J. (2006). The depolymerizing kinesin MCAK uses lattice diffusion to rapidly target microtubule ends. *Nature*, *441*(1). https://doi.org/10.1038/nature04736

Hepler, P. K., McIntosh, J. R., & Cleland, S. (1970). Intermicrotubule bridges in mitotic spindle apparatus. In *Journal of Cell Biology* (Vol. 45, Issue 2). https://doi.org/10.1083/jcb.45.2.438

Hertzer, K. M., Ems-McClung, S. C., Kline-Smith, S. L., Lipkin, T. G., Gilbert, S. P., & Walczak, C. E. (2006). Full-length dimeric MCAK is a more efficient microtubule depolymerase than minimal domain monomeric MCAK. *Molecular Biology of the Cell*, *17*(2). https://doi.org/10.1091/mbc.E05-08-0821

Hirokawa, N. (1998). Kinesin and dynein superfamily proteins and the mechanism of organelle transport. In *Science* (Vol. 279, Issue 5350). https://doi.org/10.1126/science.279.5350.519

Hirokawa, N., Noda, Y., Tanaka, Y., & Niwa, S. (2009). Kinesin superfamily motor proteins and intracellular transport. In *Nature Reviews Molecular Cell Biology* (Vol. 10, Issue 10). https://doi.org/10.1038/nrm2774

Holmfeldt, P., Zhang, X., Stenmark, S., Walczak, C. E., & Gullberg, M. (2005). CaMKIIγ-mediated inactivation of the Kin I kinesin MCAK is essential for bipolar spindle formation. *EMBO Journal*, *24*(6). https://doi.org/10.1038/sj.emboj.7600601

Hood, E. A., Kettenbach, A. N., Gerber, S. A., & Compton, D. A. (2012). Plk1 regulates the kinesin-13 protein Kif2b to promote faithful chromosome segregation. *Molecular Biology of the Cell*, *23*(12). https://doi.org/10.1091/mbc.E11-12-1013

Howard, J., & Hyman, A. A. (2003). Dynamics and mechanics of the microtubule plus end. In *Nature* (Vol. 422, Issue 6933). https://doi.org/10.1038/nature01600

Hubner, N. C., Bird, A. W., Cox, J., Splettstoesser, B., Bandilla, P., Poser, I., Hyman, A., & Mann, M. (2010). Quantitative proteomics combined with BAC TransgeneOmics reveals in vivo protein interactions. *Journal of Cell Biology*, *189*(4). https://doi.org/10.1083/jcb.200911091

Inoué, S., & Salmon, E. D. (1995). Force generation by microtubule assembly/disassembly in mitosis and related movements. In *Molecular Biology of the Cell* (Vol. 6, Issue 12). https://doi.org/10.1091/mbc.6.12.1619

Janke, C., Ortiz, J., Lechner, J., Shevchenko, A., Shevchenko, A., Magiera, M. M., Schramm, C., & Schiebel, E. (2001). The budding yeast proteins Spc24p and Spc25p interact with Ndc80p and Nuf2p at the kinetochore and are important for kinetochore clustering and checkpoint control. *EMBO Journal*, *20*(4). https://doi.org/10.1093/emboj/20.4.777

Jiang, K., Toedt, G., Montenegro Gouveia, S., Davey, N. E., Hua, S., Van Der Vaart, B., Grigoriev, I., Larsen, J., Pedersen, L. B., Bezstarosti, K., Lince-Faria, M., Demmers, J., Steinmetz, M. O., Gibson, T. J., & Akhmanova, A. (2012). A proteome-wide screen for mammalian SxIP motif-containing microtubule plus-end tracking proteins. *Current Biology*, *22*(19). https://doi.org/10.1016/j.cub.2012.07.047

Kallio, M. J., McCleland, M. L., Todd Stukenberg, P., & Gorbsky, G. J. (2002). Inhibition of Aurora B kinase blocks chromosome segregation, overrides the spindle checkpoint, and perturbs microtubule dynamics in mitosis. *Current Biology*, *12*(11). https://doi.org/10.1016/S0960-9822(02)00887-4

Kapoor, T. M. (2017). Metaphase spindle assembly. In *Biology* (Vol. 6, Issue 1). https://doi.org/10.3390/biology6010008

Katayama, H., Brinkley, W. R., & Sen, S. (2003). The Aurora kinases: Role in cell transformation and tumorigenesis. In *Cancer and Metastasis Reviews* (Vol. 22, Issue 4). https://doi.org/10.1023/A:1023789416385

Kelly, A. E., & Funabiki, H. (2009). Correcting aberrant kinetochore microtubule attachments: an Aurora B-centric view. In *Current Opinion in Cell Biology* (Vol. 21, Issue 1). https://doi.org/10.1016/j.ceb.2009.01.004

Kirschner, M., & Mitchison, T. (1986). Beyond self-assembly: From microtubules to morphogenesis. In *Cell* (Vol. 45, Issue 3). https://doi.org/10.1016/0092-8674(86)90318-1

Kufer, T. A., Silljé, H. H. W., Körner, R., Gruss, O. J., Meraldi, P., & Nigg, E. A. (2002). Human TPX2 is required for targeting Aurora-A kinase to the spindle. *Journal of Cell Biology*, *158*(4). https://doi.org/10.1083/jcb.200204155

Lan, W., Zhang, X., Kline-Smith, S. L., Rosasco, S. E., Barrett-Wilt, G. A., Shabanowitz, J., Hunt, D. F., Walczak, C. E., & Stukenberg, P. T. (2004). Aurora B Phosphorylates Centromeric MCAK and Regulates Its Localization and Microtubule Depolymerization Activity. *Current Biology*, *14*(4). https://doi.org/10.1016/j.cub.2004.01.055

Lara-Gonzalez, P., & Taylor, S. S. (2012). Cohesion Fatigue Explains Why Pharmacological Inhibition of the APC/C Induces a Spindle Checkpoint-Dependent Mitotic Arrest. *PLoS ONE*, *7*(11). https://doi.org/10.1371/journal.pone.0049041

Lukas, J., Lukas, C., & Bartek, J. (2004). Mammalian cell cycle checkpoints: Signalling pathways and their organization in space and time. In *DNA Repair* (Vol. 3, Issues 8–9). https://doi.org/10.1016/j.dnarep.2004.03.006

Maney, T., Wagenbach, M., & Wordeman, L. (2001). Molecular Dissection of the Microtubule Depolymerizing Activity of Mitotic Centromere-associated Kinesin. *Journal of Biological Chemistry*, *276*(37). https://doi.org/10.1074/jbc.M106626200

Manning, A. L., Ganem, N. J., Bakhoum, S. F., Wagenbach, M., Wordeman, L., & Compton, D. A. (2007). The kinesin-13 proteins Kif2a, Kif2b, and Kif2c/MCAK have distinct roles during mitosis in human cells. *Molecular Biology of the Cell*, *18*(8). https://doi.org/10.1091/mbc.E07-02-0110

McClelland, S. E., Borusu, S., Amaro, A. C., Winter, J. R., Belwal, M., McAinsh, A. D., & Meraldi, P. (2007). The CENP-A NAC/CAD kinetochore complex controls chromosome congression and spindle bipolarity. *EMBO Journal*, *26*(24). https://doi.org/10.1038/sj.emboj.7601927

McDonald, K. L., O'Toole, E. T., Mastronarde, D. N., & McIntosh, J. R. (1992). Kinetochore microtubules in PTK cells. *Journal of Cell Biology*, *118*(2). https://doi.org/10.1083/jcb.118.2.369

McHugh, T., Zou, J., Volkov, V. A., Bertin, A., Talapatra, S. K., Rappsilber, J., Dogterom, M., & Welburn, J. P. I. (2019). The depolymerase activity of MCAK shows a graded response to Aurora B kinase phosphorylation through allosteric regulation. *Journal of Cell Science*, *132*(4). https://doi.org/10.1242/jcs.228353

McNally, F. J., & Roll-Mecak, A. (2018). Microtubule-severing enzymes: From cellular functions to molecular mechanism. In *Journal of Cell Biology* (Vol. 217, Issue 12). https://doi.org/10.1083/jcb.201612104

Miki, H., Setou, M., Kaneshiro, K., & Hirokawa, N. (2001). All kinesin superfamily protein, KIF, genes in mouse and human. *Proceedings of the National Academy of Sciences of the United States of America*, *98*(13). https://doi.org/10.1073/pnas.111145398

Mitchison, T., & Kirschner, M. (1984). Dynamic instability of microtubule growth. *Nature*, *312*(5991). https://doi.org/10.1038/312237a0

Mitchison, T., & Kirschner, M. (1988). Cytoskeletal dynamics and nerve growth. In *Neuron* (Vol. 1, Issue 9). https://doi.org/10.1016/0896-6273(88)90124-9

Murata-Hori, M., & Wang, Y. L. (2002). The kinase activity of aurora B is required for kinetochore-microtubule interactions during mitosis. *Current Biology*, *12*(11). https://doi.org/10.1016/S0960-9822(02)00848-5

Musacchio, A., & Desai, A. (2017). A molecular view of kinetochore assembly and function. In *Biology* (Vol. 6, Issue 1). https://doi.org/10.3390/biology6010005

Musacchio, A., & Salmon, E. D. (2007). The spindle-assembly checkpoint in space and time. In *Nature Reviews Molecular Cell Biology* (Vol. 8, Issue 5). https://doi.org/10.1038/nrm2163

Nehlig, A., Molina, A., Rodrigues-Ferreira, S., Honoré, S., & Nahmias, C. (2017). Regulation of end-binding protein EB1 in the control of microtubule dynamics. In *Cellular and Molecular Life Sciences* (Vol. 74, Issue 13). https://doi.org/10.1007/s00018-017-2476-2

Nixon, F. M., Gutiérrez-Caballero, C., Hood, F. E., Booth, D. G., Prior, I. A., & Royle, S. J. (2015). The mesh is a network of microtubule connectors that stabilizes individual kinetochore fibers of the mitotic spindle. *ELife*, *4*(JUNE2015). https://doi.org/10.7554/eLife.07635

Norbury, C., & Nurse, P. (1992). ANIMAL CELL CYCLES AND THEIR CONTROL. *Annual Review of Biochemistry*, *61*(1). https://doi.org/10.1146/annurev.bi.61.070192.002301

Ohi, R., Sapra, T., Howard, J., & Mitchison, T. J. (2004). Differentiation of cytoplasmic and meiotic spindle assembly MCAK functions by Aurora B-dependent phosphorylation. *Molecular Biology of the Cell*, *15*(6). https://doi.org/10.1091/mbc.E04-02-0082

Okada, M., Cheeseman, I. M., Hori, T., Okawa, K., McLeod, I. X., Yates, J. R., Desai, A., & Fukagawa, T. (2006). The cenp-H–I complex is required for the efficient incorporation of newly synthesized CENP-A into centromeres. *Nature Cell Biology*, *8*(5). https://doi.org/10.1038/ncb1396

Ovechkina, Y., Wagenbach, M., & Wordeman, L. (2002). K-loop insertion restores microtubule depolymerizing activity of a 'neckless' MCAK mutant. *Journal of Cell Biology*, *159*(4). https://doi.org/10.1083/jcb.200205089

Pardee, A. B. (1974). A restriction point for control of normal animal cell proliferation. *Proceedings of the National Academy of Sciences of the United States of America*, *71*(4). https://doi.org/10.1073/pnas.71.4.1286

Peterman, E. J. G., & Scholey, J. M. (2009). Mitotic Microtubule Crosslinkers: Insights from Mechanistic Studies. In *Current Biology* (Vol. 19, Issue 23). https://doi.org/10.1016/j.cub.2009.10.047

Peters, J. M. (2006). The anaphase promoting complex/cyclosome: A machine designed to destroy. In *Nature Reviews Molecular Cell Biology* (Vol. 7, Issue 9). https://doi.org/10.1038/nrm1988

Petry, S. (2016). Mechanisms of Mitotic Spindle Assembly. *Annual Review of Biochemistry*, *85*. https://doi.org/10.1146/annurev-biochem-060815-014528

Pinsky, B. A., & Biggins, S. (2005). The spindle checkpoint: Tension versus attachment. In *Trends in Cell Biology* (Vol. 15, Issue 9). https://doi.org/10.1016/j.tcb.2005.07.005

Popov, A. V., Pozniakovsky, A., Arnal, I., Antony, C., Ashford, A. J., Kinoshita, K., Tournebize, R., Hyman, A. A., & Karsenti, E. (2001). XMAP215 regulates microtubule dynamics through two distinct domains. *EMBO Journal*, *20*(3). https://doi.org/10.1093/emboj/20.3.397

Prosser, S. L., & Pelletier, L. (2017). Mitotic spindle assembly in animal cells: A fine balancing act. In *Nature Reviews Molecular Cell Biology* (Vol. 18, Issue 3). https://doi.org/10.1038/nrm.2016.162

Przewloka, M. R., Venkei, Z., Bolanos-Garcia, V. M., Debski, J., Dadlez, M., & Glover, D. M. (2011). CENP-C is a structural platform for kinetochore assembly. *Current Biology*, *21*(5). https://doi.org/10.1016/j.cub.2011.02.005

Rieder, C. L. (1981). The structure of the cold-stable kinetochore fiber in metaphase PtK1 cells. *Chromosoma*, *84*(1). https://doi.org/10.1007/BF00293368

Rieder, C. L. (2005). Kinetochore fiber formation in animal somatic cells: Dueling mechanisms come to a draw. In *Chromosoma* (Vol. 114, Issue 5). https://doi.org/10.1007/s00412-005-0028-2

Rieder, C. L., Cole, R. W., Khodjakov, A., & Sluder, G. (1995). The checkpoint delaying anaphase in response to chromosome monoorientation is mediated by an inhibitory

signal produced by unattached kinetochores. *Journal of Cell Biology*, *130*(4). https://doi.org/10.1083/jcb.130.4.941

Ritter, A., Kreis, N. N., Louwen, F., Wordeman, L., & Yuan, J. (2016). Molecular insight into the regulation and function of MCAK. In *Critical Reviews in Biochemistry and Molecular Biology* (Vol. 51, Issue 4). https://doi.org/10.1080/10409238.2016.1178705

Rogers, S. L., Rogers, G. C., Sharp, D. J., & Vale, R. D. (2002). Drosophila EB1 is important for proper assembly, dynamics, and positioning of the mitotic spindle. *Journal of Cell Biology*, *158*(5). https://doi.org/10.1083/jcb.200202032

Rondelet, A., Lin, Y. C., Singh, D., Porfetye, A. T., Thakur, H. C., Hecker, A., Brinkert, P., Schmidt, N., Bendre, S., Müller, F., Mazul, L., Widlund, P. O., Bange, T., Hiller, M., Vetter, I. R., & Bird, A. W. (2020). Clathrin's adaptor interaction sites are repurposed to stabilize microtubules during mitosis. *Journal of Cell Biology*, *219*(2). https://doi.org/10.1083/jcb.201907083

Roostalu, J., & Surrey, T. (2017). Microtubule nucleation: Beyond the template. In *Nature Reviews Molecular Cell Biology* (Vol. 18, Issue 11). https://doi.org/10.1038/nrm.2017.75

Sammak, P. J., & Borisy, G. G. (1988). Direct observation of microtubule dynamics in living cells. *Nature*, *332*(6166). https://doi.org/10.1038/332724a0

Sanhaji, M., Ritter, A., Belsham, H. R., Friel, C. T., Roth, S., Louwen, F., & Yuan, J. (2014). Polo-like kinase 1 regulates the stability of the mitotic centromere-associated kinesin in mitosis. *Oncotarget*, *5*(10). https://doi.org/10.18632/oncotarget.1861

Santaguida, S., & Musacchio, A. (2009). The life and miracles of kinetochores. In *EMBO Journal* (Vol. 28, Issue 17). https://doi.org/10.1038/emboj.2009.173

Schafer, K. A. (1998). The Cell Cycle: A Review. In *Veterinary Pathology* (Vol. 35, Issue 6). https://doi.org/10.1177/030098589803500601

Scolz, M., Widlund, P. O., Piazza, S., Bublik, D. R., Reber, S., Peche, L. Y., Ciani, Y., Hubner, N., Isokane, M., Monte, M., Ellenberg, J., Hyman, A. A., Schneider, C., & Bird, A. W. (2012). GTSE1 Is a Microtubule Plus-End Tracking Protein That Regulates EB1-Dependent Cell Migration. *PLoS ONE*, *7*(12). https://doi.org/10.1371/journal.pone.0051259

Screpanti, E., De Antoni, A., Alushin, G. M., Petrovic, A., Melis, T., Nogales, E., & Musacchio, A. (2011). Direct binding of Cenp-C to the Mis12 complex joins the inner and outer kinetochore. *Current Biology*, *21*(5). https://doi.org/10.1016/j.cub.2010.12.039

Sessa, F., Mapelli, M., Ciferri, C., Tarricone, C., Areces, L. B., Schneider, T. R., Stukenberg, P. T., & Musacchio, A. (2005). Mechanism of Aurora B activation by INCENP and inhibition by hesperadin. *Molecular Cell*, *18*(3). https://doi.org/10.1016/j.molcel.2005.03.031

Sharp, D. J., Rogers, G. C., & Scholey, J. M. (2000). Microtubule motors in mitosis. In *Nature* (Vol. 407, Issue 6800). https://doi.org/10.1038/35024000

Stevermann, L., & Liakopoulos, D. (2012). Molecular mechanisms in spindle positioning: Structures and new concepts. In *Current Opinion in Cell Biology* (Vol. 24, Issue 6). https://doi.org/10.1016/j.ceb.2012.10.005

Sun, S. C., & Kim, N. H. (2012). Spindle assembly checkpoint and its regulators in meiosis. *Human Reproduction Update*, *18*(1). https://doi.org/10.1093/humupd/dmr044

Takahashi, T., Futamura, M., Yoshimi, N., Sano, J., Katada, M., Takagi, Y., Kimura, M., Yoshioka, T., Okano, Y., & Saji, S. (2000). Centrosomal kinases, HsAIRK1 and HsAIRK3, are overexpressed in primary colorectal cancers. *Japanese Journal of Cancer Research*, *91*(10). https://doi.org/10.1111/j.1349-7006.2000.tb00878.x

Takizawa, C. G., & Morgan, D. O. (2000). Control of mitosis by changes in the subcellular location of cyclin-B1-Cdk1 and Cdc25C. In *Current Opinion in Cell Biology* (Vol. 12, Issue 6). https://doi.org/10.1016/S0955-0674(00)00149-6

Talapatra, S. K., Harker, B., & Welburn, J. P. I. (2015). The C-terminal region of the motor protein MCAK controls its structure and activity through a conformational switch. *ELife*, *2015*(4). https://doi.org/10.7554/eLife.06421

Tanenbaum, M. E., MacUrek, L., Van Der Vaart, B., Galli, M., Akhmanova, A., & Medema, R. H. (2011). A complex of Kif18b and MCAK promotes microtubule depolymerization and is negatively regulated by aurora kinases. *Current Biology*, *21*(16). https://doi.org/10.1016/j.cub.2011.07.017

Terada, Y., Uetake, Y., & Kuriyama, R. (2003). Interaction of Aurora-A and centrosomin at the microtubule-nucleating site in Drosophila and mammalian cells. *Journal of Cell Biology*, *162*(5). https://doi.org/10.1083/jcb.200305048

Tsai, M. Y., & Zheng, Y. (2005). Aurora A kinase-coated beads function as microtubule-organizing centers and enhance RanGTP-induced spindle assembly. *Current Biology*, *15*(23). https://doi.org/10.1016/j.cub.2005.10.054

Uehara, R., Tsukada, Y., Kamasaki, T., Poser, I., Yoda, K., Gerlich, D. W., & Goshima, G. (2013). Aurora B and Kif2A control microtubule length for assembly of a functional

central spindle during anaphase. *Journal of Cell Biology*, *202*(4). https://doi.org/10.1083/jcb.201302123

van der Vaart, B., Akhmanova, A., & Straube, A. (2009). Regulation of microtubule dynamic instability. *Biochemical Society Transactions*, *37*(5). https://doi.org/10.1042/BST0371007

Van Vugt, M. A. T. M., & Medema, R. H. (2005). Getting in and out of mitosis with Polo-like kinase-1. In *Oncogene* (Vol. 24, Issue 17). https://doi.org/10.1038/sj.onc.1208617

Vitre, B., Coquelle, F. M., Heichette, C., Garnier, C., Chrétien, D., & Arnal, I. (2008). EB1 regulates microtubule dynamics and tubulin sheet closure in vitro. *Nature Cell Biology*, *10*(4). https://doi.org/10.1038/ncb1703

Walczak, C. E., Mitchison, T. J., & Desai, A. (1996). XKCM1: A Xenopus kinesin-related protein that regulates microtubule dynamics during mitotic spindle assembly. *Cell*, *84*(1). https://doi.org/10.1016/S0092-8674(00)80991-5

Wang, W., Jiang, Q., Argentini, M., Cornu, D., Gigant, B., Knossow, M., & Wang, C. (2012). Kif2C minimal functional domain has unusual nucleotide binding properties that are adapted to microtubule depolymerization. *Journal of Biological Chemistry*, *287*(18). https://doi.org/10.1074/jbc.M111.317859

Weir, J. R., Faesen, A. C., Klare, K., Petrovic, A., Basilico, F., Fischböck, J., Pentakota, S., Keller, J., Pesenti, M. E., Pan, D., Vogt, D., Wohlgemuth, S., Herzog, F., & Musacchio, A. (2016). Insights from biochemical reconstitution into the architecture of human kinetochores. *Nature*, *537*(7619). https://doi.org/10.1038/nature19333

Weisenberg, R. C., Borisy, G. G., & Taylor, E. W. (1968). The Colchicine-Binding Protein of Mammalian Brain and Its Relation to Microtubules. *Biochemistry*, *7*(12). https://doi.org/10.1021/bi00852a043

Wigge, P. A., & Kilmartin, J. V. (2001). The Ndc80p complex from Saccharomyces cerevisiae contains conserved centromere components and has a function in chromosome segregation. *Journal of Cell Biology*, *152*(2). https://doi.org/10.1083/jcb.152.2.349

Wilbur, J. D., & Heald, R. (2013). Mitotic spindle scaling during Xenopus development by kif2a and importin α. *ELife*, *2013*(2). https://doi.org/10.7554/eLife.00290

Willems, E., Dedobbeleer, M., Digregorio, M., Lombard, A., Lumapat, P. N., & Rogister, B. (2018). The functional diversity of Aurora kinases: A comprehensive review. In *Cell Division* (Vol. 13, Issue 1). https://doi.org/10.1186/s13008-018-0040-6

Witt, P. L., Ris, H., & Borisy, G. G. (1981). Structure of kinetochore fibers: Microtubule continuity and inter-microtubule bridges. *Chromosoma*, *83*(4). https://doi.org/10.1007/BF00328277

Wordeman, L., & Mitchison, T. J. (1995). Identification and partial characterization of mitotic centromere-associated kinesin, a kinesin-related protein that associates with centromeres during mitosis. *Journal of Cell Biology*, *128*(1–2). https://doi.org/10.1083/jcb.128.1.95

Zhang, X., Lan, W., Ems-McClung, S. C., Stukenberg, P. T., & Walczak, C. E. (2007). Aurora B phosphorylates multiple sites on mitotic centromere-associated kinesin to spatially and temporally regulate its function. *Molecular Biology of the Cell*, *18*(9). https://doi.org/10.1091/mbc.E07-01-0086

Zong, H., Carnes, S. K., Moe, C., Walczak, C. E., & Ems-McClung, S. C. (2016). The far C-terminus of MCAK regulates its conformation and spindle pole focusing. *Molecular Biology of the Cell*, *27*(9). https://doi.org/10.1091/mbc.E15-10-0699

Acknowledgements

I extend my deepest appreciation to my PhD advisors, Prof. Dr. Andrea Musacchio and Dr. Alex Bird, for their guidance and support throughout my research. Dr. Bird's faith in my abilities and liberal approach to mentoring has been invaluable, while Prof. Dr. Musacchio's willingness to supervise during challenging times and his insightful contributions were crucial to the development of my work.

Special thanks go to the members of Department 1 and the Bird-Vader lab, whose collective wisdom has been a cornerstone of my research journey. Yu Chih Lin deserves particular mention for introducing me to essential techniques and the culture of our lab. I am indebted to Divya Singh for her unflagging assistance in both my professional endeavors and personal challenges. Her readiness to share her vast knowledge has been a great comfort. Vivek B. Raina's encouragement has been a personal beacon, inspiring me throughout this project.

I owe a debt of gratitude to Farid Alizadeh for his assistance in establishing TIRF microscopy assays, and to Arnaud Rondelet and Nadine Schmidt for their mentorship in cell biology. I am thankful for Andreas Hecker and Bhagyashree Mullay's camaraderie and collaboration in concurrent projects. I extend my gratitude to Valentina Piano and Stefano Maffini for their help in learning new techniques and troubleshooting various technical hurdles. Dr. Tanja Bange and Franziska Müller have been instrumental in supporting my mass spectrometry experiments, for which I am grateful.

My TAC members, Dr. Stefan Westermann and Dr. Dominic Boos, have offered invaluable advice that has significantly enhanced my work. The financial and educational support of IMPRS-CMB has been a foundation of my PhD journey, for which I am thankful. Christa Hornemann, my student mentor, has shown unparalleled compassion and support from day one. I am deeply thankful for your nurturing presence. I am grateful to Antje Peukert and Lucia Sironi for their assistance with administrative and scientific challenges.

I cherish the moments with Suruchi Sethi and Amal Alex, whose company provided much-needed respite. Akhilesh P. Nandan's guidance in navigating the nuances of Dortmund and his friendship have enriched my experience in Germany. Pragya Jattoo's caring friendship and her ability to uplift spirits with her gentle words have been a source of constant support.

Lastly, my heart is full of affection for those who have been my steadfast companions on this journey. To Dolvin S, your love has been my anchor, and your belief in me has illuminated paths I feared to tread. Mirsana Ebrahimkutty, your wise counsel and unwavering support have been the north star guiding my scholarly pursuits. And to Revathy Lakshmi Pulpetta and Ishamol Shaji, your presence in my life is a treasure beyond words—my twin beacons of hope in times of darkness. Your boundless love have been the quiet force behind my every step forward. Thank you all for being the family chosen by heart, not by blood.

"Der Lebenslauf ist in der Online-Version aus Gründen des Datenschutzes nicht enthalten."

Einverständniserklärung

Ich versichere, dass ich meine Dissertation:

“A molecular study on phospho-regulation of microtubule depolymerase MCAK via GTSE1 ”

selbstständig, ohne unerlaubte Hilfe angefertigt und mich dabei keiner anderen als der von mir ausdrücklich bezeichneten Quellen und Hilfen bedient habe. Die Dissertation wurde in der jetzigen oder einer ähnlichen Form noch bei keiner anderen Hochschule eingereicht und hat noch keinen sonstigen Prüfungszwecken gedient.

Dortmund, 19.03.2024 _____

Devika Namboodiri